Guide for the Design and Construction of Externally Bonded FRP Systems for Strengthening Concrete Structures

Reported by ACI Committee 440

American Concrete Institute®

American Concrete Institute®
Advancing concrete knowledge

Guide for the Design and Construction of Externally Bonded FRP Systems for Strengthening Concrete Structures

Order information: ACI documents are available in print, by download, on CD-ROM, through electronic subscription, or reprint and may be obtained by contacting ACI.

Most ACI standards and committee reports are gathered together in the annually revised *ACI Manual of Concrete Practice* (MCP).

Guide for the Design and Construction of Externally Bonded FRP Systems for Strengthening Concrete Structures

Reported by ACI Committee 440

John P. Busel
Chair

Carol K. Shield
Secretary

Tarek Alkhrdaji[*]	Russell Gentry	James G. Korff	Andrea Prota
Charles E. Bakis	Janos Gergely	Michael W. Lee	Hayder A. Rasheed
Lawrence C. Bank	William J. Gold	Maria Lopez de Murphy	Sami H. Rizkalla
Abdeldjelil Belarbi	Nabil F. Grace	Ibrahim M. Mahfouz	Morris Schupack
Brahim Benmokrane	Mark F. Green	Orange S. Marshall	Rajan Sen
Luke A. Bisby	Zareh B. Gregorian	Amir Mirmiran	Khaled A. Soudki[*]
Gregg J. Blaszak	Doug D. Gremel	Ayman S. Mosallam	Samuel A. Steere, III
Timothy E. Bradberry	Shawn P. Gross	John J. Myers	Gamil S. Tadros
Gordon L. Brown, Jr.	H. R. Trey Hamilton, III	Antonio Nanni	Jay Thomas
Vicki L. Brown	Issam E. Harik	Kenneth Neale	Houssam A. Toutanji
Raafat El-Hacha	Kent A. Harries	John P. Newhook	J. Gustavo Tumialan
Garth J. Fallis	Mark P. Henderson	Ayman M. Okeil	Milan Vatovec
Amir Z. Fam	Bohdan N. Horeczko	Carlos E. Ospina	Stephanie Walkup
Edward R. Fyfe	Vistasp M. Karbhari	Max L. Porter	David White

Fiber-reinforced polymer (FRP) systems for strengthening concrete structures are an alternative to traditional strengthening techniques, such as steel plate bonding, section enlargement, and external post-tensioning. FRP strengthening systems use FRP composite materials as supplemental externally bonded reinforcement. FRP systems offer advantages over traditional strengthening techniques: they are lightweight, relatively easy to install, and are noncorrosive. Due to the characteristics of FRP materials as well as the behavior of members strengthened with FRP, specific guidance on the use of these systems is needed. This document offers general information on the history and use of FRP strengthening systems; a description of the unique material properties of FRP; and committee recommendations on the engineering, construction, and inspection of FRP systems used to strengthen concrete structures. The proposed guidelines are based on the knowledge gained from experimental research, analytical work, and field applications of FRP systems used to strengthen concrete structures.

Keywords: aramid fibers; bridges; buildings; carbon fibers; concrete; corrosion; crack widths; cracking; cyclic loading; deflection; development length; earthquake-resistant; fatigue; fiber-reinforced polymers; flexure; shear; stress; structural analysis; structural design; torsion.

CONTENTS

PART 1—GENERAL
CHAPTER 1—INTRODUCTION AND SCOPE
1.1—Introduction

The strengthening or retrofitting of existing concrete structures to resist higher design loads, correct strength loss due to deterioration, correct design or construction deficiencies, or increase ductility has traditionally been accomplished using conventional materials and construction techniques. Externally bonded steel plates, steel or concrete jackets, and external post-tensioning are just some of the many traditional techniques available.

Composite materials made of fibers in a polymeric resin, also known as fiber-reinforced polymers (FRPs), have emerged as an alternative to traditional materials for repair and rehabilitation. For the purposes of this document, an FRP system is defined as the fibers and resins used to create the composite laminate, all applicable resins used to bond it to the concrete substrate, and all applied coatings used to protect the constituent materials. Coatings used exclusively for aesthetic reasons are not considered part of an FRP system.

FRP materials are lightweight, noncorrosive, and exhibit high tensile strength. These materials are readily available in several forms, ranging from factory-made laminates to dry fiber sheets that can be wrapped to conform to the geometry of a structure before adding the polymer resin. The relatively thin profiles of cured FRP systems are often desirable in applications where aesthetics or access is a concern.

The growing interest in FRP systems for strengthening and retrofitting can be attributed to many factors. Although the fibers and resins used in FRP systems are relatively expensive compared with traditional strengthening materials such as concrete and steel, labor and equipment costs to install FRP systems are often lower (Nanni 1999). FRP systems can also be used in areas with limited access where traditional techniques would be difficult to implement.

The basis for this document is the knowledge gained from a comprehensive review of experimental research, analytical work, and field applications of FRP strengthening systems. Areas where further research is needed are highlighted in this document and compiled in Appendix C.

1.2—Scope and limitations

This document provides guidance for the selection, design, and installation of FRP systems for externally strengthening concrete structures. Information on material properties, design, installation, quality control, and maintenance of FRP systems used as external reinforcement is presented. This information can be used to select an FRP system for increasing the strength and stiffness of reinforced concrete beams or the ductility of columns and other applications.

A significant body of research serves as the basis for this document. This research, conducted over the past 25 years, includes analytical studies, experimental work, and monitored field applications of FRP strengthening systems. Based on the available research, the design procedures outlined in this document are considered to be conservative. It is important to specifically point out the areas of the document that still require research.

The durability and long-term performance of FRP materials has been the subject of much research; however, this research remains ongoing. The design guidelines in this document do account for environmental degradation and long-term durability by suggesting reduction factors for various environments. Long-term fatigue and creep are also addressed by stress limitations indicated in this document. These factors and limitations are considered conservative. As more research becomes available, however, these factors will be modified, and the specific environmental conditions and loading conditions to which they should apply will be better defined. Additionally, the coupling effect of environmental conditions and loading conditions still requires further study. Caution is advised in applications where the FRP system is subjected simultaneously to extreme environmental and stress conditions. The factors associated with the long-term durability of the FRP system may also affect the tensile modulus of elasticity of the material used for design.

Many issues regarding bond of the FRP system to the substrate remain the focus of a great deal of research. For both flexural and shear strengthening, there are many different varieties of debonding failure that can govern the strength of an FRP-strengthened member. While most of the debonding modes have been identified by researchers, more accurate methods of predicting debonding are still needed. Throughout the design procedures, significant limitations on the strain level achieved in the FRP material (and thus, the stress level achieved) are imposed to conservatively account for debonding failure modes. Future development of these design procedures should include more thorough methods of predicting debonding.

The document gives guidance on proper detailing and installation of FRP systems to prevent many types of debonding failure modes. Steps related to the surface preparation and proper termination of the FRP system are vital in achieving the levels of strength predicted by the procedures in this document. Some research has been conducted on various methods of anchoring FRP strengthening systems (by mechanical or other means). It is important to recognize, however, that methods of anchoring these systems are highly problematic due to the brittle, anisotropic nature of composite materials. Any proposed method of anchorage should be heavily scrutinized before field implementation.

The design equations given in this document are the result of research primarily conducted on moderately sized and proportioned members. Caution should be given to applications involving strengthening of very large members or strengthening in disturbed regions (D-regions) of structural members such as deep beams, corbels, and dapped beam ends. When warranted, specific limitations on the size of members and the state of stress are given in this document.

This document applies only to FRP strengthening systems used as additional tensile reinforcement. It is not recommended

to use these systems as compressive reinforcement. While FRP materials can support compressive stresses, there are numerous issues surrounding the use of FRP for compression. Microbuckling of fibers can occur if any resin voids are present in the laminate; laminates themselves can buckle if not properly adhered or anchored to the substrate, and highly unreliable compressive strengths result from misaligning fibers in the field. This document does not address the construction, quality control, and maintenance issues that would be involved with the use of the material for this purpose, nor does it address the design concerns surrounding such applications. The use of the types of FRP strengthening systems described in this document to resist compressive forces is strongly discouraged.

This document does not specifically address masonry (concrete masonry units, brick, or clay tile) construction, including masonry walls. Research completed to date, however, has shown that FRP systems can be used to strengthen masonry walls, and many of the guidelines contained in this document may be applicable (Triantafillou 1998b; Ehsani et al. 1997; Marshall et al. 1999).

1.3—Applications and use

FRP systems can be used to rehabilitate or restore the strength of a deteriorated structural member, retrofit or strengthen a sound structural member to resist increased loads due to changes in use of the structure, or address design or construction errors. The licensed design professional should determine if an FRP system is a suitable strengthening technique before selecting the type of FRP system.

To assess the suitability of an FRP system for a particular application, the licensed design professional should perform a condition assessment of the existing structure that includes establishing its existing load-carrying capacity, identifying deficiencies and their causes, and determining the condition of the concrete substrate. The overall evaluation should include a thorough field inspection, a review of existing design or as-built documents, and a structural analysis in accordance with ACI 364.1R. Existing construction documents for the structure should be reviewed, including the design drawings, project specifications, as-built information, field test reports, past repair documentation, and maintenance history documentation. The licensed design professional should conduct a thorough field investigation of the existing structure in accordance with ACI 437R and other applicable ACI documents. As a minimum, the field investigation should determine the following:

- Existing dimensions of the structural members;
- Location, size, and cause of cracks and spalls;
- Location and extent of corrosion of reinforcing steel;
- Presence of active corrosion;
- Quantity and location of existing reinforcing steel;
- In-place compressive strength of concrete; and
- Soundness of the concrete, especially the concrete cover, in all areas where the FRP system is to be bonded to the concrete.

The tensile strength of the concrete on surfaces where the FRP system may be installed should be determined by conducting a pull-off adhesion test in accordance with ACI 503R. The in-place compressive strength of concrete should be determined using cores in accordance with ACI 318-05 requirements. The load-carrying capacity of the existing structure should be based on the information gathered in the field investigation, the review of design calculations and drawings, and as determined by analytical methods. Load tests or other methods can be incorporated into the overall evaluation process if deemed appropriate.

1.3.1 *Strengthening limits*—In general, to prevent sudden failure of the member in case the FRP system is damaged, strengthening limits are imposed such that the increase in the load-carrying capacity of a member strengthened with an FRP system be limited. The philosophy is that a loss of FRP reinforcement should not cause member failure under sustained service load. Specific guidance, including load combinations for assessing member integrity after loss of the FRP system, is provided in Part 4.

FRP systems used to increase the strength of an existing member should be designed in accordance with Part 4, which includes a comprehensive discussion of load limitations, rational load paths, effects of temperature and environment on FRP systems, loading considerations, and effects of reinforcing steel corrosion on FRP system integrity.

1.3.2 *Fire and life safety*—FRP-strengthened structures should comply with all applicable building and fire codes. Smoke generation and flame spread ratings should be satisfied for the assembly according to applicable building codes depending on the classification of the building. Smoke and flame spread ratings should be determined in accordance with ASTM E84. Coatings (Apicella and Imbrogno 1999) and insulation systems (Bisby et al. 2005a; Williams et al. 2006) can be used to limit smoke and flame spread.

Because of the degradation of most FRP materials at high temperature, the strength of externally bonded FRP systems is assumed to be lost completely in a fire, unless it can be demonstrated that the FRP temperature remains below its critical temperature (for example, FRP with a fire-protection system). The critical temperature of an FRP strengthening system should be taken as the lowest glass-transition temperature T_g of the components of the repair system, as defined in Section 1.3.3. The structural member without the FRP system should possess sufficient strength to resist all applicable service loads during a fire, as discussed in Section 9.2.1. The fire endurance of FRP-strengthened concrete members may be improved through the use of certain resins, coatings, insulation systems, or other methods of fire protection (Bisby et al. 2005b). Specific guidance, including load combinations and a rational approach to calculating structural fire endurance, is given in Part 4.

1.3.3 *Maximum service temperature*—The physical and mechanical properties of the resin components of FRP systems are influenced by temperature and degrade at temperatures close to and above their glass-transition temperature T_g (Bisby et al. 2005b). The T_g for FRP systems typically ranges from 140 to 180 °F (60 to 82 °C) for existing, commercially available FRP systems. The T_g for a particular FRP system can be obtained from the system manufacturer

or through testing according to ASTM D4065. The T_g is the midpoint of the temperature range over which the resin changes from a glassy state to a viscoelastic state that occurs over a temperature range of approximately 54 °F (30 °C). This change in state will degrade the mechanical and bond properties of the cured laminates. For a dry environment, it is generally recommended that the anticipated service temperature of an FRP system not exceed T_g – 27 °F (T_g – 15 °C) (Luo and Wong 2002; Xian and Karbhari 2007). Further research is needed to determine the critical service temperature for FRP systems in other environments. This recommendation is for elevated service temperatures such as those found in hot regions or certain industrial environments. The specific case of fire is described in more detail in Section 9.2.1. In cases where the FRP will be exposed to a moist environment, the wet glass-transition temperature T_{gw} should be used.

1.3.4 *Minimum concrete substrate strength*—FRP systems work on sound concrete, and should not be considered for applications on structural members containing corroded reinforcing steel or deteriorated concrete unless the substrate is repaired in accordance with Section 6.4. Concrete distress, deterioration, and corrosion of existing reinforcing steel should be evaluated and addressed before the application of the FRP system. Concrete deterioration concerns include, but are not limited to, alkali-silica reactions, delayed ettringite formation, carbonation, longitudinal cracking around corroded reinforcing steel, and laminar cracking at the location of the steel reinforcement.

The existing concrete substrate strength is an important parameter for bond-critical applications, including flexure or shear strengthening. It should possess the necessary strength to develop the design stresses of the FRP system through bond. The substrate, including all bond surfaces between repaired areas and the original concrete, should have sufficient direct tensile and shear strength to transfer force to the FRP system. The tensile strength should be at least 200 psi (1.4 MPa) as determined by using a pull-off type adhesion test per ICRI 03739. FRP systems should not be used when the concrete substrate has a compressive strength f_c' less than 2500 psi (17 MPa). Contact-critical applications, such as column wrapping for confinement that rely only on intimate contact between the FRP system and the concrete, are not governed by this minimum value. Design stresses in the FRP system are developed by deformation or dilation of the concrete section in contact-critical applications.

The application of FRP systems will not stop the ongoing corrosion of existing reinforcing steel (El-Maaddawy et al. 2006). If steel corrosion is evident or is degrading the concrete substrate, placement of FRP reinforcement is not recommended without arresting the ongoing corrosion and repairing any degradation to the substrate.

1.4—Use of FRP systems

This document refers to commercially available FRP systems consisting of fibers and resins combined in a specific manner and installed by a specific method. These systems have been developed through material characterization and structural testing. Untested combinations of fibers and resins could result in an unexpected range of properties as well as potential material incompatibilities. Any FRP system considered for use should have sufficient test data demonstrating adequate performance of the entire system in similar applications, including its method of installation.

The use of FRP systems developed through material characterization and structural testing, including well-documented proprietary systems, is recommended. The use of untested combinations of fibers and resins should be avoided. A comprehensive set of test standards for FRP systems has been developed by several organizations, including ASTM, ACI, ICRI, and ISIS Canada. Available standards from these organizations are outlined in Appendix B.

CHAPTER 2—NOTATION AND DEFINITIONS
2.1—Notation

A_c = cross-sectional area of concrete in compression member, in.^{2} (mm^2)

A_e = cross-sectional area of effectively confined concrete section, in.^{2} (mm^2)

A_f = area of FRP external reinforcement, in.^{2} (mm^2)

$A_{fanchor}$ = area of transverse FRP U-wrap for anchorage of flexural FRP reinforcement

A_{fv} = area of FRP shear reinforcement with spacing s, in.^{2} (mm^2)

A_g = gross area of concrete section, in.^{2} (mm^2)

A_p = area of prestressed reinforcement in tension zone, in.^{2} (mm^2)

A_s = area of nonprestressed steel reinforcement, in.^{2} (mm^2)

A_{si} = area of i-th layer of longitudinal steel reinforcement, in.^{2} (mm^2)

A_{st} = total area of longitudinal reinforcement, in.^{2} (mm^2)

a_b = smaller cross-sectional dimension for rectangular FRP bars, in. (mm)

b = width of compression face of member, in. (mm)

 = short side dimension of compression member of prismatic cross section, in. (mm)

b_b = larger cross-sectional dimension for rectangular FRP bars, in. (mm)

b_w = web width or diameter of circular section, in. (mm)

C_E = environmental reduction factor

c = distance from extreme compression fiber to the neutral axis, in. (mm)

D = diameter of compression member of circular cross section, in. (mm)

d = distance from extreme compression fiber to centroid of tension reinforcement, in. (mm)

d_f = effective depth of FRP flexural reinforcement, in. (mm)

d_{fv} = effective depth of FRP shear reinforcement, in. (mm)

 = depth of FRP shear reinforcement as shown in Fig. 11.2, in. (mm)

d_i = distance from centroid of i-th layer of longitudinal steel reinforcement to geometric centroid of cross section, in. (mm)

d_p = distance from extreme compression fiber to centroid of prestressed reinforcement, in. (mm)

= diagonal distance of prismatic cross section (diameter of equivalent circular column), in. (mm) = $\sqrt{b^2 + h^2}$

E_2 = slope of linear portion of stress-strain model for FRP-confined concrete, psi (MPa)

E_c = modulus of elasticity of concrete, psi (MPa)

E_f = tensile modulus of elasticity of FRP, psi (MPa)

E_{ps} = modulus of elasticity of prestressing steel, psi (MPa)

E_s = modulus of elasticity of steel, psi (MPa)

e_s = eccentricity of prestressing steel with respect to centroidal axis of member at support, in. (mm)

e_m = eccentricity of prestressing steel with respect to centroidal axis of member at midspan, in. (mm)

f_c = compressive stress in concrete, psi (MPa)

f_c' = specified compressive strength of concrete, psi (MPa)

$\overline{f_c'}$ = mean ultimate tensile strength of FRP based on a population of 20 or more tensile tests per ASTM D3039, psi (MPa)

$\sqrt{f_c'}$ = square root of specified compressive strength of concrete

f_{cc}' = compressive strength of confined concrete, psi (MPa)

f_{co}' = compressive strength of unconfined concrete; also equal to $0.85f_c'$, psi (MPa)

$f_{c,s}$ = compressive stress in concrete at service condition, psi (MPa)

f_f = stress level in FRP reinforcement, psi (MPa)

f_{fd} = design stress of externally bonded FRP reinforcement, psi (MPa)

f_{fe} = effective stress in the FRP; stress level attained at section failure, psi (MPa)

$f_{f,s}$ = stress level in FRP caused by a moment within elastic range of member, psi (MPa)

f_{fu} = design ultimate tensile strength of FRP, psi (MPa)

f_{fu}^* = ultimate tensile strength of the FRP material as reported by the manufacturer, psi (MPa)

f_l = maximum confining pressure due to FRP jacket, psi (MPa)

f_{ps} = stress in prestressed reinforcement at nominal strength, psi (MPa)

$f_{ps,s}$ = stress in prestressed reinforcement at service load, psi (MPa)

f_{pu} = specified tensile strength of prestressing tendons, psi (MPa)

f_s = stress in nonprestressed steel reinforcement, psi (MPa)

f_{si} = stress in the i-th layer of longitudinal steel reinforcement, psi (MPa)

$f_{s,s}$ = stress level in nonprestressed steel reinforcement at service loads, psi (MPa)

f_y = specified yield strength of nonprestressed steel reinforcement, psi (MPa)

h = overall thickness or height of a member, in. (mm)

= long side cross-sectional dimension of rectangular compression member, in. (mm)

h_f = member flange thickness, in. (mm)

I_{cr} = moment of inertia of cracked section transformed to concrete, in.^{4} (mm^4)

I_{tr} = moment of inertia of uncracked section transformed to concrete, in.^{4} (mm^4)

k = ratio of depth of neutral axis to reinforcement depth measured from extreme compression fiber

k_1 = modification factor applied to κ_v to account for concrete strength

k_2 = modification factor applied to κ_v to account for wrapping scheme

k_f = stiffness per unit width per ply of the FRP reinforcement, lb/in. (N/mm); $k_f = E_f t_f$

L_e = active bond length of FRP laminate, in. (mm)

l_{db} = development length of near-surface-mounted (NSM) FRP bar, in. (mm)

l_{df} = development length of FRP system, in. (mm)

M_{cr} = cracking moment, in.-lb (N-mm)

M_n = nominal flexural strength, in.-lb (N-mm)

M_{nf} = contribution of FRP reinforcement to nominal flexural strength, lb-in. (N-mm)

M_{np} = contribution of prestressing reinforcement to nominal flexural strength, lb-in. (N-mm)

M_{ns} = contribution of steel reinforcement to nominal flexural strength, lb-in. (N-mm)

M_s = service moment at section, in.-lb (N-mm)

M_{snet} = service moment at section beyond decompression, in.-lb (N-mm)

M_u = factored moment at a section, in.-lb (N-mm)

n = number of plies of FRP reinforcement

n_f = modular ratio of elasticity between FRP and concrete = E_f/E_c

n_s = modular ratio of elasticity between steel and concrete = E_s/E_c

P_e = effective force in prestressing reinforcement (after allowance for all prestress losses), lb (N)

P_n = nominal axial compressive strength of a concrete section, lb (N)

$\overline{p_{fu}}$ = mean tensile strength per unit width per ply of FRP reinforcement, lb/in. (N/mm)

p_{fu}^* = ultimate tensile strength per unit width per ply of FRP reinforcement, lb/in. (N/mm); $p_{fu}^* = f_{fu}^* t_f$

R_n = nominal strength of a member

$R_{n\phi}$ = nominal strength of a member subjected to elevated temperatures associated with a fire

r = radius of gyration of a section, in. (mm)

r_c = radius of edges of a prismatic cross section confined with FRP, in. (mm)

S_{DL} = dead load effects

S_{LL} = live load effects

T_g = glass-transition temperature, °F (°C)

T_{gw} = wet glass-transition temperature, °F (°C)

T_{ps} = tensile force in prestressing steel, lb (N)

t_f = nominal thickness of one ply of FRP reinforcement, in. (mm)

V_c = nominal shear strength provided by concrete with steel flexural reinforcement, lb (N)

V_f = nominal shear strength provided by FRP stirrups, lb (N)

V_n = nominal shear strength, lb (N)

V_s = nominal shear strength provided by steel stirrups, lb (N)

w_f = width of FRP reinforcing plies, in. (mm)

y_b = distance from centroidal axis of gross section, neglecting reinforcement, to extreme bottom fiber, in./in. (mm/mm)

y_t = vertical coordinate within compression region measured from neutral axis position. It corresponds to transition strain ε_t', in. (mm)

α_1 = multiplier on f_c' to determine intensity of an equivalent rectangular stress distribution for concrete

α_L = longitudinal coefficient of thermal expansion, in./in./°F (mm/mm/°C)

α_T = transverse coefficient of thermal expansion, in./in./°F (mm/mm/°C)

β_1 = ratio of depth of equivalent rectangular stress block to depth of the neutral axis

ε_b = strain level in concrete substrate developed by a given bending moment (tension is positive), in./in. (mm/mm)

ε_{bi} = strain level in concrete substrate at time of FRP installation (tension is positive), in./in. (mm/mm)

ε_c = strain level in concrete, in./in. (mm/mm)

ε_c' = maximum strain of unconfined concrete corresponding to f_c', in./in. (mm/mm); may be taken as 0.002

ε_{ccu} = ultimate axial compressive strain of confined concrete corresponding to $0.85f_{cc}'$ in a lightly confined member (member confined to restore its concrete design compressive strength), or ultimate axial compressive strain of confined concrete corresponding to failure in a heavily confined member (Fig. 12.1)

$\varepsilon_{c,s}$ = strain level in concrete at service, in./in. (mm/mm)

ε_{ct} = concrete tensile strain at level of tensile force resultant in post-tensioned flexural members, in./in. (mm/mm)

ε_{cu} = ultimate axial strain of unconfined concrete corresponding to $0.85f_{co}'$ or maximum usable strain of unconfined concrete, in./in. (mm/mm), which can occur at $0.85f_c'$ or 0.003, depending on the obtained stress-strain curve

ε_f = strain level in the FRP reinforcement, in./in. (mm/ mm)

ε_{fd} = debonding strain of externally bonded FRP reinforcement, in./in. (mm/mm)

ε_{fe} = effective strain level in FRP reinforcement attained at failure, in./in. (mm/mm)

ε_{fu} = design rupture strain of FRP reinforcement, in./in. (mm/mm)

$\overline{\varepsilon_{fu}}$ = mean rupture strain of FRP reinforcement based on a population of 20 or more tensile tests per ASTM D3039, in./in. (mm/mm)

ε_{fu}^* = ultimate rupture strain of FRP reinforcement, in./in. (mm/mm)

ε_{pe} = effective strain in prestressing steel after losses, in./in. (mm/mm)

ε_{pi} = initial strain level in prestressed steel reinforcement, in./in. (mm/mm)

ε_{pnet} = net strain in flexural prestressing steel at limit state after prestress force is discounted (excluding strains due to effective prestress force after losses), in./in. (mm/mm)

$\varepsilon_{pnet,s}$ = net strain in prestressing steel beyond decompression at service, in./in. (mm/mm)

ε_{ps} = strain in prestressed reinforcement at nominal strength, in./in. (mm/mm)

$\varepsilon_{ps,s}$ = strain in prestressing steel at service load, in./in. (mm/mm)

ε_s = strain level in nonprestessed steel reinforcement, in./in. (mm/mm)

ε_{sy} = strain corresponding to yield strength of nonprestressed steel reinforcement, in./in. (mm/mm)

ε_t = net tensile strain in extreme tension steel at nominal strength, in./in. (mm/mm)

ε_t' = transition strain in stress-strain curve of FRP-confined concrete, in./in. (mm/mm)

ϕ = strength reduction factor

κ_a = efficiency factor for FRP reinforcement in determination of f_{cc}' (based on geometry of cross section)

κ_b = efficiency factor for FRP reinforcement in determination of ε_{ccu} (based on geometry of cross section)

κ_v = bond-dependent coefficient for shear

κ_ε = efficiency factor equal to 0.55 for FRP strain to account for the difference between observed rupture strain in confinement and rupture strain determined from tensile tests

ρ_f = FRP reinforcement ratio

ρ_g = ratio of area of longitudinal steel reinforcement to cross-sectional area of a compression member (A_s/bh)

ρ_s = ratio of nonprestressed reinforcement

σ = standard deviation

τ_b = average bond strength for NSM FRP bars, psi (MPa)

ψ_f = FRP strength reduction factor

 = 0.85 for flexure (calibrated based on design material properties)

 = 0.85 for shear (based on reliability analysis) for three-sided FRP U-wrap or two-sided strengthening schemes

 = 0.95 for shear fully wrapped sections

2.2—Definitions and acronyms

The following definitions clarify terms pertaining to FRP that are not commonly used in reinforced concrete practice. These definitions are specific to this document, and are not applicable to other ACI documents.

AFRP—aramid fiber-reinforced polymer.

batch—quantity of material mixed at one time or in one continuous process.

binder—chemical treatment applied to the random arrangement of fibers to give integrity to mats, roving, and fabric. Specific binders are used to promote chemical compatibility with the various laminating resins used.

carbon fiber-reinforced polymer (CFRP)—a composite material comprising a polymer matrix reinforced with carbon fiber cloth, mat, or strands.

catalyst—a substance that accelerates a chemical reaction and enables it to proceed under conditions more mild than otherwise required and that is not, itself, permanently changed by the reaction. See **initiator** or **hardener**.

coating, intumescent—a covering that blisters to form a heat shield when exposed to fire.

composite—engineering materials (for example, concrete and fiber-reinforced polymer) made from two or more constituent materials that remain distinct, but combine to form materials with properties not possessed by any of the constituent materials individually; the constituent materials are generally characterized as matrix and reinforcement or matrix and aggregate.

contact-critical application—strengthening or repair system that relies on load transfer from the substrate to the system material achieved through bearing or horizontal shear transfer at the interface.

content, fiber—the amount of fiber present in a composite, usually expressed as a percentage volume fraction or weight fraction of the composite.

content, resin—the amount of resin in a fiber-reinforced polymer composite laminate, expressed as either a percentage of total mass or total volume.

creep-rupture—breakage of a material under sustained loading at stresses less than the tensile strength.

cross-linking—forming covalent bonds linking one polymer molecule to another (also **polymerization**). Note: an increased number of cross-links per polymer molecule increases strength and modulus at the expense of ductility.

cure, A-stage—early period after mixing at which components of a thermosetting resin remain soluble and fusible.

cure, B-stage—an intermediate period at which the components of a thermosetting resin have reacted sufficiently to produce a material that can be handled and processed, yet not sufficiently to produce specified final properties.

cure, full—period at which components of a thermosetting resin have reacted sufficiently for the resin to produce specified final properties (antonym: undercure).

cure, thermosetting resin—inducing a reaction leading to cross-linking in a thermosetting resin using chemical initiators, catalysts, radiation, heat, or pressure.

curing agent—a catalytic or reactive agent that induces cross-linking in a thermosetting resin (also **hardener** or **initiator**).

debonding—failure of cohesive or adhesive bond at the interface between a substrate and a strengthening or repair system.

delamination—a planar separation in a material that is roughly parallel to the surface of the material.

durability—the ability of a material to resist weathering action, chemical attack, abrasion, and other conditions of service.

e-glass—a family of glass with a calcium alumina borosilicate composition and a maximum alkali content of 2.0%. A general-purpose fiber that is used in reinforced polymers.

epoxy—a thermosetting polymer that is the reaction product of epoxy resin and an amino hardener (see also **resin, epoxy**).

fabric—a two-dimensional network of woven, nonwoven, knitted, or stitched fibers.

fiber—a slender and greatly elongated solid material, generally with a length at least 100 times its diameter, that has properties making it desirable for use as reinforcement.

fiber, aramid—fiber in which chains of aromatic polyamide molecules are oriented along the fiber axis to exploit the strength of the chemical bond.

fiber, carbon—fiber produced by heating organic precursor materials containing a substantial amount of carbon, such as rayon, polyacrylonitrile (PAN), or pitch in an inert environment and at temperatures of 2700 °F (1500 °C) or greater.

fiber, glass—filament drawn from an inorganic fusion typically comprising silica-based material that has cooled without crystallizing. Types of glass fibers include alkali resistant (AR-glass), general purpose (E-glass), high strength (S-glass), and boron free (ECR-glass).

fiber content—see **content, fiber**.

fiber fly—short filaments that break off dry fiber tows or yarns during handling and become airborne; usually classified as a nuisance dust.

fiber-reinforced polymer (FRP)—a general term for a composite material comprising a polymer matrix reinforced with fibers in the form of fabric, mat, strands, or any other fiber form. See **composite**.

fiber volume fraction—the ratio of the volume of fibers to the volume of the composite containing the fibers.

fiber weight fraction—the ratio of the weight of fibers to the weight of the composite containing the fibers.

filament—see **fiber**.

filler—a finely divided, relatively inert material, such as pulverized limestone, silica, or colloidal substances, added to portland cement, paint, resin, or other materials to reduce shrinkage, improve workability, reduce cost, or reduce density.

fire retardant—additive or coating used to reduce the tendency of a resin to burn; these can be added to the resin or coated on the surface of the FRP.

flow—movement of uncured resin under gravity loads or differential pressure.

FRP—fiber-reinforced polymer.

glass fiber-reinforced polymer (GFRP)—a composite material comprising a polymer matrix reinforced with glass fiber cloth, mat, or strands.

grid, FRP—a rigid array of interconnected FRP elements that can be used to reinforce concrete.

hardener—in a two-component adhesive or coating, the chemical component that causes the resin component to cure.

impregnate—to saturate fibers with resin or binder.

initiator—a chemical (most commonly organic peroxides) used to start the curing process for unsaturated polyester and vinyl ester resins. See also **catalyst**.

lamina—a single layer of fabric or mat reinforcing bound together in a cured resin matrix.

laminate—multiple plies or lamina molded together.

layup—the process of placing reinforcing material and resin system in position for molding.

layup, wet—the process of placing the reinforcing material in the mold or its final position and applying the resin as a liquid.

length, development—the bonded length required to achieve the design strength of a reinforcement at a critical section.

load, sustained—a constant load that in structures is due to dead load and long-term live load.

mat—a thin layer of randomly oriented chopped filaments, short fibers (with or without a carrier fabric), or long random filaments loosely held together with a binder and used as reinforcement for a FRP composite material.

matrix—the resin or binders that hold the fibers in FRP together, transfer load to the fibers, and protect them against environmental attack and damage due to handling.

modulus of elasticity—the ratio of normal stress to corresponding strain for tensile or compressive stress below the proportional limit of the material; also referred to as elastic modulus, Young's modulus, and Young's modulus of elasticity; denoted by the symbol E.

monomer—an organic molecule of relatively low molecular weight that creates a solid polymer by reacting with itself or other compounds of low molecular weight.

NSM—near-surface-mounted.

pitch—viscid substance obtained as a residue of petroleum or coal tar and used as a precursor in the manufacture of some carbon fibers.

ply—see **lamina**.

polyacrylonitrile (**PAN**)—a polymer-based material that is spun into a fiber form and used as a precursor in the manufacturer of some carbon fibers.

polyester—one of a large group of synthetic resins, mainly produced by reaction of dibasic acids with dihydroxy alcohols; commonly prepared for application by mixing with a vinyl-group monomer and free-radical catalysts at ambient temperatures and used as binders for resin mortars and concretes, fiber laminates (mainly glass), adhesives, and the like. Commonly referred to as "unsaturated polyester."

polymer—the product of polymerization; more commonly a rubber or resin consisting of large molecules formed by polymerization.

polymerization—the reaction in which two or more molecules of the same substance combine to form a compound containing the same elements and in the same proportions but of higher molecular weight.

polyurethane—reaction product of an isocyanate with any of a wide variety of other compounds containing an active hydrogen group; used to formulate tough, abrasion-resistant coatings.

postcuring—application of elevated temperature to material containing thermosetting resin to increase the level of polymer cross-linking and enhance the final material properties. See **cure, thermosetting resin**.

pot life—time interval, after mixing of thermosetting resin and initiators, during which the mixture can be applied without degrading the final performance of the resulting polymer composite beyond specified limits.

prepreg—a sheet of fabric or mat containing resin or binder usually advanced to the B-stage and ready for final forming and cure.

pultrusion—a continuous process for manufacturing fiber-reinforced polymer composites in which resin is impregnated on fiber reinforcements (roving or mats) and are pulled through a shaping and curing die, typically to produce composites with uniform cross sections.

resin—generally a thermosetting polymer used as the matrix and binder in FRP composites.

resin content—see **content, resin**.

resin, epoxy—a class of organic chemical bonding systems used in the preparation of special coatings or adhesives for concrete or as binders in epoxy-resin mortars, concretes, and FRP composites.

resin, phenolic—a thermosetting resin produced by the condensation reaction of an aromatic alcohol with an aldehyde (usually a phenol with formaldehyde).

resin, thermoset—a material that hardens by an irreversible three-dimensional cross-linking of monomers, typically when subjected to heat or light energy and subsequently will not soften.

roving—a parallel bundle of continuous yarns, tows, or fibers with little or no twist.

shear, interlaminar—force tending to produce a relative displacement along the plane of the interface between two laminae.

shelf life—the length of time packaged materials can be stored under specified conditions and remain usable.

sizing—surface treatment applied to filaments to impart desired processing, durability, and bond attributes.

substrate—any material on the surface of which another material is applied.

temperature, glass-transition—the midpoint of the temperature range over which an amorphous material (such as glass or a high polymer) changes from (or to) a brittle, vitreous state to (or from) a plastic state.

thermoset—resin that is formed by cross-linking polymer chains. Note: A thermoset cannot be melted and recycled because the polymer chains form a three-dimensional network.

tow—an untwisted bundle of continuous filaments.

vinylester resin—a thermosetting reaction product of epoxy resin with a polymerizable unsaturated acid (usually methacrylic acid) that is then diluted with a reactive monomer (usually styrene).

volatile organic compound (**VOC**)—an organic compound that vaporizes under normal atmospheric conditions and is defined by the U.S. Environmental Protection agency

as any compound of carbon, excluding carbon monoxide, carbon dioxide, carbonic acid, metallic carbides or carbonates, and ammonium carbonate, which participates in atmospheric photochemical reactions.

volume fraction—see **fiber volume fraction**.

wet layup—see **layup, wet**.

wet-out—the process of coating or impregnating roving, yarn, or fabric to fill the voids between the strands and filaments with resin; it is also the condition at which this state is achieved.

witness panel—a small mockup manufactured under conditions representative of field application, to confirm that prescribed procedures and materials will yield specified mechanical and physical properties.

yarn—a twisted bundle of continuous filaments.

CHAPTER 3—BACKGROUND INFORMATION

Externally bonded FRP systems have been used to strengthen and retrofit existing concrete structures around the world since the mid-1980s. The number of projects using FRP systems worldwide has increased dramatically, from a few 20 years ago to several thousand today. Structural elements strengthened with externally bonded FRP systems include beams, slabs, columns, walls, joints/connections, chimneys and smokestacks, vaults, domes, tunnels, silos, pipes, and trusses. Externally bonded FRP systems have also been used to strengthen masonry, timber, steel, and cast-iron structures. The idea of strengthening concrete structures with externally bonded reinforcement is not new. Externally bonded FRP systems were developed as alternatives to traditional external reinforcing techniques such as steel plate bonding and steel or concrete column jacketing. The initial development of externally bonded FRP systems for the retrofit of concrete structures occurred in the 1980s in both Europe and Japan.

3.1—Historical development

In Europe, FRP systems were developed as alternates to steel plate bonding. Bonding steel plates to the tension zones of concrete members with adhesive resins were shown to be viable techniques for increasing their flexural strengths (Fleming and King 1967). This technique has been used to strengthen many bridges and buildings around the world. Because steel plates can corrode, leading to a deterioration of the bond between the steel and concrete, and because they are difficult to install, requiring the use of heavy equipment, researchers have looked to FRP materials as an alternative to steel. Experimental work using FRP materials for retrofitting concrete structures was reported as early as 1978 in Germany (Wolf and Miessler 1989). Research in Switzerland led to the first applications of externally bonded FRP systems to reinforced concrete bridges for flexural strengthening (Meier 1987; Rostasy 1987).

FRP systems were first applied to reinforced concrete columns for providing additional confinement in Japan in the 1980s (Fardis and Khalili 1981; Katsumata et al. 1987). A sudden increase in the use of FRPs in Japan was observed after the 1995 Hyogoken-Nanbu earthquake (Nanni 1995).

Researchers in the United States have had a long and continuous interest in fiber-based reinforcement for concrete structures since the 1930s. Development and research into the use of these materials for retrofitting concrete structures, however, started in the 1980s through the initiatives of the National Science Foundation (NSF) and the Federal Highway Administration (FHWA). The research activities led to the construction of many field projects that encompassed a wide variety of environmental conditions. Previous research and field applications for FRP rehabilitation and strengthening are described in ACI 440R and conference proceedings (Neale 2000; Dolan et al. 1999; Sheheta et al. 1999; Saadatmanesh and Ehsani 1998; Benmokrane and Rahman 1998; Neale and Labossière 1997; Hassan and Rizkalla 2002; Shield et al. 2005).

The development of codes and standards for externally bonded FRP systems is ongoing in Europe, Japan, Canada, and the United States. Within the last 10 years, the Japan Society of Civil Engineers (JSCE), the Japan Concrete Institute (JCI), and the Railway Technical Research Institute (RTRI) published several documents related to the use of FRP materials in concrete structures.

In Europe, Task Group 9.3 of the International Federation for Structural Concrete (FIB) published a bulletin on design guidelines for externally bonded FRP reinforcement for reinforced concrete structures (International Federation for Structural Concrete 2001).

The Canadian Standards Association (CSA) and ISIS have been active in developing guidelines for FRP systems. Section 16, "Fiber Reinforced Structures," of the Canadian Highway Bridge Design Code was completed in 2006 (CAN/CSA-S6-06), and CSA approved CSA S806-00.

In the United States, criteria for evaluating FRP systems are available to the construction industry (ICBO AC125; CALTRANS Division of Structures 1996; Hawkins et al. 1998).

3.2—Commercially available externally bonded FRP systems

FRP systems come in a variety of forms, including wet layup systems and precured systems. FRP system forms can be categorized based on how they are delivered to the site and installed. The FRP system and its form should be selected based on the acceptable transfer of structural loads and the ease and simplicity of application. Common FRP system forms suitable for the strengthening of structural members are listed in Sections 3.2.1 through 3.2.4.

3.2.1 *Wet layup systems*—Wet layup FRP systems consist of dry unidirectional or multidirectional fiber sheets or fabrics impregnated with a saturating resin on site. The saturating resin, along with the compatible primer and putty, bonds the FRP sheets to the concrete surface. Wet layup systems are saturated in place and cured in place and, in this sense, are analogous to cast-in-place concrete. Three common types of wet layup systems are listed as follows:

1. Dry unidirectional fiber sheets where the fibers run predominantly in one planar direction;

2. Dry multidirectional fiber sheets or fabrics where the fibers are oriented in at least two planar directions; and

3. Dry fiber tows that are wound or otherwise mechanically applied to the concrete surface. The dry fiber tows are impregnated with resin on site during the winding operation.

3.2.2 *Prepreg systems*—Prepreg FRP systems consist of partially cured unidirectional or multidirectional fiber sheets or fabrics that are preimpregnated with a saturating resin in the manufacturer's facility. Prepreg systems are bonded to the concrete surface with or without an additional resin application, depending on specific system requirements. Prepreg systems are saturated off-site and, like wet layup systems, cured in place. Prepreg systems usually require additional heating for curing. Prepreg system manufacturers should be consulted for storage and shelf-life recommendations and curing procedures. Three common types of prepreg FRP systems are:

1. Preimpregnated unidirectional fiber sheets where the fibers run predominantly in one planar direction;

2. Preimpregnated multidirectional fiber sheets or fabrics where the fibers are oriented in at least two planar directions; and

3. Preimpregnated fiber tows that are wound or otherwise mechanically applied to the concrete surface.

3.2.3 *Precured systems*—Precured FRP systems consist of a wide variety of composite shapes manufactured off site. Typically, an adhesive, along with the primer and putty, is used to bond the precured shapes to the concrete surface. The system manufacturer should be consulted for recommended installation procedures. Precured systems are analogous to precast concrete. Three common types of precured systems are:

1. Precured unidirectional laminate sheets, typically delivered to the site in the form of large flat stock or as thin ribbon strips coiled on a roll;

2. Precured multidirectional grids, typically delivered to the site coiled on a roll; and

3. Precured shells, typically delivered to the site in the form of shell segments cut longitudinally so they can be opened and fitted around columns or other members; multiple shell layers are bonded to the concrete and to each other to provide seismic confinement.

3.2.4 *Near-surface-mounted (NSM) systems*—Surface-embedded (NSM) FRP systems consist of circular or rectangular bars or plates installed and bonded into grooves made on the concrete surface. A suitable adhesive is used to bond the FRP bar into the groove, and is cured in-place. The NSM system manufacturer should be consulted for recommended adhesives. Two common FRP bar types used for NSM applications are:

1. Round bars usually manufactured using pultrusion processes, typically delivered to the site in the form of single bars or in a roll depending on bar diameter; and

2. Rectangular bars and plates usually manufactured using pultrusion processes, typically delivered to the site in a roll.

PART 2—MATERIALS
CHAPTER 4—CONSTITUENT
MATERIALS AND PROPERTIES

The physical and mechanical properties of FRP materials presented in this chapter explain the behavior and properties affecting their use in concrete structures. The effects of factors such as loading history and duration, temperature, and moisture on the properties of FRP are discussed.

FRP strengthening systems come in a variety of forms (wet layup, prepreg, and precured). Factors such as fiber volume, type of fiber, type of resin, fiber orientation, dimensional effects, and quality control during manufacturing all play a role in establishing the characteristics of an FRP material. The material characteristics described in this chapter are generic and do not apply to all commercially available products. Standard test methods are being developed by several organizations, including ASTM, ACI, and CSA, to characterize certain FRP products. In the interim, however, the licensed design professional is encouraged to consult with the FRP system manufacturer to obtain the relevant characteristics for a specific product and the applicability of those characteristics.

4.1—Constituent materials

The constituent materials used in commercially available FRP repair systems, including all resins, primers, putties, saturants, adhesives, and fibers, have been developed for the strengthening of structural concrete members based on materials and structural testing.

4.1.1 *Resins*—A wide range of polymeric resins, including primers, putty fillers, saturants, and adhesives, are used with FRP systems. Commonly used resin types, including epoxy, vinyl esters, and polyesters, have been formulated for use in a wide range of environmental conditions. FRP system manufacturers use resins that have:

- Compatibility with and adhesion to the concrete substrate;
- Compatibility with and adhesion to the FRP composite system;
- Resistance to environmental effects, including but not limited to moisture, salt water, temperature extremes, and chemicals normally associated with exposed concrete;
- Filling ability;
- Workability;
- Pot life consistent with the application; and
- Compatibility with and adhesion to the reinforcing fiber; and
- Development of appropriate mechanical properties for the FRP composite.

4.1.1.1 *Primer*—Primer is used to penetrate the surface of the concrete, providing an improved adhesive bond for the saturating resin or adhesive.

4.1.1.2 *Putty fillers*—Putty is used to fill small surface voids in the substrate, such as bug holes, and to provide a smooth surface to which the FRP system can bond. Filled surface voids also prevent bubbles from forming during curing of the saturating resin.

4.1.1.3 *Saturating resin*—Saturating resin is used to impregnate the reinforcing fibers, fix them in place, and provide a shear load path to effectively transfer load between fibers. The saturating resin also serves as the adhesive for wet layup systems, providing a shear load path between the previously primed concrete substrate and the FRP system

Table 4.1—Typical densities of FRP materials, lb/ft³ (g/cm³)

Steel	GFRP	CFRP	AFRP
490 (7.9)	75 to 130 (1.2 to 2.1)	90 to 100 (1.5 to 1.6)	75 to 90 (1.2 to 1.5)

Table 4.2—Typical coefficients of thermal expansion for FRP materials[*]

Direction	Coefficient of thermal expansion, $\times 10^{-6}$/°F ($\times 10^{-6}$/°C)		
	GFRP	CFRP	AFRP
Longitudinal, α_L	3.3 to 5.6 (6 to 10)	–0.6 to 0 (–1 to 0)	–3.3 to –1.1 (–6 to –2)
Longitudinal, α_T	10.4 to 12.6 (19 to 23)	12 to 27 (22 to 50)	33 to 44 (60 to 80)

[*]Typical values for fiber-volume fractions ranging from 0.5 to 0.7.

4.1.1.4 *Adhesives—*Adhesives are used to bond precured FRP laminate and NSM systems to the concrete substrate. The adhesive provides a shear load path between the concrete substrate and the FRP reinforcing system. Adhesives are also used to bond together multiple layers of precured FRP laminates.

4.1.2 *Fibers—*Continuous glass, aramid, and carbon fibers are common reinforcements used with FRP systems. The fibers give the FRP system its strength and stiffness. Typical ranges of the tensile properties of fibers are given in Appendix A. A more detailed description of fibers is given in ACI 440R.

4.1.3 *Protective coatings—*The protective coating protects the bonded FRP reinforcement from potentially damaging environmental and mechanical effects. Coatings are typically applied to the exterior surface of the cured FRP system after the adhesive or saturating resin has cured. The protection systems are available in a variety of forms. These include:
- Polymer coatings that are generally epoxy or polyurethanes;
- Acrylic coatings that can be either straight acrylic systems or acrylic cement-based systems. The acrylic systems can also come in different textures;
- Cementitious systems that may require roughening of the FRP surface (such as broadcasting sand into wet resin) and can be installed in the same manner as they would be installed on a concrete surface; and
- Intumescent coatings that are polymer-based coatings used to control flame spread and smoke generation per code requirements.

There are several reasons why protection systems are used to protect FRP systems that have been installed on concrete surfaces. These include:
- *Ultraviolet light protection—*The epoxy used as part of the FRP strengthening system will be affected over time by exposure to ultraviolet light. There are a number of available methods used to protect the system from ultraviolet light. These include: acrylic coatings, cementitious surfacing, aliphatic polyurethane coatings, and others. Certain types of vinylester resins have higher ultraviolet light durability than epoxy resins;
- *Fire protection—*Fire protection systems are discussed in Sections 1.3.2 and 9.2.1;

- *Vandalism—*Protective systems that are to resist vandalism should be hard and durable. There are different levels of vandalism protection from polyurethane coatings that will resist cutting and scraping to cementitious overlays that provide much more protection;
- *Impact, abrasion, and wear—*Protection systems for impact, abrasion, and wear are similar to those used for vandalism protection; however, abrasion and wear are different than vandalism in that they result from continuous exposure rather than a one-time event, and their protection systems are usually chosen for their hardness and durability;
- *Aesthetics—*Protective topcoats may be used to conceal the FRP system. These may be acrylic latex coatings that are gray in color to match bare concrete, or they may be various other colors and textures to match the existing structure;
- *Chemical resistance—*Exposure to harsh chemicals, such as strong acids, may damage the FRP system. In such environments, coatings with better chemical resistance, such as urethanes and novolac epoxies, may be used; and
- *Submersion in potable water—*In applications where the FRP system is to be submerged in potable water, the FRP system may leach compounds into the water supply. Protective coatings that do not leach harmful chemicals into the water may be used as a barrier between the FRP system and the potable water supply.

4.2—Physical properties

4.2.1 *Density—*FRP materials have densities ranging from 75 to 130 lb/ft³ (1.2 to 2.1 g/cm³), which is four to six times lower than that of steel (Table 4.1). The reduced density leads to lower transportation costs, reduces added dead load on the structure, and can ease handling of the materials on the project site.

4.2.2 *Coefficient of thermal expansion—*The coefficients of thermal expansion of unidirectional FRP materials differ in the longitudinal and transverse directions, depending on the types of fiber, resin, and volume fraction of fiber. Table 4.2 lists the longitudinal and transverse coefficients of thermal expansion for typical unidirectional FRP materials. Note that a negative coefficient of thermal expansion indicates that the material contracts with increased temperature and expands with decreased temperature. For reference, concrete has a coefficient of thermal expansion that varies from 4×10^{-6} to 6×10^{-6}/°F (7×10^{-6} to 11×10^{-6}/°C), and is usually assumed to be isotropic (Mindess and Young 1981). Steel has an isotropic coefficient of thermal expansion of 6.5×10^{-6}/°F (11.7×10^{-6}/°C). See Section 9.3.1 for design considerations regarding thermal expansion.

4.2.3 *Effects of high temperatures—*Beyond the T_g, the elastic modulus of a polymer is significantly reduced due to changes in its molecular structure. The value of T_g depends on the type of resin but is normally in the region of 140 to 180 °F (60 to 82 °C). In an FRP composite material, the fibers, which exhibit better thermal properties than the resin, can continue to support some load in the longitudinal direction

until the temperature threshold of the fibers is reached. This can occur at temperatures exceeding 1800 °F (1000 °C) for carbon fibers, and 350 °F (175 °C) for aramid fibers. Glass fibers are capable of resisting temperatures in excess of 530 °F (275 °C). Due to a reduction in force transfer between fibers through bond to the resin, however, the tensile properties of the overall composite are reduced. Test results have indicated that temperatures of 480 °F (250 °C), much higher than the resin T_g, will reduce the tensile strength of GFRP and CFRP materials in excess of 20% (Kumahara et al. 1993). Other properties affected by the shear transfer through the resin, such as bending strength, are reduced significantly at lower temperatures (Wang and Evans 1995).

For bond-critical applications of FRP systems, the properties of the polymer at the fiber-concrete interface are essential in maintaining the bond between FRP and concrete. At a temperature close to its T_g, however, the mechanical properties of the polymer are significantly reduced, and the polymer begins to lose its ability to transfer stresses from the concrete to the fibers.

4.3—Mechanical properties

4.3.1 *Tensile behavior*—When loaded in direct tension, unidirectional FRP materials do not exhibit any plastic behavior (yielding) before rupture. The tensile behavior of FRP materials consisting of one type of fiber material is characterized by a linear elastic stress-strain relationship until failure, which is sudden and brittle.

The tensile strength and stiffness of an FRP material is dependent on several factors. Because the fibers in an FRP material are the main load-carrying constituents, the type of fiber, the orientation of fibers, the quantity of fibers, and method and conditions in which the composite is produced affect the tensile properties of the FRP material. Due to the primary role of the fibers and methods of application, the properties of an FRP repair system are sometimes reported based on the net-fiber area. In other instances, such as in precured laminates, the reported properties are based on the gross-laminate area.

The gross-laminate area of an FRP system is calculated using the total cross-sectional area of the cured FRP system, including all fibers and resin. The gross-laminate area is typically used for reporting precured laminate properties where the cured thickness is constant and the relative proportion of fiber and resin is controlled.

The net-fiber area of an FRP system is calculated using the known area of fiber, neglecting the total width and thickness of the cured system; thus, resin is excluded. The net-fiber area is typically used for reporting properties of wet layup systems that use manufactured fiber sheets and field-installed resins. The wet layup installation process leads to controlled fiber content and variable resin content.

System properties reported using the gross-laminate area have higher relative thickness dimensions and lower relative strength and modulus values, whereas system properties reported using the net-fiber area have lower relative thickness dimensions and higher relative strength and modulus values. Regardless of the basis for the reported values, the load-carrying strength ($f_{fu}A_f$) and axial stiffness ($A_f E_f$) of the composite remain constant. (The calculation of FRP system properties using both gross-laminate and net-fiber property methods is illustrated in Part 5.) Properties reported based on the net-fiber area are not the properties of the bare fibers. When tested as a part of a cured composite, the measured tensile strength and ultimate rupture strain of the net-fiber are typically lower than those measured based on a dry fiber test. The properties of an FRP system should be characterized as a composite, recognizing not just the material properties of the individual fibers, but also the efficiency of the fiber-resin system, the fabric architecture, and the method used to create the composite. The mechanical properties of all FRP systems, regardless of form, should be based on the testing of laminate samples with known fiber content.

The tensile properties of some commercially available FRP strengthening systems are given in Appendix A. The tensile properties of a particular FRP system, however, can be obtained from the FRP system manufacturer or using the test appropriate method as described in ACI 440.3R and ASTM D3039 and D7205. Manufacturers should report an ultimate tensile strength, which is defined as the mean tensile strength of a sample of test specimens minus three times the standard deviation ($f_{fu}^* = \overline{f_{fu}} - 3\sigma$) and, similarly, report an ultimate rupture strain ($\varepsilon_{fu}^* = \overline{\varepsilon_{fu}} - 3\sigma$). This approach provides a 99.87% probability that the actual ultimate tensile properties will exceed these statistically-based design values for a standard sample distribution (Mutsuyoshi et al. 1990). Young's modulus should be calculated as the chord modulus between 0.003 and 0.006 strain, in accordance with ASTM D3039. A minimum number of 20 replicate test specimens should be used to determine the ultimate tensile properties. The manufacturer should provide a description of the method used to obtain the reported tensile properties, including the number of tests, mean values, and standard deviations.

4.3.2 *Compressive behavior*—Externally bonded FRP systems should not be used as compression reinforcement due to insufficient testing validating its use in this type of application. While it is not recommended to rely on externally bonded FRP systems to resist compressive stresses, the following section is presented to fully characterize the behavior of FRP materials.

Coupon tests on FRP laminates used for repair on concrete have shown that the compressive strength of FRP is lower than the tensile strength (Wu 1990). The mode of failure for FRP laminates subjected to longitudinal compression can include transverse tensile failure, fiber microbuckling, or shear failure. The mode of failure depends on the type of fiber, the fiber-volume fraction, and the type of resin. Compressive strengths of 55, 78, and 20% of the tensile strength have been reported for GFRP, CFRP, and AFRP, respectively (Wu 1990). In general, compressive strengths are higher for materials with higher tensile strengths, except in the case of AFRP, where the fibers exhibit nonlinear behavior in compression at a relatively low level of stress.

The compressive modulus of elasticity is usually smaller than the tensile modulus of elasticity of FRP materials. Test reports on samples containing a 55 to 60% volume fraction

of continuous E-glass fibers in a matrix of vinyl ester or isophthalic polyester resin have indicated a compressive modulus of elasticity of 5000 to 7000 ksi (34,000 to 48,000 MPa) (Wu 1990). According to reports, the compressive modulus of elasticity is approximately 80% for GFRP, 85% for CFRP, and 100% for AFRP of the tensile modulus of elasticity for the same product (Ehsani 1993).

4.4—Time-dependent behavior

4.4.1 *Creep-rupture*—FRP materials subjected to a constant load over time can suddenly fail after a time period referred to as the endurance time. This type of failure is known as creep-rupture. As the ratio of the sustained tensile stress to the short-term strength of the FRP laminate increases, endurance time decreases. The endurance time also decreases under adverse environmental conditions, such as high temperature, ultraviolet-radiation exposure, high alkalinity, wet and dry cycles, or freezing-and-thawing cycles.

In general, carbon fibers are the least susceptible to creep-rupture; aramid fibers are moderately susceptible, and glass fibers are most susceptible. Creep-rupture tests have been conducted on 0.25 in. (6 mm) diameter FRP bars reinforced with glass, aramid, and carbon fibers. The FRP bars were tested at different load levels at room temperature. Results indicated that a linear relationship exists between creep-rupture strength and the logarithm of time for all load levels. The ratios of stress level at creep-rupture after 500,000 hours (about 50 years) to the initial ultimate strength of the GFRP, AFRP, and CFRP bars were extrapolated to be approximately 0.3, 0.5, and 0.9, respectively (Yamaguchi et al. 1997; Malvar 1998). Recommendations on sustained stress limits imposed to avoid creep-rupture are given in the design section of this guide. As long as the sustained stress in the FRP is below the creep rupture stress limits, the strength of the FRP is available for nonsustained loads.

4.4.2 *Fatigue*—A substantial amount of data for fatigue behavior and life prediction of stand-alone FRP materials is available (National Research Council 1991). Most of these data were generated from materials typically used by the aerospace industry. Despite the differences in quality and consistency between aerospace and commercial-grade FRP materials, some general observations on the fatigue behavior of FRP materials can be made. Unless specifically stated otherwise, the following cases being reviewed are based on a unidirectional material with approximately 60% fiber-volume fraction and subjected to tension-tension sinusoidal cyclic loading at:

- A frequency low enough to not cause self-heating;
- Ambient laboratory environments;
- A stress ratio (ratio of minimum applied stress to maximum applied stress) of 0.1; and
- A direction parallel to the principal fiber alignment.

Test conditions that raise the temperature and moisture content of FRP materials generally degrade the ambient environment fatigue behavior.

Of all types of FRP composites for infrastructure applications, CFRP is the least prone to fatigue failure. An endurance limit of 60 to 70% of the initial static ultimate strength of CFRP is typical. On a plot of stress versus the logarithm of the number of cycles at failure (S-N curve), the downward slope for CFRP is usually approximately 5% of the initial static ultimate strength per decade of logarithmic life. At 1 million cycles, the fatigue strength is generally between 60 and 70% of the initial static ultimate strength and is relatively unaffected by the moisture and temperature exposures of concrete structures unless the resin or fiber/resin interface is substantially degraded by the environment.

In ambient-environment laboratory tests (Mandell and Meier 1983), individual glass fibers demonstrated delayed rupture caused by stress corrosion, which had been induced by the growth of surface flaws in the presence of even minute quantities of moisture. When many glass fibers were embedded into a matrix to form an FRP composite, a cyclic tensile fatigue effect of approximately 10% loss in the initial static strength per decade of logarithmic lifetime was observed (Mandell 1982). This fatigue effect is thought to be due to fiber-fiber interactions and is not dependent on the stress corrosion mechanism described for individual fibers. Usually, no clear fatigue limit can be defined. Environmental factors can play an important role in the fatigue behavior of glass fibers due to their susceptibility to moisture, alkaline, or acidic solutions.

Aramid fibers, for which substantial durability data are available, appear to behave reasonably well in fatigue. Neglecting in this context the rather poor durability of all aramid fibers in compression, the tension-tension fatigue behavior of an impregnated aramid fiber strand is excellent. Strength degradation per decade of logarithmic lifetime is approximately 5 to 6% (Roylance and Roylance 1981). While no distinct endurance limit is known for AFRP, 2-million-cycle endurance limits of commercial AFRP tendons for concrete applications have been reported in the range of 54 to 73% of the ultimate tensile strength (Odagiri et al. 1997). Based on these findings, Odagiri et al. suggested that the maximum stress be set to 0.54 to 0.73 times the tensile strength. Because the slope of the applied stress versus logarithmic endurance time of AFRP is similar to the slope of the stress versus logarithmic cyclic lifetime data, the individual fibers appear to fail by a strain-limited, creep-rupture process. This lifetime-limiting mechanism in commercial AFRP bars is accelerated by exposure to moisture and elevated temperature (Roylance and Roylance 1981; Rostasy 1997).

4.5—Durability

Many FRP systems exhibit reduced mechanical properties after exposure to certain environmental factors, including high temperature, humidity, and chemical exposure. The exposure environment, duration of the exposure, resin type and formulation, fiber type, and resin-curing method are some of the factors that influence the extent of the reduction in mechanical properties. These factors are discussed in more detail in Section 9.3. The tensile properties reported by the manufacturer are based on testing conducted in a laboratory environment, and do not reflect the effects of environmental exposure. These properties should be adjusted in accordance with Section 9.4 to account for the anticipated service

environment to which the FRP system may be exposed during its service life.

4.6—FRP systems qualification

FRP systems should be qualified for use on a project on the basis of independent laboratory test data of the FRP-constituent materials and the laminates made with them, structural test data for the type of application being considered, and durability data representative of the anticipated environment. Test data provided by the FRP system manufacturer demonstrating the proposed FRP system should meet all mechanical and physical design requirements, including tensile strength, durability, resistance to creep, bond to substrate, and T_g, should be considered.

FRP composite systems that have not been fully tested should not be considered for use. Mechanical properties of FRP systems should be determined from tests on laminates manufactured in a process representative of their field installation. Mechanical properties should be tested in general conformance with the procedures listed in Appendix B. Modifications of standard testing procedures may be permitted to emulate field assemblies.

The specified material-qualification programs should require sufficient laboratory testing to measure the repeatability and reliability of critical properties. Testing of multiple batches of FRP materials is recommended. Independent structural testing can be used to evaluate a system's performance for the specific application.

PART 3—RECOMMENDED CONSTRUCTION REQUIREMENTS
CHAPTER 5—SHIPPING, STORAGE, AND HANDLING

5.1—Shipping

FRP system constituent materials should be packaged and shipped in a manner that conforms to all applicable federal and state packaging and shipping codes and regulations. Packaging, labeling, and shipping for thermosetting resin materials are controlled by CFR 49. Many materials are classified as corrosive, flammable, or poisonous in Subchapter C (CFR 49) under "Hazardous Materials Regulations."

5.2—Storage

5.2.1 *Storage conditions*—To preserve the properties and maintain safety in the storage of FRP system constituent materials, the materials should be stored in accordance with the manufacturer's recommendations. Certain constituent materials, such as reactive curing agents, hardeners, initiators, catalysts, and cleaning solvents, have safety-related requirements, and should be stored in a manner as recommended by the manufacturer and OSHA. Catalysts and initiators (usually peroxides) should be stored separately.

5.2.2 *Shelf life*—The properties of the uncured resin components can change with time, temperature, or humidity. Such conditions can affect the reactivity of the mixed system and the uncured and cured properties. The manufacturer sets a recommended shelf life within which the properties of the resin-based materials should continue to meet or exceed

stated performance criteria. Any component material that has exceeded its shelf life, has deteriorated, or has been contaminated should not be used. FRP materials deemed unusable should be disposed of in a manner specified by the manufacturer and acceptable to state and federal environmental control regulations.

5.3—Handling

5.3.1 *Material safety data sheet*—Material safety data sheets (MSDS) for all FRP constituent materials and components should be obtained from the manufacturers, and should be accessible at the job site.

5.3.2 *Information sources*—Detailed information on the handling and potential hazards of FRP constituent materials can be found in information sources, such as ACI and ICRI reports, company literature and guides, OSHA guidelines, and other government informational documents. ACI 503R is specifically noted as a general guideline for the safe handling of epoxy and other resin adhesive compounds.

5.3.3 *General handling hazards*—Thermosetting resins describe a generic family of products that includes unsaturated polyesters, vinyl esters, epoxy, and polyurethane resins. The materials used with them are generally described as hardeners, curing agents, peroxide initiators, isocyanates, fillers, and flexibilizers. There are precautions that should be observed when handling thermosetting resins and their component materials. Some general hazards that may be encountered when handling thermosetting resins are listed as:

- Skin irritation, such as burns, rashes, and itching;
- Skin sensitization, which is an allergic reaction similar to that caused by poison ivy, building insulation, or other allergens;
- Breathing organic vapors from cleaning solvents, monomers, and diluents;
- With a sufficient concentration in air, explosion or fire of flammable materials when exposed to heat, flames, pilot lights, sparks, static electricity, cigarettes, or other sources of ignition;
- Exothermic reactions of mixtures of materials causing fires or personal injury; and
- Nuisance dust caused by grinding or handling of the cured FRP materials (manufacturer's literature should be consulted for specific hazards).

The complexity of thermosetting resins and associated materials makes it essential that labels and the MSDS are read and understood by those working with these products. CFR 16, Part 1500, regulates the labeling of hazardous substances and includes thermosetting-resin materials. ANSI Z-129.1 provides further guidance regarding classification and precautions.

5.3.4 *Personnel safe handling and clothing*—Disposable suits and gloves are suitable for handling fiber and resin materials. Disposable rubber or plastic gloves are recommended and should be discarded after each use. Gloves should be resistant to resins and solvents. Safety glasses or goggles should be used when handling resin components and solvents. Respiratory protection, such as dust masks or respirators, should be used when fiber fly, dust, or organic

vapors are present, or during mixing and placing of resins if required by the FRP system manufacturer.

5.3.5 *Workplace safe handling*—The workplace should be well ventilated. Surfaces should be covered as needed to protect against contamination and resin spills. Each FRP system constituent material has different handling and storage requirements to prevent damage. The material manufacturer should be consulted for guidance. Some resin systems are potentially dangerous during mixing of the components. The manufacturer's literature should be consulted for proper mixing procedures, and the MSDS for specific handling hazards. Ambient cure resin formulations produce heat when curing, which in turn accelerates the reaction. Uncontrolled reactions, including fuming, fire, or violent boiling, may occur in containers holding a mixed mass of resin; therefore, containers should be monitored.

5.3.6 *Cleanup and disposal*—Cleanup can involve use of flammable solvents, and appropriate precautions should be observed. Cleanup solvents are available that do not present the same flammability concerns. All waste materials should be contained and disposed of as prescribed by the prevailing environmental authority.

CHAPTER 6—INSTALLATION

Procedures for installing FRP systems have been developed by the system manufacturers and often differ between systems. In addition, installation procedures can vary within a system, depending on the type and condition of the structure. This chapter presents general guidelines for the installation of FRP systems. Contractors trained in accordance with the installation procedures developed by the system manufacturer should install FRP systems. Deviations from the procedures developed by the FRP system manufacturer should not be allowed without consulting with the manufacturer.

6.1—Contractor competency

The FRP system installation contractor should demonstrate competency for surface preparation and application of the FRP system to be installed. Contractor competency can be demonstrated by providing evidence of training and documentation of related work previously completed by the contractor or by actual surface preparation and installation of the FRP system on portions of the structure. The FRP system manufacturer or its authorized agent should train the contractor's application personnel in the installation procedures of its system and ensure they are competent to install the system.

6.2—Temperature, humidity, and moisture considerations

Temperature, relative humidity, and surface moisture at the time of installation can affect the performance of the FRP system. Conditions to be observed before and during installation include surface temperature of the concrete, air temperature, relative humidity, and corresponding dew point.

Primers, saturating resins, and adhesives should generally not be applied to cold or frozen surfaces. When the surface temperature of the concrete surface falls below a minimum level as specified by the FRP system manufacturer, improper saturation of the fibers and improper curing of the resin constituent materials can occur, compromising the integrity of the FRP system. An auxiliary heat source can be used to raise the ambient and surface temperature during installation. The heat source should be clean and not contaminate the surface or the uncured FRP system.

Resins and adhesives should generally not be applied to damp or wet surfaces unless they have been formulated for such applications. FRP systems should not be applied to concrete surfaces that are subject to moisture vapor transmission. The transmission of moisture vapor from a concrete surface through the uncured resin materials typically appears as surface bubbles and can compromise the bond between the FRP system and the substrate.

6.3—Equipment

Some FRP systems have unique equipment designed specifically for the application of the materials for one particular system. This equipment can include resin impregnators, sprayers, lifting/positioning devices, and winding machines. All equipment should be clean and in good operating condition. The contractor should have personnel trained in the operation of all equipment. Personal protective equipment, such as gloves, masks, eye guards, and coveralls, should be chosen and worn for each employee's function. All supplies and equipment should be available in sufficient quantities to allow continuity in the installation project and quality assurance.

6.4—Substrate repair and surface preparation

The behavior of concrete members strengthened or retrofitted with FRP systems is highly dependent on a sound concrete substrate and proper preparation and profiling of the concrete surface. An improperly prepared surface can result in debonding or delamination of the FRP system before achieving the design load transfer. The general guidelines presented in this chapter should be applicable to all externally bonded FRP systems. Specific guidelines for a particular FRP system should be obtained from the FRP system manufacturer. Substrate preparation can generate noise, dust, and disruption to building occupants.

6.4.1 *Substrate repair*—All problems associated with the condition of the original concrete and the concrete substrate that can compromise the integrity of the FRP system should be addressed before surface preparation begins. ACI 546R and ICRI 03730 detail methods for the repair and surface preparation of concrete. All concrete repairs should meet the requirements of the design drawings and project specifications. The FRP system manufacturer should be consulted on the compatibility of the FRP system with materials used for repairing the substrate.

6.4.1.1 *Corrosion-related deterioration*—Externally bonded FRP systems should not be applied to concrete substrates suspected of containing corroded reinforcing steel. The expansive forces associated with the corrosion process are difficult to determine, and could compromise the structural integrity of the externally applied FRP system. The cause(s) of the corrosion should be addressed, and the

corrosion-related deterioration should be repaired before the application of any externally bonded FRP system.

6.4.1.2 *Injection of cracks*—Cracks that are 0.010 in. (0.3 mm) and wider can affect the performance of the externally bonded FRP system through delamination or fiber crushing. Consequently, cracks wider than 0.010 in. (0.3 mm) should be pressure injected with epoxy before FRP installation in accordance with ACI 224.1R. Smaller cracks exposed to aggressive environments may require resin injection or sealing to prevent corrosion of existing steel reinforcement. Crack-width criteria for various exposure conditions are given in ACI 224.1R.

6.4.2 *Surface preparation*—Surface preparation requirements should be based on the intended application of the FRP system. Applications can be categorized as bond-critical or contact-critical. Bond-critical applications, such as flexural or shear strengthening of beams, slabs, columns, or walls, require an adhesive bond between the FRP system and the concrete. Contact-critical applications, such as confinement of columns, only require intimate contact between the FRP system and the concrete. Contact-critical applications do not require an adhesive bond between the FRP system and the concrete substrate, although one is often provided to facilitate installation.

6.4.2.1 *Bond-critical applications*—Surface preparation for bond-critical applications should be in accordance with recommendations of ACI 546R and ICRI 03730. The concrete or repaired surfaces to which the FRP system is to be applied should be freshly exposed and free of loose or unsound materials. Where fibers wrap around the corners of rectangular cross sections, the corners should be rounded to a minimum 0.5 in. (13 mm) radius to prevent stress concentrations in the FRP system and voids between the FRP system and the concrete. Roughened corners should be smoothed with putty. Obstructions, inside corners, concave surfaces, and embedded objects can affect the performance of the FRP system, and should be addressed. Obstructions and embedded objects may need to be removed before installing the FRP system. Inside corners and concave surfaces may require special detailing to ensure that the bond of the FRP system to the substrate is maintained. Surface preparation can be accomplished using abrasive or water-blasting techniques. All laitance, dust, dirt, oil, curing compound, existing coatings, and any other matter that could interfere with the bond of the FRP system to the concrete should be removed. Bug holes and other small surface voids should be completely exposed during surface profiling. After the profiling operations are complete, the surface should be cleaned and protected before FRP installation so that no materials that can interfere with bond are redeposited on the surface.

The concrete surface should be prepared to a minimum concrete surface profile (CSP) 3 as defined by the ICRI-surface-profile chips. The FRP system manufacturer should be consulted to determine if more aggressive surface profiling is necessary. Localized out-of-plane variations, including form lines, should not exceed 1/32 in. (1 mm) or the tolerances recommended by the FRP system manufacturer. Localized out-of-plane variations can be removed by grinding, before abrasive or water blasting, or can be smoothed over using resin-based putty if the variations are very small. Bug holes and voids should be filled with resin-based putty.

All surfaces to receive the strengthening system should be as dry as recommended by the FRP system manufacturer. Water in the pores can inhibit resin penetration and reduce mechanical interlock. Moisture content should be evaluated in accordance with the requirements of ACI 503.4.

6.4.2.2 *Contact-critical applications*—In applications involving confinement of structural concrete members, surface preparation should promote continuous intimate contact between the concrete surface and the FRP system. Surfaces to be wrapped should, at a minimum, be flat or convex to promote proper loading of the FRP system. Large voids in the surface should be patched with a repair material compatible with the existing concrete.

Materials with low compressive strength and elastic modulus, such as plaster, can reduce the effectiveness of the FRP system and should be removed.

6.4.3 *Surface-embedded systems*—NSM systems are typically installed in grooves cut onto the concrete surface. The existing steel reinforcement should not be damaged while cutting the groove. The soundness of the concrete surface should be checked before installing the bar. The inside faces of the groove should be cleaned to ensure adequate bond with concrete. The resulting groove should be free of laitance or other compounds that may interfere with bond. The moisture content of the parent concrete should be controlled to suit the bonding properties of the adhesive. The grooves should be completely filled with the adhesive. The adhesive should be specified by the NSM system manufacturer.

6.5—Mixing of resins

Mixing of resins should be done in accordance with the FRP system manufacturer's recommended procedure. All resin components should be at the proper temperature and mixed in the correct ratio until there is a uniform and complete mixing of components. Resin components are often contrasting colors, so full mixing is achieved when color streaks are eliminated. Resins should be mixed for the prescribed mixing time and visually inspected for uniformity of color. The material manufacturer should supply recommended batch sizes, mixture ratios, mixing methods, and mixing times.

Mixing equipment can include small electrically powered mixing blades or specialty units, or resins can be mixed by hand stirring, if needed. Resin mixing should be in quantities sufficiently small to ensure that all mixed resin can be used within the resin's pot life. Mixed resin that exceeds its pot life should not be used because the viscosity will continue to increase and will adversely affect the resin's ability to penetrate the surface or saturate the fiber sheet.

6.6—Application of FRP systems

Fumes can accompany the application of some FRP resins. FRP systems should be selected with consideration for their

impact on the environment, including emission of volatile organic compounds and toxicology.

6.6.1 *Primer and putty*—Where required, primer should be applied to all areas on the concrete surface where the FRP system is to be placed. The primer should be placed uniformly on the prepared surface at the manufacturer's specified rate of coverage. The applied primer should be protected from dust, moisture, and other contaminants before applying the FRP system.

Putty should be used in an appropriate thickness and sequence with the primer as recommended by the FRP manufacturer. The system-compatible putty, which is typically a thickened resin-based paste, should be used only to fill voids and smooth surface discontinuities before the application of other materials. Rough edges or trowel lines of cured putty should be ground smooth before continuing the installation.

Before applying the saturating resin or adhesive, the primer and putty should be allowed to cure as specified by the FRP system manufacturer. If the putty and primer are fully cured, additional surface preparation may be required before the application of the saturating resin or adhesive. Surface preparation requirements should be obtained from the FRP system manufacturer.

6.6.2 *Wet layup systems*—Wet layup FRP systems are typically installed by hand using dry fiber sheets and a saturating resin, typically per the manufacturer's recommendations. The saturating resin should be applied uniformly to all prepared surfaces where the system is to be placed. The fibers can also be impregnated in a separate process using a resin-impregnating machine before placement on the concrete surface.

The reinforcing fibers should be gently pressed into the uncured saturating resin in a manner recommended by the FRP system manufacturer. Entrapped air between layers should be released or rolled out before the resin sets. Sufficient saturating resin should be applied to achieve full saturation of the fibers.

Successive layers of saturating resin and fiber materials should be placed before the complete cure of the previous layer of resin. If previous layers are cured, interlayer surface preparation, such as light sanding or solvent application as recommended by the system manufacturer, may be required.

6.6.3 *Machine-applied systems*—Machine-applied systems can use resin-preimpregnated tows or dry-fiber tows. Prepreg tows are impregnated with saturating resin off-site and delivered to the work site as spools of prepreg tow material. Dry fibers are impregnated at the job site during the winding process.

Wrapping machines are primarily used for the automated wrapping of concrete columns. The tows can be wound either horizontally or at a specified angle. The wrapping machine is placed around the column and automatically wraps the tow material around the perimeter of the column while moving up and down the column.

After wrapping, prepreg systems should be cured at an elevated temperature. Usually, a heat source is placed around the column for a predetermined temperature and time schedule in accordance with the manufacturer's recommen-

dations. Temperatures are controlled to ensure consistent quality. The resulting FRP jackets do not have any seams or welds because the tows are continuous. In all of the previous application steps, the FRP system manufacturer's recommendations should be followed.

6.6.4 *Precured systems*—Precured systems include shells, strips, and open grid forms that are typically installed with an adhesive. Adhesives should be uniformly applied to the prepared surfaces where precured systems are to be placed, except in certain instances of concrete confinement where adhesion of the FRP system to the concrete substrate may not be required.

Precured laminate surfaces to be bonded should be clean and prepared in accordance with the manufacturer's recommendation. The precured sheets or curved shells should be placed on or into the wet adhesive in a manner recommended by the FRP manufacturer. Entrapped air between layers should be released or rolled out before the adhesive sets. Adhesive should be applied at a rate recommended by the FRP manufacturer to a minimum concrete surface profile (CSP) 3 as defined by the ICRI-surface-profile chips to ensure full bonding of successive layers (ICRI 03732).

6.6.5 *NSM systems*—NSM systems consist of installing rectangular or circular FRP bars in grooves cut onto the concrete surface and bonded in place using an adhesive. Grooves should be dimensioned to ensure adequate adhesive around the bars. Figure 13.4 gives typical groove dimensions for NSM FRP rods and plates. NSM systems can be used on the topside of structural members and for overhead applications. There are many application methods and types of adhesive that have been successfully used in the field for NSM systems. Adhesive type and installation method should be specified by the NSM system manufacturer.

6.6.6 *Protective coatings*—Coatings should be compatible with the FRP strengthening system and applied in accordance with the manufacturer's recommendations. Typically, the use of solvents to clean the FRP surface before installing coatings is not recommended due to the deleterious effects that solvents can have on the polymer resins. The FRP system manufacturer should approve any use of solvent-wipe preparation of FRP surfaces before the application of protective coatings.

The coatings should be periodically inspected and maintenance should be provided to ensure the effectiveness of the coatings.

6.7—Alignment of FRP materials

The FRP-ply orientation and ply-stacking sequence should be specified. Small variations in angle, as little as 5 degrees, from the intended direction of fiber alignment can cause a substantial reduction in strength and modulus. Deviations in ply orientation should only be made if approved by the licensed design professional.

Sheet and fabric materials should be handled in a manner to maintain the fiber straightness and orientation. Fabric kinks, folds, or other forms of severe waviness should be reported to the licensed design professional.

6.8—Multiple plies and lap splices

Multiple plies can be used, provided that all plies are fully impregnated with the resin system, the resin shear strength is sufficient to transfer the shearing load between plies, and the bond strength between the concrete and FRP system is sufficient. For long spans, multiple lengths of fiber material or precured stock can be used to continuously transfer the load by providing adequate lap splices. Lap splices should be staggered, unless noted otherwise by the licensed design professional. Lap splice details, including lap length, should be based on testing and installed in accordance with the manufacturer's recommendations. Due to the unique characteristics of some FRP systems, multiple plies and lap splices are not always possible. Specific guidelines on lap splices are given in Chapter 13.

6.9—Curing of resins

Curing of resins is a time-temperature-dependent phenomenon. Ambient-cure resins can take several days to reach full cure. Temperature extremes or fluctuations can retard or accelerate the resin curing time. The FRP system manufacturer may offer several prequalified grades of resin to accommodate these situations.

Elevated cure systems require the resin to be heated to a specific temperature for a specified period of time. Various combinations of time and temperature within a defined envelope should provide full cure of the system.

All resins should be cured according to the manufacturer's recommendation. Field modification of resin chemistry should not be permitted.

Cure of installed plies should be monitored before placing subsequent plies. Installation of successive layers should be halted if there is a curing anomaly.

6.10—Temporary protection

Adverse temperatures; direct contact by rain, dust, or dirt; excessive sunlight; high humidity; or vandalism can damage an FRP system during installation and cause improper cure of the resins. Temporary protection, such as tents and plastic screens, may be required during installation and until the resins have cured. If temporary shoring is required, the FRP system should be fully cured before removing the shoring and allowing the structural member to carry the design loads. In the event of suspected damage to the FRP system during installation, the licensed design professional should be notified and the FRP system manufacturer consulted.

CHAPTER 7—INSPECTION, EVALUATION, AND ACCEPTANCE

Quality-assurance and quality-control (QA/QC) programs and criteria are to be maintained by the FRP system manufacturers, the installation contractors, and others associated with the project. Quality assurance (QA) is typically an owner or a licensed professional activity, while quality control (QC) is a contractor or supplier activity. The QC program should be comprehensive and cover all aspects of the strengthening project, and should be detailed in the project specifications by a licensed professional. The degree of QC and the scope of testing, inspection, and record keeping depends on the size and complexity of the project.

Quality assurance is achieved through a set of inspections and applicable tests to document the acceptability of the installation. Project specifications should include a requirement to provide a QA plan for the installation and curing of all FRP materials. The plan should include personnel safety issues, application and inspection of the FRP system, location and placement of splices, curing provisions, means to ensure dry surfaces, QA samples, cleanup, and the required submittals listed in Section 14.3.

7.1—Inspection

FRP systems and all associated work should be inspected as required by the applicable codes. In the absence of such requirements, the inspection should be conducted by or under the supervision of a licensed design professional or a qualified inspector. Inspectors should be knowledgeable of FRP systems and be trained in the installation of FRP systems. The qualified inspector should require compliance with the design drawings and project specifications. During the installation of the FRP system, daily inspection should be conducted and should include:

- Date and time of installation;
- Ambient temperature, relative humidity, and general weather observations;
- Surface temperature of concrete;
- Surface dryness per ACI 503.4;
- Surface preparation methods and resulting profile using the ICRI-surface-profile-chips;
- Qualitative description of surface cleanliness;
- Type of auxiliary heat source, if applicable;
- Widths of cracks not injected with epoxy;
- Fiber or precured laminate batch number(s) and approximate location in structure;
- Batch numbers, mixture ratios, mixing times, and qualitative descriptions of the appearance of all mixed resins, including primers, putties, saturants, adhesives, and coatings mixed for the day;
- Observations of progress of cure of resins;
- Conformance with installation procedures;
- Pull-off test results: bond strength, failure mode, and location;
- FRP properties from tests of field sample panels or witness panels, if required;
- Location and size of any delaminations or air voids; and
- General progress of work.

The inspector should provide the licensed design professional or owner with the inspection records and witness panels. Records and witness panels should be retained for a minimum of 10 years or a period specified by the licensed design professional. The installation contractor should retain sample cups of mixed resin and maintain a record of the placement of each batch.

7.2—Evaluation and acceptance

FRP systems should be evaluated and accepted or rejected based on conformance or nonconformance with the design

drawings and specifications. FRP system material properties, installation within specified placement tolerances, presence of delaminations, cure of resins, and adhesion to substrate should be included in the evaluation. Placement tolerances including fiber orientation, cured thickness, ply orientation, width and spacing, corner radii, and lap splice lengths should be evaluated.

Witness panel and pulloff tests are used to evaluate the installed FRP system. In-place load testing can also be used to confirm the installed behavior of the FRP-strengthened member (Nanni and Gold 1998).

7.2.1 *Materials*—Before starting the project, the FRP system manufacturer should submit certification of specified material properties and identification of all materials to be used. Additional material testing can be conducted if deemed necessary based on the complexity and intricacy of the project. Evaluation of delivered FRP materials can include tests for tensile strength, infrared spectrum analysis, T_g, gel time, pot life, and adhesive shear strength. These tests are usually performed on material samples sent to a laboratory, according to the QC test plan. Tests for pot life of resins and curing hardness are usually conducted on site. Materials that do not meet the minimum requirements as specified by the licensed design professional should be rejected.

Witness panels can be used to evaluate the tensile strength and modulus, lap splice strength, hardness, and T_g of the FRP system installed and cured on site using installation procedures similar to those used to install and cure the FRP system. During installation, flat panels of predetermined dimensions and thickness can be fabricated on site according to a predetermined sampling plan. After curing on-site, the panels can then be sent to a laboratory for testing. Witness panels can be retained or submitted to an approved laboratory in a timely manner for testing of strength and T_g. Strength and elastic modulus of FRP materials can be determined in accordance with the requirements of Section 4.3.1 and ACI 440.3R (Test Method L.2) or CSA S806-02. The properties to be evaluated by testing should be specified. The licensed design professional may waive or alter the frequency of testing.

Some FRP systems, including precured and machine-wound systems, do not lend themselves to the fabrication of small, flat, witness panels. For these cases, the licensed design professional can modify the requirements to include test panels or samples provided by the manufacturer.

During installation, sample cups of mixed resin should be prepared according to a predetermined sampling plan and retained for testing to determine the level of cure (see Section 7.2.4).

7.2.2 *Fiber orientation*—Fiber or precured-laminate orientation should be evaluated by visual inspection. Fiber waviness—a localized appearance of fibers that deviate from the general straight-fiber line in the form of kinks or waves—should be evaluated for wet layup systems.

Fiber or precured laminate misalignment of more than 5 degrees from that specified on the design drawings (approximately 1 in./ft [80 mm/m]) should be reported to the licensed design professional for evaluation and acceptance.

7.2.3 *Delaminations*—The cured FRP system should be evaluated for delaminations or air voids between multiple plies or between the FRP system and the concrete. Inspection methods should be capable of detecting delaminations of 2 in.^{2} (1300 mm^2) or greater. Methods such as acoustic sounding (hammer sounding), ultrasonics, and thermography can be used to detect delaminations.

The effect of delaminations or other anomalies on the structural integrity and durability of the FRP system should be evaluated. Delamination size, location, and quantity relative to the overall application area should be considered in the evaluation.

General acceptance guidelines for wet layup systems are:
- Small delaminations less than 2 in.^{2} each (1300 mm^2) are permissible as long as the delaminated area is less than 5% of the total laminate area and there are no more than 10 such delaminations per 10 ft^2 (1 m^2);
- Large delaminations, greater than 25 in.^{2} (16,000 mm^2), can affect the performance of the installed FRP and should be repaired by selectively cutting away the affected sheet and applying an overlapping sheet patch of equivalent plies; and
- Delaminations less than 25 in.^{2} (16,000 mm^2) may be repaired by resin injection or ply replacement, depending on the size and number of delaminations and their locations.

For precured FRP systems, each delamination should be evaluated and repaired in accordance with the licensed design professional's direction. Upon completion of the repairs, the laminate should be reinspected to verify that the repair was properly accomplished.

7.2.4 *Cure of resins*—The relative cure of FRP systems can be evaluated by laboratory testing of witness panels or resin-cup samples using ASTM D3418. The relative cure of the resin can also be evaluated on the project site by physical observation of resin tackiness and hardness of work surfaces or hardness of retained resin samples. The FRP system manufacturer should be consulted to determine the specific resin-cure verification requirements. For precured systems, adhesive-hardness measurements should be made in accordance with the manufacturer's recommendation.

7.2.5 *Adhesion strength*—For bond-critical applications, tension adhesion testing of cored samples should be conducted using the methods in ACI 503R or ASTM D4541 or the method described by ACI 440.3R, Test Method L.1. Such tests cannot be performed when using NSM systems. The sampling frequency should be specified. Tension adhesion strengths should exceed 200 psi (1.4 MPa), and should exhibit failure of the concrete substrate. Lower strengths or failure between the FRP system and the concrete or between plies should be reported to the licensed design professional for evaluation and acceptance. For NSM strengthening, sample cores may be extracted to visually verify the consolidation of the resin adhesive around the FRP bar. The location of this core should be chosen such that the continuity of the FRP reinforcement is maintained (that is, at the ends of the NSM bars).

7.2.6 *Cured thickness*—Small core samples, typically 0.5 in. (13 mm) in diameter, may be taken to visually ascertain the

cured laminate thickness or number of plies. Cored samples required for adhesion testing also can be used to ascertain the laminate thickness or number of plies. The sampling frequency should be specified. Taking samples from high-stress areas or splice areas should be avoided. For aesthetic reasons, the cored hole can be filled and smoothed with a repair mortar or the FRP system putty. If required, a 4 to 8 in. (100 to 200 mm) overlapping FRP sheet patch of equivalent plies may be applied over the filled and smoothed core hole immediately after taking the core sample. The FRP sheet patch should be installed in accordance with the manufacturer's installation procedures.

CHAPTER 8—MAINTENANCE AND REPAIR
8.1—General

As with any strengthening or retrofit repair, the owner should periodically inspect and assess the performance of the FRP system used for strengthening or retrofit repair of concrete members. The causes of any damage or deficiencies detected during routine inspections should be identified and addressed before performing any repairs or maintenance.

8.2—Inspection and assessment

8.2.1 *General inspection*—A visual inspection looks for changes in color, debonding, peeling, blistering, cracking, crazing, deflections, indications of reinforcing-bar corrosion, and other anomalies. In addition, ultrasonic, acoustic sounding (hammer tap), or thermographic tests may indicate signs of progressive delamination.

8.2.2 *Testing*—Testing can include pull-off tension tests (Section 7.2.5) or conventional structural loading tests.

8.2.3 *Assessment*—Test data and observations are used to assess any damage and the structural integrity of the strengthening system. The assessment can include a recommendation for repairing any deficiencies and preventing recurrence of degradation,

8.3—Repair of strengthening system

The method of repair for the strengthening system depends on the causes of the damage, the type of material, the form of degradation, and the level of damage. Repairs to the FRP system should not be undertaken without first identifying and addressing the causes of the damage.

Minor damage should be repaired, including localized FRP laminate cracking or abrasions that affect the structural integrity of the laminate. Minor damage can be repaired by bonding FRP patches over the damaged area. The FRP patches should possess the same characteristics, such as thickness or ply orientation, as the original laminate. The FRP patches should be installed in accordance with the material manufacturer's recommendation. Minor delaminations can be repaired by resin injection. Major damage, including peeling and debonding of large areas, may require removal of the affected area, reconditioning of the cover concrete, and replacement of the FRP laminate.

8.4—Repair of surface coating

In the event that the surface-protective coating should be replaced, the FRP laminate should be inspected for structural damage or deterioration. The surface coating may be replaced using a process approved by the system manufacturer.

PART 4—DESIGN RECOMMENDATIONS
CHAPTER 9—GENERAL DESIGN CONSIDERATIONS

General design recommendations are presented in this chapter. The recommendations presented are based on the traditional reinforced concrete design principles stated in the requirements of ACI 318-05 and knowledge of the specific mechanical behavior of FRP reinforcement.

FRP strengthening systems should be designed to resist tensile forces while maintaining strain compatibility between the FRP and the concrete substrate. FRP reinforcement should not be relied on to resist compressive forces. It is acceptable, however, for FRP tension reinforcement to experience compression due to moment reversals or changes in load pattern. The compressive strength of the FRP reinforcement, however, should be neglected.

9.1—Design philosophy

These design recommendations are based on limit-states-design principles. This approach sets acceptable levels of safety for the occurrence of both serviceability limit states (excessive deflections and cracking) and ultimate limit states (failure, stress rupture, and fatigue). In assessing the nominal strength of a member, the possible failure modes and subsequent strains and stresses in each material should be assessed. For evaluating the serviceability of a member, engineering principles, such as modular ratios and transformed sections, can be used.

FRP strengthening systems should be designed in accordance with ACI 318-05 strength and serviceability requirements using the strength and load factors stated in ACI 318-05. Additional reduction factors applied to the contribution of the FRP reinforcement are recommended by this guide to reflect uncertainties inherent in FRP systems compared with steel reinforced and prestressed concrete. These reduction factors were determined based on statistical evaluation of variability in mechanical properties, predicted versus full-scale test results, and field applications. FRP-related reduction factors were calibrated to produce reliability indexes typically above 3.5. Reliability indexes between 3.0 and 3.5 can be encountered in cases where relatively low ratios of steel reinforcement combined with high ratios of FRP reinforcement are used. Such cases are less likely to be encountered in design because they violate the strength-increase limits of Section 9.2. Reliability indexes for FRP-strengthened members are determined based on the approach used for reinforced concrete buildings (Nowak and Szerszen 2003; Szerszen and Nowak 2003). In general, lower reliability is expected in retrofitted and repaired structures than in new structures.

9.2—Strengthening limits

Careful consideration should be given to determine reasonable strengthening limits. These limits are imposed to guard against collapse of the structure should bond or other

failure of the FRP system occur due to damage, vandalism, or other causes. The unstrengthened structural member, without FRP reinforcement, should have sufficient strength to resist a certain level of load. In the event that the FRP system is damaged, the structure will still be capable of resisting a reasonable level of load without collapse. The existing strength of the structure should be sufficient to resist a level of load as described by Eq. (9-1)

$$(\phi R_n)_{existing} \geq (1.1S_{DL} + 0.75S_{LL})_{new} \qquad (9\text{-}1)$$

A dead load factor of 1.1 is used because a relatively accurate assessment of the existing dead loads of the structure can be determined. A live load factor of 0.75 is used to exceed the statistical mean of yearly maximum live load factor of 0.5, as given in ASCE 7-05. The minimum strengthening limit of Eq. (9-1) will allow the strengthened member to maintain sufficient structural capacity until the damaged FRP has been repaired.

In cases where the design live load acting on the member to be strengthened has a high likelihood of being present for a sustained period of time, a live load factor of 1.0 should be used instead of 0.75 in Eq. (9-1). Examples include library stack areas, heavy storage areas, warehouses, and other occupancies with a live load exceeding 150 lb/ft^2 (730 kg/m^2).

More specific limits for structures requiring a fire endurance rating are given in Section 9.2.1.

9.2.1 *Structural fire endurance*—The level of strengthening that can be achieved through the use of externally bonded FRP reinforcement is often limited by the code-required fire-resistance rating of a structure. The polymer resins currently used in wet layup and prepreg FRP systems and the polymer adhesives used in precured FRP systems suffer deterioration of mechanical and bond properties at temperatures close to or exceeding the Tg of the polymer (Bisby et al. 2005b). While the Tg can vary significantly, depending on the polymer chemistry, a typical range for field-applied resins and adhesives is 140 to 180 °F (60 to 82 °C).

Although the FRP system itself has a low fire endurance, a combination of the FRP system with an existing concrete structure may still have an adequate level of fire endurance. This occurs because an insulation system can improve the overall fire rating of a reinforced concrete member by providing protection to its components, concrete, and reinforcing steel. The insulation system can delay strength degradation of the concrete and steel due to fire exposure and increase their residual strengths, thus increasing the fire rating of the member. Hence, with proper insulation, the fire rating of a member can be increased even with the FRP contribution ignored (Bisby et al. 2005a; Williams et al. 2006). This is attributable to the inherent fire endurance of the existing concrete structure alone. To investigate the fire endurance of an FRP-strengthened concrete structure, it is important to recognize that the strength of traditional reinforced concrete structures is somewhat reduced during exposure to the high temperatures associated with a fire event as well. The yield strength of reinforcing steel and the compressive strength of concrete are reduced. As a result, the overall

resistance of a reinforced concrete member to load effects is reduced. This concept is used in ACI 216R to provide a method of computing the fire endurance of concrete members. ACI 216R suggests limits that maintain a reasonable level of safety against complete collapse of the structure in the event of a fire.

By extending the concepts established in ACI 216R to FRP-strengthened reinforced concrete, limits on strengthening can be used to ensure a strengthened structure will not collapse in a fire event. A member's resistance to load effects, with reduced steel and concrete strengths and without the strength of the FRP reinforcement, can be computed. This resistance can then be compared with the load demand on the member to ensure the structure will not collapse under service loads and elevated temperatures.

The nominal strength of a structural member with a fire resistance rating should satisfy the conditions of Eq. (9-2) if it is to be strengthened with an FRP system. The load effects, S_{DL} and S_{LL}, should be determined using the current load requirements for the structure. If the FRP system is meant to allow greater load-carrying strength, such as an increase in live load, the load effects should be computed using these greater loads. The nominal strength at high temperature should be greater than the strengthened service load on the member (ACI 216R should be used for ASTM E119 fire scenarios)

$$R_{n\theta} \geq S_{DL} + S_{LL} \qquad (9\text{-}2)$$

The nominal resistance of the member at an elevated temperature $R_{n\theta}$ may be determined using the guidelines outlined in ACI 216R or through testing. The nominal resistance $R_{n\theta}$ should be calculated based on the reduced properties of the existing member. The resistance should be computed for the time period required by the structure's fire-resistance rating—for example, a 2-hour fire rating—and should not account for the contribution of the FRP system, unless the FRP temperature can be demonstrated to remain below a critical temperature for FRP. The critical temperature for the FRP may be defined as the temperature at which significant deterioration of FRP properties has occurred. More research is needed to accurately identify critical temperatures for different types of FRP. Until better information on the properties of FRP at high temperature is available, the critical temperature of an FRP strengthening system can be taken as the lowest T_g of the components of the system.

Furthermore, if the FRP system is meant to address a loss in strength, such as deterioration, the resistance should reflect this loss. The fire endurance of FRP materials and FRP strengthening systems can be improved through the use of polymers having high T_g or using fire protection (Bisby et al. 2005a).

9.2.2 *Overall structural strength*—While FRP systems are effective in strengthening members for flexure and shear and providing additional confinement, other modes of failure, such as punching shear and bearing capacity of footings, may be only slightly affected by FRP systems (Sharaf et al.

2006). All members of a structure should be capable of withstanding the anticipated increase in loads associated with the strengthened members.

Additionally, analysis should be performed on the member strengthened by the FRP system to check that under overload conditions the strengthened member will fail in a flexural mode rather than in a shear mode.

9.2.3 *Seismic applications*—The majority of research into seismic strengthening of structures has dealt with strengthening of columns. FRP systems confine columns to improve concrete compressive strength, reduce required splice length, and increase the shear strength (Priestley et al. 1996). Limited information is available for strengthening building frames in seismic zones. When beams or floors in building frames in seismic zones are strengthened, the strength and stiffness of both the beam/floor and column should be checked to ensure the formation of the plastic hinge away from the column and the joint (Mosallam et al. 2000).

9.3—Selection of FRP systems

9.3.1 *Environmental considerations*—Environmental conditions uniquely affect resins and fibers of various FRP systems. The mechanical properties (for example, tensile strength, ultimate tensile strain, and elastic modulus) of some FRP systems degrade under exposure to certain environments, such as alkalinity, salt water, chemicals, ultraviolet light, high temperatures, high humidity, and freezing-and-thawing cycles. The material properties used in design should account for this degradation in accordance with Section 9.4.

The licensed design professional should select an FRP system based on the known behavior of that system in the anticipated service conditions. Some important environmental considerations that relate to the nature of the specific systems are given as follows. Specific information can be obtained from the FRP system manufacturer.

- *Alkalinity/acidity*—The performance of an FRP system over time in an alkaline or acidic environment depends on the matrix material and the reinforcing fiber. Dry, unsaturated bare, or unprotected carbon fiber is resistant to both alkaline and acidic environments, while bare glass fiber can degrade over time in these environments. A properly applied resin matrix, however, should isolate and protect the fiber from the alkaline/acidic environment and retard deterioration. The FRP system selected should include a resin matrix resistant to alkaline and acidic environments. Sites with high alkalinity and high moisture or relative humidity favor the selection of carbon-fiber systems over glass-fiber systems;

- *Thermal expansion*—FRP systems may have thermal expansion properties that are different from those of concrete. In addition, the thermal expansion properties of the fiber and polymer constituents of an FRP system can vary. Carbon fibers have a coefficient of thermal expansion near zero whereas glass fibers have a coefficient of thermal expansion similar to concrete. The polymers used in FRP strengthening systems typically have coefficients of thermal expansion roughly five times

that of concrete. Calculation of thermally-induced strain differentials are complicated by variations in fiber orientation, fiber volume fraction (ratio of the volume of fibers to the volume of fibers and resins in an FRP), and thickness of adhesive layers. Experience (Motavalli et al. 1997; Soudki and Green 1997; Green et al. 1998) indicates, however, that thermal expansion differences do not affect bond for small ranges of temperature change, such as ±50 °F (±28 °C); and

- *Electrical conductivity*—GFRP and AFRP are effective electrical insulators, whereas CFRP is conductive. To avoid potential galvanic corrosion of steel elements, carbon-based FRP materials should not come in direct contact with steel.

9.3.2 *Loading considerations*—Loading conditions uniquely affect different fibers of FRP systems. The licensed design professional should select an FRP system based on the known behavior of that system in the anticipated service conditions.

Some important loading considerations that relate to the nature of the specific systems are given below. Specific information should be obtained from material manufacturers.

- *Impact tolerance*—AFRP and GFRP systems demonstrate better tolerance to impact than CFRP systems; and

- *Creep-rupture and fatigue*—CFRP systems are highly resistive to creep-rupture under sustained loading and fatigue failure under cyclic loading. GFRP systems are more sensitive to both loading conditions.

9.3.3 *Durability considerations*—Durability of FRP systems is the subject of considerable ongoing research (Steckel et al. 1999). The licensed design professional should select an FRP system that has undergone durability testing consistent with the application environment. Durability testing may include hot-wet cycling, alkaline immersion, freezing-and-thawing cycling, ultraviolet exposure, dry heat, and salt water.

Any FRP system that completely encases or covers a concrete section should be investigated for the effects of a variety of environmental conditions including those of freezing and thawing, steel corrosion, alkali and silica aggregate reactions, water entrapment, vapor pressures, and moisture vapor transmission (Masoud and Soudki 2006; Soudki and Green 1997; Porter et al. 1997; Christensen et al. 1996; Toutanji 1999). Many FRP systems create a moisture-impermeable layer on the surface of the concrete. In areas where moisture vapor transmission is expected, adequate means should be provided to allow moisture to escape from the concrete structure.

9.3.4 *Protective-coating selection considerations*—A coating or insulation system can be applied to the installed FRP system to protect it from exposure to certain environmental conditions (Bisby et al. 2005a; Williams et al. 2006). The thickness and type of coating should be selected based on the requirements of the composite repair; resistance to environmental effects such as moisture, salt water, temperature extremes, fire, impact, and UV exposure; resistance to site-specific effects; and resistance to vandalism. Coatings are relied on to retard the degradation of the mechanical properties

Table 9.1—Environmental reduction factor for various FRP systems and exposure conditions

Exposure conditions	Fiber type	Environmental reduction factor C_E
Interior exposure	Carbon	0.95
	Glass	0.75
	Aramid	0.85
Exterior exposure (bridges, piers, and unenclosed parking garages)	Carbon	0.85
	Glass	0.65
	Aramid	0.75
Aggressive environment (chemical plants and wastewater treatment plants)	Carbon	0.85
	Glass	0.50
	Aramid	0.70

of the FRP systems. The coatings should be periodically inspected and maintained to ensure the effectiveness of the coatings.

External coatings or thickened coats of resin over fibers can protect them from damage due to impact or abrasion. In high-impact or traffic areas, additional levels of protection may be necessary. Portland-cement plaster and polymer coatings are commonly used for protection where minor impact or abrasion is anticipated.

9.4—Design material properties

Unless otherwise stated, the material properties reported by manufacturers, such as the ultimate tensile strength, typically do not consider long-term exposure to environmental conditions and should be considered as initial properties. Because long-term exposure to various types of environments can reduce the tensile properties and creep-rupture and fatigue endurance of FRP laminates, the material properties used in design equations should be reduced based on the environmental exposure condition.

Equations (9-3) through (9-5) give the tensile properties that should be used in all design equations. The design ultimate tensile strength should be determined using the environmental reduction factor given in Table 9.1 for the appropriate fiber type and exposure condition

$$f_{fu} = C_E f_{fu}^* \qquad (9\text{-}3)$$

Similarly, the design rupture strain should also be reduced for environmental exposure conditions

$$\varepsilon_{fu} = C_E \varepsilon_{fu}^* \qquad (9\text{-}4)$$

Because FRP materials are linear elastic until failure, the design modulus of elasticity for unidirectional FRP can be determined from Hooke's law. The expression for the modulus of elasticity, given in Eq. (9-5), recognizes that the modulus is typically unaffected by environmental conditions. The modulus given in this equation will be the same as the initial value reported by the manufacturer

$$E_f = f_{fu}/\varepsilon_{fu} \qquad (9\text{-}5)$$

The constituent materials, fibers, and resins of an FRP system affect its durability and resistance to environmental exposure. The environmental reduction factors given in Table 9.1 are conservative estimates based on the relative durability of each fiber type. As more research information is developed and becomes available, these values will be refined. The methodology regarding the use of these factors, however, will remain unchanged. When available, durability test data for FRP systems with and without protective coatings may be obtained from the manufacturer of the FRP system under consideration.

As Table 9.1 illustrates, if the FRP system is located in a relatively benign environment, such as indoors, the reduction factor is closer to unity. If the FRP system is located in an aggressive environment where prolonged exposure to high humidity, freezing-and-thawing cycles, salt water, or alkalinity is expected, a lower reduction factor should be used. The reduction factor can reflect the use of a protective coating if the coating has been shown through testing to lessen the effects of environmental exposure and the coating is maintained for the life of the FRP system.

CHAPTER 10—FLEXURAL STRENGTHENING

Bonding FRP reinforcement to the tension face of a concrete flexural member with fibers oriented along the length of the member will provide an increase in flexural strength. Increases in overall flexural strength from 10 to 160% have been documented (Meier and Kaiser 1991; Ritchie et al. 1991; Sharif et al. 1994). When taking into account the strengthening limits of Section 9.2 and ductility and serviceability limits, however, strength increases of up to 40% are more reasonable.

This chapter does not apply to FRP systems used to enhance the flexural strength of members in the expected plastic hinge regions of ductile moment frames resisting seismic loads. The design of such applications, if used, should examine the behavior of the strengthened frame, considering that the strengthened sections have much-reduced rotation and curvature capacities. In this case, the effect of cyclic load reversal on the FRP reinforcement should be investigated.

10.1—Nominal strength

The strength design approach requires that the design flexural strength of a member exceed its required factored moment as indicated by Eq. (10-1). The design flexural strength ϕM_n refers to the nominal strength of the member multiplied by a strength reduction factor, and the factored moment M_u refers to the moment calculated from factored loads (for example, $\alpha_{DL}M_{DL} + \alpha_{LL}M_{LL} + ...$)

$$\phi M_n \geq M_u \qquad (10\text{-}1)$$

This guide recommends that the factored moment M_u of a section be calculated by use of load factors as required by ACI 318-05. In addition, an additional strength reduction factor for FRP, ψ_f, should be applied to the flexural contribution of the FRP reinforcement alone, M_{nf}, as described in Section

(a) Behavior of flexural member having bonded reinforcement on soffit

(b) Debonding initiated by flexural and/or shear cracks

(c) Cover delamination initiated at curtailment of bonded FRP reinforcement
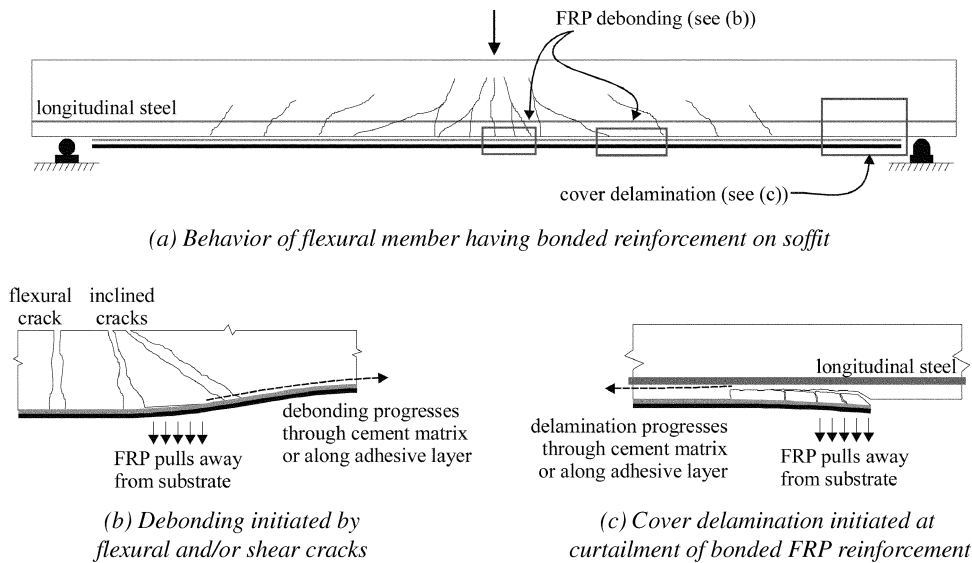
Fig. 10.1—Debonding and delamination of externally bonded FRP systems.

10.2.10. The additional strength reduction factor, ψ_f, is used to improve the reliability of strength prediction and accounts for the different failure modes observed for FRP-strengthened members (delamination of FRP reinforcement).

The nominal flexural strength of FRP-strengthened concrete members with mild steel reinforcement and with bonded prestressing steel can be determined based on strain compatibility, internal force equilibrium, and the controlling mode of failure. For members with unbonded prestressed steel, strain compatibility does not apply and the stress in the unbonded tendons at failure depends on the overall deformation of the member and is assumed to be approximately the same at all sections. No specific guidelines on FRP strengthening of concrete members with unbonded prestressing steel are provided at this time.

10.1.1 *Failure modes*—The flexural strength of a section depends on the controlling failure mode. The following flexural failure modes should be investigated for an FRP-strengthened section (GangaRao and Vijay 1998):

- Crushing of the concrete in compression before yielding of the reinforcing steel;
- Yielding of the steel in tension followed by rupture of the FRP laminate;
- Yielding of the steel in tension followed by concrete crushing;
- Shear/tension delamination of the concrete cover (cover delamination); and
- Debonding of the FRP from the concrete substrate (FRP debonding).

Concrete crushing is assumed to occur if the compressive strain in the concrete reaches its maximum usable strain ($\varepsilon_c = \varepsilon_{cu} = 0.003$). Rupture of the externally bonded FRP is assumed to occur if the strain in the FRP reaches its design rupture strain ($\varepsilon_f = \varepsilon_{fu}$) before the concrete reaches its maximum usable strain.

Cover delamination or FRP debonding can occur if the force in the FRP cannot be sustained by the substrate (Fig. 10.1).

Such behavior is generally referred to as debonding, regardless of where the failure plane propagates within the FRP-adhesive-substrate region. Guidance to avoid the cover delamination failure mode is given in Chapter 13.

Away from the section where externally bonded FRP terminates, a failure controlled by FRP debonding may govern (Fig. 10.1(b)). To prevent such an intermediate crack-induced debonding failure mode, the effective strain in FRP reinforcement should be limited to the strain level at which debonding may occur, ε_{fd}, as defined in Eq. (10-2)

$$\varepsilon_{fd} = 0.083\sqrt{\frac{f'_c}{nE_f t_f}} \leq 0.9\varepsilon_{fu} \quad \text{in in.-lb units}$$

$$\varepsilon_{fd} = 0.41\sqrt{\frac{f'_c}{nE_f t_f}} \leq 0.9\varepsilon_{fu} \quad \text{in SI units}$$

(10-2)

Equation (10-2) takes a modified form of the debonding strain equation proposed by Teng et al. (2001, 2004) that was based on committee evaluation of a significant database for flexural beam tests exhibiting FRP debonding failure. The proposed equation was calibrated using average measured values of FRP strains at debonding and the database for flexural tests experiencing intermediate crack-induced debonding to determine the best fit coefficient of 0.083 (0.41 in SI units). Reliability of FRP contribution to flexural strength is addressed by incorporating an additional strength reduction factor for FRP ψ_f in addition to the strength reduction factor ϕ per ACI 318-05 for structural concrete.

Transverse clamping with FRP layers improves bond behavior relative to that predicted by Eq. (10-2). Provision of transverse clamping FRP U-wraps along the length of the flexural FRP reinforcement has been observed to result in increased FRP strain at debonding. An improvement of up to 30% increase in debonding strain has been observed (CECS-146 (2003)). Further research is needed to understand

the influence of transverse FRP on the debonding strain of longitudinal FRP.

For NSM FRP applications, the value of ε_{fd} may vary from $0.6\varepsilon_{fu}$ to $0.9\varepsilon_{fu}$ depending on many factors such as member dimensions, steel and FRP reinforcement ratios, and surface roughness of the FRP bar. Based on existing studies (Hassan and Rizkalla 2003; De Lorenzis et al. 2004; Kotynia 2005), the committee recommends the use of $\varepsilon_{fd} = 0.7\varepsilon_{fu}$. To achieve the debonding design strain of NSM FRP bars ε_{fd}, the bonded length should be greater than the development length given in Chapter 13.

10.2—Reinforced concrete members

This section presents guidance on the calculation of the flexural strengthening effect of adding longitudinal FRP reinforcement to the tension face of a reinforced concrete member. A specific illustration of the concepts in this section applied to strengthening of existing rectangular sections reinforced in the tension zone with nonprestressed steel is given. The general concepts outlined herein can, however, be extended to nonrectangular shapes (T-sections and I-sections) and to members with compression steel reinforcement.

10.2.1 *Assumptions*—The following assumptions are made in calculating the flexural resistance of a section strengthened with an externally applied FRP system:

- Design calculations are based on the dimensions, internal reinforcing steel arrangement, and material properties of the existing member being strengthened;
- The strains in the steel reinforcement and concrete are directly proportional to the distance from the neutral axis. That is, a plane section before loading remains plane after loading;
- There is no relative slip between external FRP reinforcement and the concrete;
- The shear deformation within the adhesive layer is neglected because the adhesive layer is very thin with slight variations in its thickness;
- The maximum usable compressive strain in the concrete is 0.003;
- The tensile strength of concrete is neglected; and
- The FRP reinforcement has a linear elastic stress-strain relationship to failure.

While some of these assumptions are necessary for the sake of computational ease, the assumptions do not accurately reflect the true fundamental behavior of FRP flexural reinforcement. For example, there will be shear deformation in the adhesive layer causing relative slip between the FRP and the substrate. The inaccuracy of the assumptions will not, however, significantly affect the computed flexural strength of an FRP-strengthened member. An additional strength reduction factor (presented in Section 10.2.10) will conservatively compensate for any such discrepancies.

10.2.2 *Shear strength*—When FRP reinforcement is being used to increase the flexural strength of a member, the member should be capable of resisting the shear forces associated with the increased flexural strength. The potential for shear failure of the section should be considered by comparing the design shear strength of the section to the required shear strength. If additional shear strength is required, FRP laminates oriented transverse to the beam longitudinal axis can be used to resist shear forces as described in Chapter 11.

10.2.3 *Existing substrate strain*—Unless all loads on a member, including self-weight and any prestressing forces, are removed before installation of FRP reinforcement, the substrate to which the FRP is applied will be strained. These strains should be considered as initial strains and should be excluded from the strain in the FRP (Arduini and Nanni 1997; Nanni and Gold 1998). The initial strain level on the bonded substrate, ε_{bi}, can be determined from an elastic analysis of the existing member, considering all loads that will be on the member during the installation of the FRP system. The elastic analysis of the existing member should be based on cracked section properties.

10.2.4 *Flexural strengthening of concave soffits*—The presence of curvature in the soffit of a concrete member may lead to the development of tensile stresses normal to the adhesive and surface to which the FRP is bonded. Such tensile stresses result when the FRP tends to straighten under load, and can promote the initiation of FRP laminate separation failure that reduces the effectiveness of the FRP flexural strengthening (Aiello et al. 2001; Eshwar et al. 2003). If the extent of the curved portion of the soffit exceeds a length of 40 in. (1.0 m) with a rise of 0.2 in. (5 mm), the surface should be made flat before strengthening. Alternately, anchor systems such as FRP anchors or U-wraps should be installed to prevent delamination (Eshwar et al. 2003).

10.2.5 *Strain level in FRP reinforcement*—It is important to determine the strain level in the FRP reinforcement at the ultimate limit state. Because FRP materials are linear elastic until failure, the level of strain in the FRP will dictate the level of stress developed in the FRP. The maximum strain level that can be achieved in the FRP reinforcement will be governed by either the strain level developed in the FRP at the point at which concrete crushes, the point at which the FRP ruptures, or the point at which the FRP debonds from the substrate. The effective strain level in the FRP reinforcement at the ultimate limit state can be found from Eq. (10-3)

$$\varepsilon_{fe} = \varepsilon_{cu}\left(\frac{d_f - c}{c}\right) - \varepsilon_{bi} \le \varepsilon_{fd} \qquad (10\text{-}3)$$

where ε_{bi} is the initial substrate strain as described in Section 10.2.3, and d_f is the effective depth of FRP reinforcement, as indicated in Fig. 10.2.

10.2.6 *Stress level in the FRP reinforcement*—The effective stress level in the FRP reinforcement is the maximum level of stress that can be developed in the FRP reinforcement before flexural failure of the section. This effective stress level can be found from the strain level in the FRP, assuming perfectly elastic behavior

$$f_{fe} = E_f \varepsilon_{fe} \qquad (10\text{-}4)$$

(a) FRP Laminates   *(b) NSM bars*
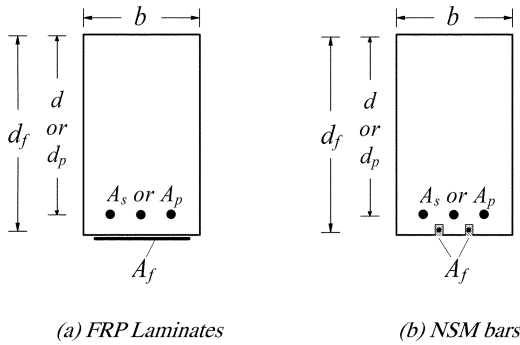
Fig. 10.2—Effective depth of FRP systems.

10.2.7 *Strength reduction factor*—The use of externally bonded FRP reinforcement for flexural strengthening will reduce the ductility of the original member. In some cases, the loss of ductility is negligible. Sections that experience a significant loss in ductility, however, should be addressed. To maintain a sufficient degree of ductility, the strain level in the steel at the ultimate limit state should be checked. For reinforced concrete members with nonprestressed steel reinforcement, adequate ductility is achieved if the strain in the steel at the point of concrete crushing or failure of the FRP, including delamination or debonding, is at least 0.005, according to the definition of a tension-controlled section as given in ACI 318-05.

The approach taken by this guide follows the philosophy of ACI 318-05. A strength reduction factor given by Eq. (10-5) should be used, where ε_t is the net tensile strain in extreme tension steel at nominal strength, as defined in ACI 318-05

$$\phi = \begin{cases} 0.90 \text{ for } \varepsilon_t \geq 0.005 \\ 0.65 + \dfrac{0.25(\varepsilon_t - \varepsilon_{sy})}{0.005 - \varepsilon_{sy}} \text{ for } \varepsilon_{sy} < \varepsilon_t < 0.005 \\ 0.65 \text{ for } \varepsilon_t \leq \varepsilon_{sy} \end{cases} \quad (10\text{-}5)$$

This equation sets the reduction factor at 0.90 for ductile sections and 0.65 for brittle sections where the steel does not yield, and provides a linear transition for the reduction factor between these two extremes (Fig. 10.3).

10.2.8 *Serviceability*—The serviceability of a member (deflections and crack widths) under service loads should satisfy applicable provisions of ACI 318-05. The effect of the FRP external reinforcement on the serviceability can be assessed using the transformed-section analysis.

To avoid inelastic deformations of reinforced concrete members with nonprestressed steel reinforcement strengthened with external FRP reinforcement, the existing internal steel reinforcement should be prevented from yielding under service load levels, especially for members subjected to cyclic loads (El-Tawil et al. 2001). The stress in the steel reinforcement under service load should be limited to 80% of the yield strength, as shown in Eq. (10-6). In addition, the compressive stress in concrete under service load should be limited to 45% of the compressive strength, as shown in Eq. (10-7)
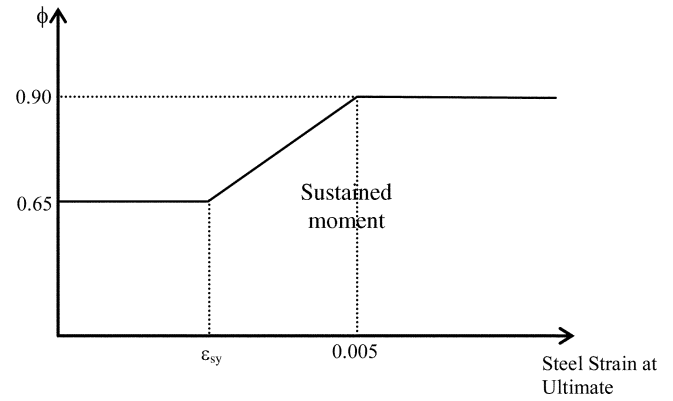
Fig. 10.3—Graphical representation of strength reduction factor.
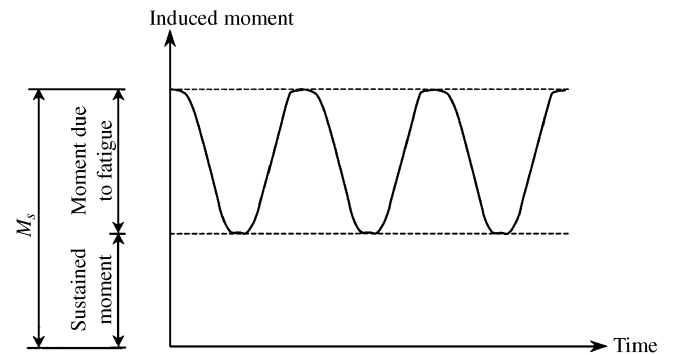
Fig. 10.4—Illustration of the level of applied moment to be used to check the stress limits in the FRP reinforcement.

$$f_{s,s} \leq 0.80 f_y \quad (10\text{-}6)$$

$$f_{c,s} \leq 0.45 f_c' \quad (10\text{-}7)$$

10.2.9 *Creep-rupture and fatigue stress limits*—To avoid creep-rupture of the FRP reinforcement under sustained stresses or failure due to cyclic stresses and fatigue of the FRP reinforcement, the stress levels in the FRP reinforcement under these stress conditions should be checked. Because these stress levels will be within the elastic response range of the member, the stresses can be computed by elastic analysis.

In Section 4.4, the creep-rupture phenomenon and fatigue characteristics of FRP material were described and the resistance to its effects by various types of fibers was examined. As stated in Section 4.4.1, research has indicated that glass, aramid, and carbon fibers can sustain approximately 0.3, 0.5, and 0.9 times their ultimate strengths, respectively, before encountering a creep-rupture problem (Yamaguchi et al. 1997; Malvar 1998). To avoid failure of an FRP-reinforced member due to creep-rupture and fatigue of the FRP, stress limits for these conditions should be imposed on the FRP reinforcement. The stress level in the FRP reinforcement can be computed using elastic analysis and an applied moment due to all sustained loads (dead loads and the sustained portion of the live load) plus the maximum moment induced in a fatigue loading cycle (Fig. 10.4). The sustained stress
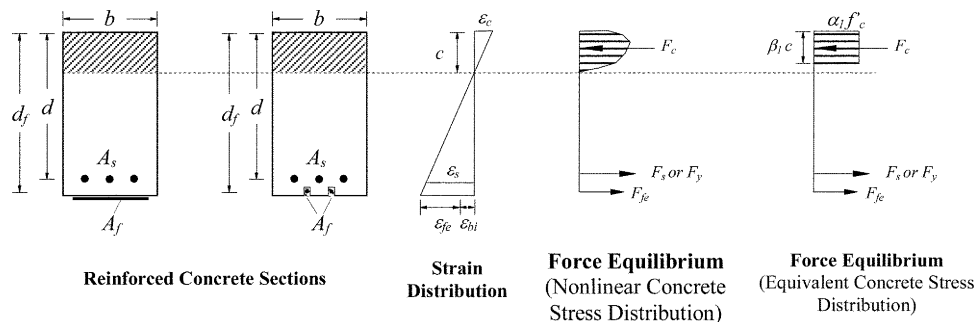
Fig. 10.5—Internal strain and stress distribution for a rectangular section under flexure at ultimate limit state.

Table 10.1—Sustained plus cyclic service load stress limits in FRP reinforcement

Stress type	Fiber type		
	GFRP	AFRP	CFRP
Sustained plus cyclic stress limit	$0.20f_{fu}$	$0.30f_{fu}$	$0.55f_{fu}$

should be limited as expressed by Eq. (10-8) to maintain safety. Values for safe sustained plus cyclic stress levels are given in Table 10.1. These values are based approximately on the stress limits previously stated in Section 4.4.1 with an imposed safety factor of 1/0.6

$$f_{f,s} \leq \text{sustained plus cyclic stress limit} \qquad (10\text{-}8)$$

10.2.10 *Ultimate strength of singly reinforced rectangular section*—To illustrate the concepts presented in this chapter, this section describes the application of these concepts to a singly-reinforced rectangular section (nonprestressed).

Figure 10.5 illustrates the internal strain and stress distribution for a rectangular section under flexure at the ultimate limit state.

The calculation procedure used to arrive at the ultimate strength should satisfy strain compatibility and force equilibrium and should consider the governing mode of failure. Several calculation procedures can be derived to satisfy these conditions. The calculation procedure described herein illustrates a trial-and-error method.

The trial-and-error procedure involves selecting an assumed depth to the neutral axis c; calculating the strain level in each material using strain compatibility; calculating the associated stress level in each material; and checking internal force equilibrium. If the internal force resultants do not equilibrate, the depth to the neutral axis should be revised and the procedure repeated.

For any assumed depth to the neutral axis c, the strain level in the FRP reinforcement can be computed from Eq. (10-3) presented in Section 10.2.5 and reprinted below for convenience. This equation considers the governing mode of failure for the assumed neutral axis depth. If the left term of the inequality controls, concrete crushing controls flexural failure of the section. If the right term of the inequality controls, FRP failure (rupture or debonding) controls flexural failure of the section

$$\varepsilon_{fe} = \varepsilon_{cu}\left(\frac{d_f - c}{c}\right) - \varepsilon_{bi} \leq \varepsilon_{fd} \qquad (10\text{-}3)$$

The effective stress level in the FRP reinforcement can be found from the strain level in the FRP, assuming perfectly elastic behavior

$$f_{fe} = E_f\varepsilon_{fe} \qquad (10\text{-}9)$$

Based on the strain level in the FRP reinforcement, the strain level in the nonprestressed steel reinforcement can be found from Eq. (10-10) using strain compatibility

$$\varepsilon_s = (\varepsilon_{fe} + \varepsilon_{bi})\left(\frac{d - c}{d_f - c}\right) \qquad (10\text{-}10)$$

The stress in the steel is determined from the strain level in the steel using its stress-strain curve

$$f_s = E_s\varepsilon_s \leq f_y \qquad (10\text{-}11)$$

With the strain and stress level in the FRP and steel reinforcement determined for the assumed neutral axis depth, internal force equilibrium may be checked using Eq. (10-12)

$$c = \frac{A_s f_s + A_f f_{fe}}{\alpha_1 f_c' \beta_1 b} \qquad (10\text{-}12)$$

The terms α_1 and β_1 in Eq. (10-12) are parameters defining a rectangular stress block in the concrete equivalent to the nonlinear distribution of stress. If concrete crushing is the controlling mode of failure (before or after steel yielding), α_1 and β_1 can be taken as the values associated with the Whitney stress block ($\alpha_1 = 0.85$ and β_1 from Section 10.2.7.3 of ACI 318-05). If FRP rupture, cover delamination, or FRP debonding occur, the Whitney stress block will give reasonably accurate results. A more accurate stress block for the strain level reached in the concrete at the ultimate-limit state may be used. Moreover, methods considering a nonlinear stress distribution in the concrete can also be used.

The depth to the neutral axis c is found by simultaneously satisfying Eq. (10-3), (10-9), (10-10), (10-11), and (10-12),
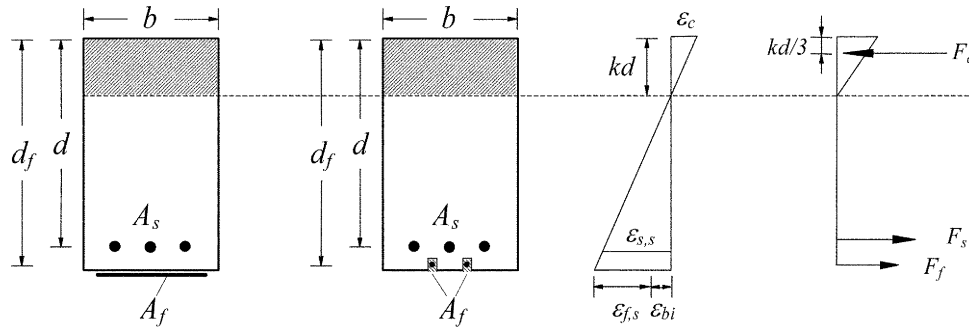
Fig. 10.6—Elastic strain and stress distribution.

thus establishing internal force equilibrium and strain compatibility. To solve for the depth of the neutral axis, *c*, an iterative solution procedure can be used. An initial value for *c* is first assumed and the strains and stresses are calculated using Eq. (10-3), (10-9), (10-10), and (10-11). A revised value for the depth of neutral axis *c* is then calculated from Eq. (10-12). The calculated and assumed values for *c* are then compared. If they agree, then the proper value of *c* is reached. If the calculated and assumed values do not agree, another value for *c* is selected, and the process is repeated until convergence is attained.

The nominal flexural strength of the section with FRP external reinforcement is computed from Eq. (10-13). An additional reduction factor for FRP, ψ_f, is applied to the flexural-strength contribution of the FRP reinforcement. The recommended value of ψ_f is 0.85. This reduction factor for the strength contribution of FRP reinforcement is based on the reliability analysis discussed in Section 9.1, which was based on the experimentally calibrated statistical properties of the flexural strength (Okeil et al. 2007)

$$M_n = A_s f_s \left(d - \frac{\beta_1 c}{2} \right) + \psi_f A_f f_{fe} \left(h - \frac{\beta_1 c}{2} \right) \qquad (10\text{-}13)$$

10.2.10.1 *Stress in steel under service loads*—The stress level in the steel reinforcement can be calculated based on a cracked-section analysis of the FRP-strengthened reinforced concrete section, as indicated by Eq. (10-14)

$$f_{s,s} = \frac{\left[M_s + \varepsilon_{bi} A_f E_f \left(d_f - \frac{kd}{3} \right) \right] (d - kd) E_s}{A_s E_s \left(d - \frac{kd}{3} \right)(d - kd) + A_f E_f \left(d_f - \frac{kd}{3} \right)(d_f - kd)} \qquad (10\text{-}14)$$

The distribution of strain and stress in the reinforced concrete section is shown in Fig. 10.6. Similar to conventional reinforced concrete, the depth to the neutral axis at service, *kd*, can be computed by taking the first moment of the areas of the transformed section. The transformed area of the FRP may be obtained by multiplying the area of FRP by the modular ratio of FRP to concrete. Although this method ignores the difference in the initial strain level of the FRP, the initial strain level does not greatly influence the depth to the neutral axis in the elastic response range of the member.

The stress in the steel under service loads computed from Eq. (10-14) should be compared against the limits described in Section 10.2.8: M_s from Eq. (10-14) equal to the moment due to all sustained loads (dead loads and the sustained portion of the live load) plus the maximum moment induced in a fatigue loading cycle, as shown in Fig. 10.4.

10.2.10.2 *Stress in FRP under service loads*—The stress level in the FRP reinforcement can be computed using Eq. (10-15) with $f_{s,s}$ from Eq. (10-14). Equation (10-15) gives the stress level in the FRP reinforcement under an applied moment within the elastic response range of the member

$$f_{f,s} = f_{s,s} \left(\frac{E_f}{E_s} \right) \frac{d_f - kd}{d - kd} - \varepsilon_{bi} E_f \qquad (10\text{-}15)$$

The stress in the FRP under service loads computed from Eq. (10-15) should be compared against the limits described in Section 10.2.9.

10.3—Prestressed concrete members

This section presents guidance on the effect of adding longitudinal FRP reinforcement to the tension face of a rectangular prestressed concrete member. The general concepts outlined herein can be extended to nonrectangular shapes (T-sections and I-sections) and to members with tension and/or compression nonprestressed steel reinforcement.

10.3.1 *Members with bonded prestressing steel*

10.3.1.1 *Assumptions*—In addition to the basic assumptions for concrete and FRP behavior for a reinforced concrete section listed in Section 10.2.1, the following assumptions are made in calculating the flexural resistance of a prestressed section strengthened with an externally applied FRP system:

• Strain compatibility can be used to determine strain in the externally bonded FRP, strain in the nonprestressed steel reinforcement, and the strain or strain change in the prestressing steel;

• Additional flexural failure mode controlled by prestressing steel rupture should be investigated;

• For cases where the prestressing steel is draped, several sections along the span of the member should be evaluated to verify strength requirements; and

• The initial strain level of the concrete substrate ε_{bi} should be calculated and excluded from the effective

strain in the FRP. The initial strain can be determined from an elastic analysis of the existing member, considering all loads that will be on the member at the time of FRP installation. Analysis should be based on the actual condition of the member (cracked or uncracked section) to determine the substrate initial strain level.

10.3.1.2 *Strain in FRP reinforcement*—The maximum strain that can be achieved in the FRP reinforcement will be governed by strain limitations due to either concrete crushing, FRP rupture, FRP debonding, or prestressing steel rupture. The effective design strain for FRP reinforcement at the ultimate-limit state for failure controlled by concrete crushing can be calculated by use of Eq. (10-16)

$$\varepsilon_{fe} = \varepsilon_{cu}\left(\frac{d_f - c}{c}\right) - \varepsilon_{bi} \le \varepsilon_{fd} \qquad (10\text{-}16)$$

For failure controlled by prestressing steel rupture, Eq. (10-17) and (10-18) can be used. For Grade 270 and 250 ksi (1860 and 1725 MPa) strand, the value of ε_{pu} to be used in Eq. (10-17) is 0.035

$$\varepsilon_{fe} = (\varepsilon_{pu} - \varepsilon_{pi})\left(\frac{d_f - c}{d_p - c}\right) - \varepsilon_{bi} \le \varepsilon_{fd} \qquad (10\text{-}17)$$

in which

$$\varepsilon_{pi} = \frac{P_e}{A_p E_p} + \frac{P_e}{A_c E_c}\left(1 + \frac{e^2}{r^2}\right) \qquad (10\text{-}18)$$

10.3.1.3 *Strength reduction factor*—To maintain a sufficient degree of ductility, the strain in the prestressing steel at the nominal strength should be checked. Adequate ductility is achieved if the strain in the prestressing steel at the nominal strength is at least 0.013. Where this strain cannot be achieved, the strength reduction factor is decreased to account for a less ductile failure. The strength reduction factor for a member prestressed with standard 270 and 250 ksi (1860 and 1725 MPa) prestressing steel is given by Eq. (10-19), where ε_{ps} is the prestressing steel strain at the nominal strength

$$\phi = \begin{cases} 0.90 \text{ for } \varepsilon_{ps} \ge 0.013 \\ 0.65 + \dfrac{0.25(\varepsilon_{ps} - 0.010)}{0.013 - 0.010} \text{ for } 0.010 < \varepsilon_{ps} < 0.013 \\ 0.65 \text{ for } \varepsilon_{ps} \le 0.010 \end{cases} \quad (10\text{-}19)$$

10.3.1.4 *Serviceability*—To avoid inelastic deformations of the strengthened member, the prestressing steel should be prevented from yielding under service load levels. The stress in the steel under service load should be limited per Eq. (10-20). In addition, the compressive stress in the concrete under service load should be limited to 45% of the compressive strength

$$f_{ps,s} \le 0.82 f_{py} \qquad (10\text{-}20a)$$

$$f_{ps,s} \le 0.74 f_{pu} \qquad (10\text{-}20b)$$

When fatigue is a concern (for example, in bridges), the stress in the prestressing steel due to live loads should be limited to 18 ksi (125 MPa) when the radii of prestressing steel curvature exceeds 29 ft (9 m), or to 10 ksi (70 MPa) when the radii of prestressing-steel curvature does not exceed 12 ft (3.6 m). A linear interpolation should be used for radii between 12 and 29 ft (3.6 and 9 m) (AASHTO 2004). These limits have been verified experimentally for prestressed members with harped and straight strands strengthened with externally bonded FRP (Rosenboom and Rizkalla 2006).

10.3.1.5 *Creep-rupture and fatigue stress limits*—To avoid creep-rupture of the FRP reinforcement under sustained stresses or failure due to cyclic stresses and fatigue of the FRP reinforcement, the stress levels in the FRP reinforcement under these stress conditions should not exceed the limits provided in Section 10.2.9.

10.3.1.6 *Nominal strength*—The calculation procedure to compute nominal strength should satisfy strain compatibility and force equilibrium, and should consider the governing mode of failure. The calculation procedure described herein uses a trial-and-error method similar to that discussed in Section 10.2.

For any assumed depth to the neutral axis, c, the effective strain and stress in the FRP reinforcement can be computed from Eq. (10-16) and (10-21), respectively. This equation considers the governing mode of failure for the assumed neutral axis depth. In Eq. (10-16), if the right side of the equality controls, concrete crushing governs flexural failure of the section. If ε_{fd} governs, then FRP rupture or debonding governs the flexural failure of the section

$$f_{fe} = E_f \varepsilon_{fe} \qquad (10\text{-}21)$$

The strain level in the prestressed steel can be found from Eq. (10-22) based on strain compatibility

$$\varepsilon_{ps} = \varepsilon_{pe} + \frac{P_e}{A_c E_c}\left(1 + \frac{e^2}{r^2}\right) + \varepsilon_{pnet} \le 0.035 \qquad (10\text{-}22)$$

in which ε_{pe} is the effective strain in the prestressing steel after losses, and ε_{pnet} is the net tensile strain in the prestressing steel beyond decompression, at the nominal strength. The value of ε_{pnet} will depend on the mode of failure, and can be calculated using Eq. (10-23)

$$\varepsilon_{pnet} = 0.003\left(\frac{d_p - c}{c}\right) \text{ for concrete crushing failure mode} \qquad (10\text{-}23a)$$

$$\varepsilon_{pnet} = (\varepsilon_{fe} + \varepsilon_{bi})\left(\frac{d_p - c}{d_f - c}\right) \qquad (10\text{-}23b)$$

for FRP rupture or debonding failure modes

The stress in the prestressing steel is calculated using the material properties of the steel. For a typical seven-wire low-

relaxation prestressing strand, the stress-strain curve may be approximated by the following equations (PCI 2004)

For Grade 250 ksi steel:

$$f_{ps} = \begin{cases} 28{,}500\varepsilon_{ps} & \text{for } \varepsilon_{ps} \leq 0.0076 \\ & \qquad \text{in in.-lb units} \\ 250 - \dfrac{0.04}{\varepsilon_{ps} - 0.0064} & \text{for } \varepsilon_{ps} > 0.0076 \end{cases}$$

$$\text{(10-24a)}$$

$$f_{ps} = \begin{cases} 196{,}500\varepsilon_{ps} & \text{for } \varepsilon_{ps} \leq 0.0076 \\ & \qquad \text{in SI units} \\ 1720 - \dfrac{0.276}{\varepsilon_{ps} - 0.0064} & \text{for } \varepsilon_{ps} > 0.0076 \end{cases}$$

For Grade 270 ksi steel:

$$f_{ps} = \begin{cases} 28{,}500\varepsilon_{ps} & \text{for } \varepsilon_{ps} \leq 0.0086 \\ & \qquad \text{in in.-lb units} \\ 270 - \dfrac{0.04}{\varepsilon_{ps} - 0.007} & \text{for } \varepsilon_{ps} > 0.0086 \end{cases}$$

$$\text{(10-24b)}$$

$$f_{ps} = \begin{cases} 196{,}500\varepsilon_{ps} & \text{for } \varepsilon_{ps} \leq 0.0086 \\ & \qquad \text{in SI units} \\ 1860 - \dfrac{0.276}{\varepsilon_{ps} - 0.007} & \text{for } \varepsilon_{ps} > 0.0086 \end{cases}$$

With the strain and stress level in the FRP and prestressing steel determined for the assumed neutral axis depth, internal force equilibrium may be checked using Eq. (10-25)

$$c = \frac{A_p f_{ps} + A_f f_{fe}}{\alpha_1 f_c' \beta_1 b} \qquad \text{(10-25)}$$

For the concrete crushing mode of failure, the equivalent compressive stress block factor α_1 can be taken as 0.85, and β_1 can be estimated per ACI 318-05. If FRP rupture, cover delamination, or FRP debonding failure occurs, the use of equivalent rectangular concrete stress block factors is appropriate. Methods considering a nonlinear stress distribution in the concrete can also be used.

The depth to the neutral axis, c, is found by simultaneously satisfying Eq. (10-21) to (10-25), thus establishing internal force equilibrium and strain compatibility. To solve for the depth of the neutral axis, c, an iterative solution procedure can be used. An initial value for c is first assumed, and the strains and stresses are calculated using Eq. (10-21) to (10-24). A revised value for the depth of neutral axis, c, is then calculated from Eq. (10-25). The calculated and assumed values for c are then compared. If they agree, then the proper value of c is reached. If the calculated and assumed values do not agree, another value for c is selected, and the process is repeated until convergence is attained.

The nominal flexural strength of the section with FRP external reinforcement can be computed using Eq. (10-26). The additional reduction factor $\psi_f = 0.85$ is applied to the flexural-strength contribution of the FRP reinforcement

$$M_n = A_p f_{ps}\left(d_p - \frac{\beta_1 c}{2}\right) + \psi_f A_f f_{fe}\left(d_f - \frac{\beta_1 c}{2}\right) \qquad \text{(10-26)}$$

10.3.1.7 *Stress in prestressing steel under service loads—* The stress level in the prestressing steel can be calculated based on the actual condition (cracked or uncracked section) of the strengthened reinforced concrete section. The strain in prestressing steel at service, $\varepsilon_{ps,s}$, can be calculated as

$$\varepsilon_{ps,\,s} = \varepsilon_{pe} + \frac{P_e}{A_c E_c}\left(1 + \frac{e^2}{r^2}\right) + \varepsilon_{pnet,\,s} \qquad \text{(10-27)}$$

in which ε_{pe} is the effective prestressing strain, and $\varepsilon_{pnet,s}$ is the net tensile strain in the prestressing steel beyond decompression at service. The value of $\varepsilon_{pnet,s}$ depends on the effective section properties at service, and can be calculated using Eq. (10-28)

$$\varepsilon_{pnet,\,s} = \frac{M_s e}{E_c I_g} \quad \text{for uncracked section at service} \quad \text{(10-28a)}$$

$$\varepsilon_{pnet,\,s} = \frac{M_{snet} e}{E_c I_{cr}} \quad \text{for cracked section at service} \quad \text{(10-28b)}$$

where M_{snet} is the net service moment beyond decompression. The stress in the prestressing steel under service loads can then be computed from Eq. (10-24), and should be compared against the limits described in Section 10.3.1.4.

10.3.1.8 *Stress in FRP under service loads—*Equation (10-29) gives the stress level in the FRP reinforcement under an applied moment within the elastic response range of the member. The calculation procedure for the initial strain ε_{bi} at the time of FRP installation will depend on the state of the concrete section at the time of FRP installation and at service condition. Prestressed sections can be uncracked at installation/ uncracked at service, uncracked at installation/cracked at service, or cracked at installation/cracked at service. The initial strain level on the bonded substrate, ε_{bi}, can be determined from an elastic analysis of the existing member, considering all loads that will be on the member during the installation of the FRP system. The elastic analysis of the existing member should be based on cracked or uncracked section properties, depending of existing conditions. In most cases, the initial strain before cracking is relatively small, and may conservatively be ignored

$$f_{f,\,s} = \left(\frac{E_f}{E_c}\right)\frac{M_s y_b}{I} - \varepsilon_{bi} E_f \qquad \text{(10-29)}$$

Depending on the actual condition at service (cracked or uncracked section), the moment of inertia I can be taken as the moment of inertia of the uncracked section transformed to concrete, I_{tr}, or the moment of inertia of the cracked section transformed to concrete, I_{cr}. The variable y_b is the

distance from the centroidal axis of the gross section, neglecting reinforcement, to the extreme bottom fiber. The computed stress in the FRP under service loads should not exceed the limits provided in Section 10.2.9.

CHAPTER 11—SHEAR STRENGTHENING

FRP systems have been shown to increase the shear strength of existing concrete beams and columns by wrapping or partially wrapping the members (Malvar et al. 1995; Chajes et al. 1995; Norris et al. 1997; Kachlakev and McCurry 2000). Orienting FRP fibers transverse to the axis of the member or perpendicular to potential shear cracks is effective in providing additional shear strength (Sato et al. 1996). Increasing the shear strength can also result in flexural failures, which are relatively more ductile in nature compared with shear failures.

11.1—General considerations

This chapter presents guidance on the calculation of added shear strength resulting from the addition of FRP shear reinforcement to a reinforced concrete beam or column. The additional shear strength that can be provided by the FRP system is based on many factors, including geometry of the beam or column, wrapping scheme, and existing concrete strength, but should always be limited in accordance with the provisions of Chapter 9.

Shear strengthening using external FRP may be provided at locations of expected plastic hinges or stress reversal and for enhancing post-yield flexural behavior of members in moment frames resisting seismic loads only by completely wrapping the section. For external FRP reinforcement in the form of discrete strips, the center-to-center spacing between the strips should not exceed the sum of $d/4$ plus the width of the strip.

11.2—Wrapping schemes

The three types of FRP wrapping schemes used to increase the shear strength of prismatic, rectangular beams, or columns are illustrated in Fig. 11.1. Completely wrapping the FRP system around the section on all four sides is the most efficient wrapping scheme and is most commonly used in column applications where access to all four sides of the column is usually available. In beam applications where an integral slab makes it impractical to completely wrap the member, the shear strength can be improved by wrapping the FRP system around three sides of the member (U-wrap) or bonding to two opposite sides of the member.

Although all three techniques have been shown to improve the shear strength of a member, completely wrapping the section is the most efficient, followed by the three-sided U-wrap. Bonding to two sides of a beam is the least efficient scheme.

In all wrapping schemes, the FRP system can be installed continuously along the span of a member or placed as discrete strips. As discussed in Section 9.3.3, the use of continuous FRP reinforcement that completely encases a member and potentially prevents migration of moisture is discouraged.
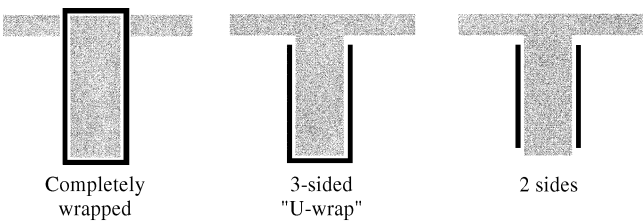
Fig. 11.1—Typical wrapping schemes for shear strengthening using FRP laminates.

Table 11.1—Recommended additional reduction factors for FRP shear reinforcement

$\psi_f = 0.95$	Completely wrapped members
$\psi_f = 0.85$	Three-side and two-opposite-sides schemes

11.3—Nominal shear strength

The design shear strength of a concrete member strengthened with an FRP system should exceed the required shear strength (Eq. (11-1)). The required shear strength of an FRP-strengthened concrete member should be computed with the load factors required by ACI 318-05. The design shear strength should be calculated by multiplying the nominal shear strength by the strength reduction factor ϕ, as specified by ACI 318-05

$$\phi V_n \geq V_u \qquad (11\text{-}1)$$

The nominal shear strength of an FRP-strengthened concrete member can be determined by adding the contribution of the FRP external shear reinforcement to the contributions from the reinforcing steel (stirrups, ties, or spirals) and the concrete (Eq. (11-2)). An additional reduction factor ψ_f is applied to the contribution of the FRP system

$$\phi V_n = \phi(V_c + V_s + \psi_f V_f) \qquad (11\text{-}2)$$

where V_c is calculated using Eq. (11-3) through Eq. (11-8) of ACI 318-05, and V_s is calculated using Section 11.5.7.2 of ACI 318-05. For prestressed members, V_c is the minimum of V_{ci} of Eq. (11-10) and V_{cw} of Eq. (11-12) of ACI 318-05. The latter may also be computed based on Eq. (11-9) when applicable (Reed et al. 2005).

Based on a reliability analysis using data from Bousselham and Chaallal (2006), Deniaud and Cheng (2001, 2003), Funakawa et al. (1997), Matthys and Triantafillou (2001), and Pellegrino and Modena (2002), the reduction factor ψ_f of 0.85 is recommended for the three-sided FRP U-wrap or two-opposite-sides strengthening schemes. Insufficient experimental data exist to perform a reliability analysis for fully-wrapped sections; however, there should be less variability with this strengthening scheme as it is less bond independent, and therefore, the reduction factor ψ_f of 0.95 is recommended. The ψ_f factor was calibrated based on design material properties. These recommendations are given in Table 11.1.

11.4—FRP contribution to shear strength

Figure 11.2 illustrates the dimensional variables used in shear-strengthening calculations for FRP laminates. The contribution of the FRP system to shear strength of a member is based on the fiber orientation and an assumed crack pattern (Khalifa et al. 1998). The shear strength provided by the FRP reinforcement can be determined by calculating the force resulting from the tensile stress in the FRP across the assumed crack. The shear contribution of the FRP shear reinforcement is then given by Eq. (11-3)

$$V_f = \frac{A_{fv}f_{fe}(\sin\alpha + \cos\alpha)d_{fv}}{s_f} \qquad (11\text{-}3)$$

where

$$A_{fv} = 2nt_fw_f \qquad (11\text{-}4)$$

The tensile stress in the FRP shear reinforcement at nominal strength is directly proportional to the level of strain that can be developed in the FRP shear reinforcement at nominal strength

$$f_{fe} = \varepsilon_{fe}E_f \qquad (11\text{-}5)$$

11.4.1 *Effective strain in FRP laminates*—The effective strain is the maximum strain that can be achieved in the FRP system at the nominal strength and is governed by the failure mode of the FRP system and of the strengthened reinforced concrete member. The licensed design professional should consider all possible failure modes and use an effective strain representative of the critical failure mode. The following subsections provide guidance on determining this effective strain for different configurations of FRP laminates used for shear strengthening of reinforced concrete members.

11.4.1.1 *Completely wrapped members*—For reinforced concrete column and beam members completely wrapped by FRP, loss of aggregate interlock of the concrete has been observed to occur at fiber strains less than the ultimate fiber strain. To preclude this mode of failure, the maximum strain used for design should be limited to 0.4% for members that can be completely wrapped with FRP (Eq. (11-6a))

$$\varepsilon_{fe} = 0.004 \le 0.75\varepsilon_{fu} \qquad (11\text{-}6a)$$

This strain limitation is based on testing (Priestley et al. 1996) and experience. Higher strains should not be used for FRP shear-strengthening applications.

11.4.1.2 *Bonded U-wraps or bonded face plies*—FRP systems that do not enclose the entire section (two- and three-sided wraps) have been observed to delaminate from the concrete before the loss of aggregate interlock of the section. For this reason, bond stresses have been analyzed to determine the usefulness of these systems and the effective strain level that can be achieved (Triantafillou 1998a). The effective strain is calculated using a bond-reduction coefficient κ_v applicable to shear

$$\varepsilon_{fe} = \kappa_v\varepsilon_{fu} \le 0.004 \qquad (11\text{-}6b)$$
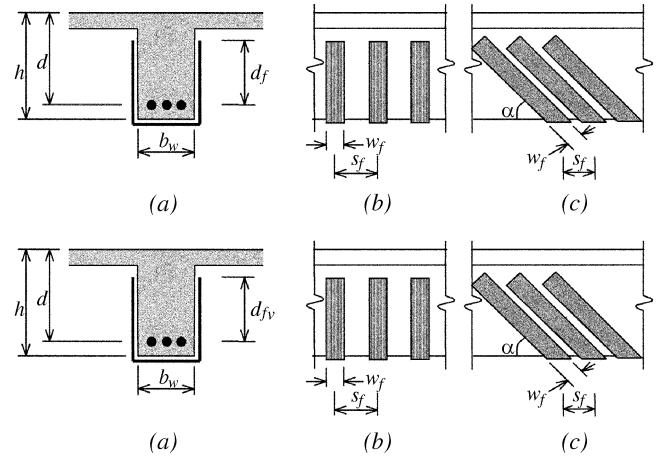
Fig. 11.2—Illustration of the dimensional variables used in shear-strengthening calculations for repair, retrofit, or strengthening using FRP laminates.

The bond-reduction coefficient is a function of the concrete strength, the type of wrapping scheme used, and the stiffness of the laminate. The bond-reduction coefficient can be computed from Eq. (11-7) through (11-10) (Khalifa et al. 1998)

$$\kappa_v = \frac{k_1k_2L_e}{468\varepsilon_{fu}} \le 0.75 \quad \text{in in.-lb units}$$

$$\kappa_v = \frac{k_1k_2L_e}{11{,}900\varepsilon_{fu}} \le 0.75 \quad \text{in SI units} \qquad (11\text{-}7)$$

The active bond length L_e is the length over which the majority of the bond stress is maintained. This length is given by Eq. (11-8)

$$L_e = \frac{2500}{(n_ft_fE_f)^{0.58}} \quad \text{in in.-lb units}$$

$$L_e = \frac{23{,}300}{(n_ft_fE_f)^{0.58}} \quad \text{in SI units} \qquad (11\text{-}8)$$

The bond-reduction coefficient also relies on two modification factors, k_1 and k_2, that account for the concrete strength and the type of wrapping scheme used, respectively. Expressions for these modification factors are given in Eq. (11-9) and (11-10)

$$k_1 = \left(\frac{f_c'}{4000}\right)^{2/3} \quad \text{in in.-lb units}$$

$$k_1 = \left(\frac{f_c'}{27}\right)^{2/3} \quad \text{in SI units} \qquad (11\text{-}9)$$

$$k_2 = \begin{cases} \dfrac{d_{fv} - L_e}{d_{fv}} & \text{for U-wraps} \\[2ex] \dfrac{d_{fv} - 2L_e}{d_{fv}} & \text{for two sides bonded} \end{cases} \qquad (11\text{-}10)$$

The methodology for determining κ_v has been validated for members in regions of high shear and low moment, such as monotonically loaded simply supported beams. Although the methodology has not been confirmed for shear strengthening in areas subjected to combined high flexural and shear stresses or in regions where the web is primarily in compression (negative moment regions), it is suggested that κ_v is sufficiently conservative for such cases. The design procedures outlined herein have been developed by a combination of analytical and empirical results (Khalifa et al. 1998).

Mechanical anchorages can be used at termination points to develop larger tensile forces (Khalifa et al. 1999). The effectiveness of such mechanical anchorages, along with the level of tensile stress they can develop, should be substantiated through representative physical testing. In no case, however, should the effective strain in FRP laminates exceed 0.004.

11.4.2 *Spacing*—Spaced FRP strips used for shear strengthening should be investigated to evaluate their contribution to the shear strength. Spacing should adhere to the limits prescribed by ACI 318-05 for internal steel shear reinforcement. The spacing of FRP strips is defined as the distance between the centerline of the strips.

11.4.3 *Reinforcement limits*—The total shear strength provided by reinforcement should be taken as the sum of the contribution of the FRP shear reinforcement and the steel shear reinforcement. The sum of the shear strengths provided by the shear reinforcement should be limited based on the criteria given for steel alone in ACI 318-05, Section 11.5.6.9. This limit is stated in Eq. (11-11)

$$V_s + V_f \leq 8\sqrt{f_c'}\,b_w d \quad \text{in in-lb units}$$
$$V_s + V_f \leq 0.66\sqrt{f_c'}\,b_w d \quad \text{in SI units}$$
(11-11)

CHAPTER 12—STRENGTHENING OF MEMBERS SUBJECTED TO AXIAL FORCE OR COMBINED AXIAL AND BENDING FORCES

Confinement of reinforced concrete columns by means of FRP jackets can be used to enhance their strength and ductility. An increase in capacity is an immediate outcome typically expressed in terms of improved peak load resistance. Ductility enhancement, on the other hand, requires more complex calculations to determine the ability of a member to sustain rotation and drift without a substantial loss in strength. This chapter applies only to members confined with FRP systems.

12.1—Pure axial compression

FRP systems can be used to increase the axial compression strength of a concrete member by providing confinement with an FRP jacket (Nanni and Bradford 1995; Toutanji 1999). Confining a concrete member is accomplished by orienting the fibers transverse to the longitudinal axis of the member. In this orientation, the transverse or hoop fibers are similar to conventional spiral or tie reinforcing steel. Any contribution of longitudinally aligned fibers to the axial compression strength of a concrete member should be neglected.
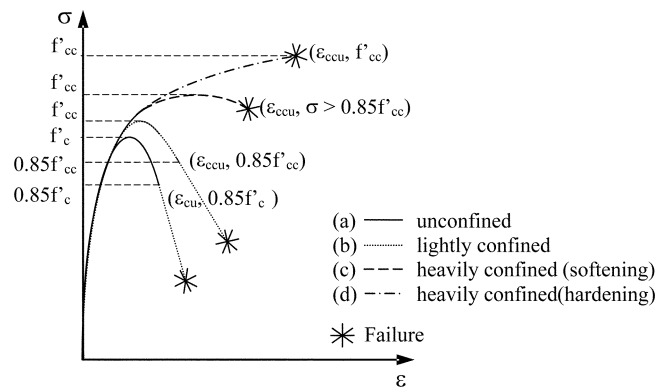
Fig. 12.1—Schematic stress-strain behavior of unconfined and confined RC columns (Rocca et al. 2006).

FRP jackets provide passive confinement to the compression member, remaining unstressed until dilation and cracking of the wrapped compression member occur. For this reason, intimate contact between the FRP jacket and the concrete member is critical.

Depending on the level of confinement, the uniaxial stress-strain curve of a reinforced concrete column could be depicted by one of the curves in Fig. 12.1, where f_c' and f_{cc}' represent the peak concrete strengths for unconfined and confined cases, respectively. These strengths are calculated as the peak load minus the contribution of the steel reinforcement, all divided by the cross-sectional area of the concrete. The ultimate strain of the unconfined member corresponding to $0.85f_c'$ (Curve (a)) is ε_{cu}. The strain ε_{ccu} corresponds to: a) $0.85f_{cc}'$ in the case of the lightly confined member (Curve (b)); and b) the failure strain in both the heavily confined-softening case (the failure stress is larger than $0.85f_{cc}'$—Curve (c)) or in the heavily confined-hardening case (Curve (d)).

The definition of ε_{ccu} at $0.85f_{cc}'$ or less is arbitrary, although consistent with modeling of conventional concrete (Hognestad 1951), and such that the descending branch of the stress-strain curve at that level of stress ($0.85f_{cc}'$ or higher) is not as sensitive to the test procedure in terms of rate of loading and stiffness of the equipment used.

The axial compressive strength of a nonslender, normal-weight concrete member confined with an FRP jacket may be calculated using the confined concrete strength (Eq. (12-1)). The axial force acting on an FRP-strengthened concrete member should be computed using the load factors required by ACI 318-05, and the axial compression strength should be calculated using the strength reduction factors ϕ for spiral and tied members required by ACI 318-05.

For nonprestressed members with existing steel spiral reinforcement

$$\phi P_n = 0.85\phi[0.85f_{cc}'(A_g - A_{st}) + f_y A_{st}]$$
(12-1a)

For nonprestressed members with existing steel-tie reinforcement

$$\phi P_n = 0.8\phi[0.85f_{cc}'(A_g - A_{st}) + f_y A_{st}]$$
(12-1b)

Several models that simulate the stress-strain behavior of FRP-confined compression sections are available in the literature (Teng et al. 2002; De Lorenzis and Tepfers 2003; Lam and Teng 2003a). The stress-strain model by Lam and Teng (2003a,b) for FRP-confined concrete has been adopted by this committee and is illustrated in Fig. 12.2 and computed using the following expressions

$$f_c = \begin{cases} E_c\varepsilon_c - \dfrac{(E_c - E_2)^2}{4f_c'}\varepsilon_c^2 & 0 \le \varepsilon_c \le \varepsilon_t' \\ f_c' + E_2\varepsilon_c & \varepsilon_t' \le \varepsilon_c \le \varepsilon_{ccu} \end{cases} \quad (12\text{-}2a)$$

$$E_2 = \frac{f_{cc}' - f_c'}{\varepsilon_{ccu}} \quad (12\text{-}2b)$$

$$\varepsilon_t' = \frac{2f_c'}{E_c - E_2} \quad (12\text{-}2c)$$

The maximum confined concrete compressive strength f_{cc}' and the maximum confinement pressure f_l are calculated using Eq. (12-3) and (12-4), respectively (Lam and Teng 2003a,b) with the inclusion of an additional reduction factor $\psi_f = 0.95$. The value of this reduction factor is based on the committee's judgment

$$f_{cc}' = f_c' = \psi_f 3.3\kappa_a f_l \quad (12\text{-}3)$$

$$f_l = \frac{2E_f n t_f \varepsilon_{fe}}{D} \quad (12\text{-}4)$$

In Eq. (12-3), f_c' is the unconfined cylinder compressive strength of concrete, and the efficiency factor κ_a accounts for the geometry of the section, circular and noncircular, as defined in Sections 12.1.1 and 12.1.2. In Eq. (12-4), the effective strain level in the FRP at failure ε_{fe} is given by

$$\varepsilon_{fe} = \kappa_\varepsilon \varepsilon_{fu} \quad (12\text{-}5)$$

The FRP strain efficiency factor κ_ε accounts for the premature failure of the FRP system (Pessiki et al. 2001), possibly due to the multiaxial state of stress to which it is subjected as opposed to the pure axial tension used for material characterization. This behavior may also be related to stress concentration regions caused by cracking of the concrete as it dilates. Based on experimental calibration using mainly CFRP-confined concrete specimens, an average value of 0.586 was computed for κ_ε by Lam and Teng (2003a). Similarly, a database of 251 test results (Harries and Carey 2003) computed a value of $\kappa_\varepsilon = 0.58$ while experimental tests on medium- and large-scale columns resulted in values of $\kappa_\varepsilon = 0.57$ and 0.61, respectively (Carey and Harries 2005).

Based on tests by Lam and Teng (2003a,b), the ratio f_l/f_c' should not be less than 0.08. This is the minimum level of confinement required to assure a nondescending second

Fig. 12.2—Lam and Teng's stress-strain model for FRP-confined concrete (Lam and Teng 2003a).

branch in the stress-strain performance, as shown by Curve (d) in Fig. 12.1. This limitation was later confirmed for circular cross sections by Spoelstra and Monti (1999) using their analytical model. A strain efficiency factor κ_ε of 0.55 and a minimum confinement ratio f_l/f_c' of 0.08 (that is, $f_{fu}nt_f/(f_c'D) \ge 0.073$) should be used.

The maximum compressive strain in the FRP-confined concrete ε_{ccu} can be found using Eq. (12-6). This strain should be limited to the value given in Eq. (12-7) to prevent excessive cracking and the resulting loss of concrete integrity. When this limit is applicable, the corresponding maximum value of f_{cc}' should be recalculated from the stress-strain curve (Concrete Society 2004).

$$\varepsilon_{ccu} = \varepsilon_c' \left(1.50 + 12\kappa_b \frac{f_l}{f_c'} \left(\frac{\varepsilon_{fe}}{\varepsilon_c'}\right)^{0.45}\right) \quad (12\text{-}6)$$

$$\varepsilon_{ccu} \le 0.01 \quad (12\text{-}7)$$

In Eq. (12-6), the efficiency factor κ_b accounts for the geometry of the section in the calculation of the ultimate axial strain, as defined in Sections 12.1.1 and 12.1.2.

Strength enhancement for compression members with f_c' of 10,000 psi (70 MPa) or higher has not been experimentally verified.

12.1.1 *Circular cross sections*—FRP jackets are most effective at confining members with circular cross sections (Demers and Neale 1999; Pessiki et al. 2001; Harries and Carey 2003; Youssef 2003; Matthys et al. 2005; Rocca et al. 2006). The FRP system provides a circumferentially uniform confining pressure to the radial expansion of the compression member when the fibers are aligned transverse to the longitudinal axis of the member. For circular cross sections, the shape factors κ_a and κ_b in Eq. (12-3) and (12-6), respectively, can be taken as 1.0.

12.1.2 *Noncircular cross sections*—Testing has shown that confining square and rectangular members with FRP jackets can provide marginal increases in the maximum axial compressive strength f_{cc}' of the member (Pessiki et al. 2001; Wang and Restrepo 2001; Harries and Carey 2003; Youssef 2003; Rocca et al. 2008). The provisions in this guide are not recommended for members featuring side aspect ratios h/b greater than 2.0, or face dimensions b or h exceeding 36 in. (900 mm), unless testing demonstrates their effectiveness.

Fig. 12.3—Equivalent circular cross section (Lam and Teng 2003b).

For noncircular cross sections, f_l in Eq. (12-4) corresponds to the maximum confining pressure of an equivalent circular cross section with diameter D equal to the diagonal of the rectangular cross section

$$D = \sqrt{b^2 + h^2} \tag{12-8}$$

The shape factors κ_a in Eq. (12-3) and κ_b in Eq. (12-6) depend on two parameters: the cross-sectional area of effectively confined concrete A_e, and the side-aspect ratio h/b, as shown in Eq. (12-9) and (12-10), respectively
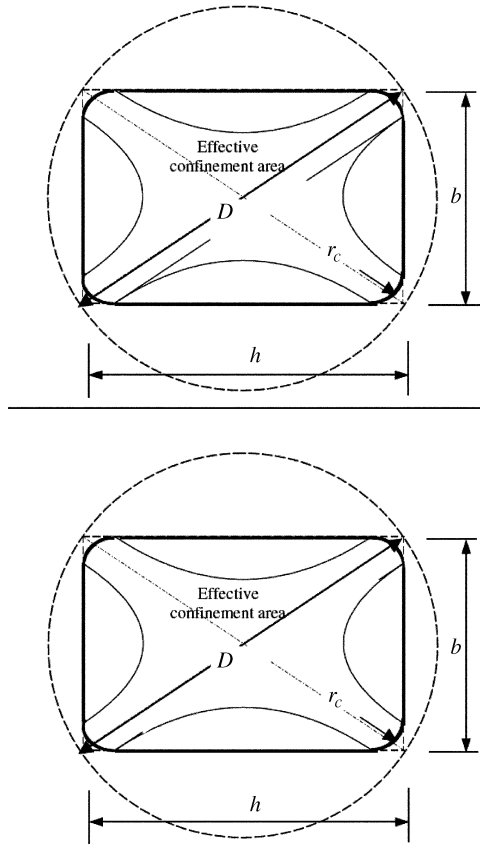
$$\kappa_a = \frac{A_e}{A_c}\left(\frac{b}{h}\right)^2 \tag{12-9}$$

$$\kappa_b = \frac{A_e}{A_c}\left(\frac{h}{b}\right)^{0.5} \tag{12-10}$$

The generally accepted theoretical approach for the definition of A_e consists of four parabolas within which the concrete is fully confined, and outside of which negligible confinement occurs (Fig. 12.3). The shape of the parabolas and the resulting effective confinement area is a function of the dimensions of the column (b and h), the radius of the corners r_c, and the longitudinal steel reinforcement ratio ρ_g, and can be expressed as

$$\frac{A_e}{A_c} = \frac{1 - \dfrac{\left[\left(\dfrac{b}{h}\right)(h - 2r_c)^2 + \left(\dfrac{h}{b}\right)(b - 2r_c)^2\right]}{3A_g} - \rho_g}{1 - \rho_g} \tag{12-11}$$

12.1.3 *Serviceability considerations*—As loads approach factored load levels, damage to the concrete in the form of significant cracking in the radial direction might occur. The FRP jacket contains the damage and maintains the structural integrity of the column. At service load levels, however, this type of damage should be avoided. In this way, the FRP jacket will only act during overloading conditions that are temporary in nature.

To ensure that radial cracking will not occur under service loads, the transverse strain in the concrete should remain below its cracking strain at service load levels. This corresponds to limiting the compressive stress in the concrete to $0.65f_c'$. In addition, the service stress in the longitudinal steel should remain below $0.60f_y$ to avoid plastic deformation under sustained or cyclic loads. By maintaining the specified stress in the concrete at service, the stress in the FRP jacket will be relatively low. The jacket is only stressed to significant levels when the concrete is transversely strained above the cracking strain and the transverse expansion becomes large. Service load stresses in the FRP jacket should never exceed the creep-rupture stress limit. In addition, axial deformations under service loads should be investigated to evaluate their effect on the performance of the structure.

12.2—Combined axial compression and bending

Wrapping with an FRP jacket can also provide strength enhancement for a member subjected to combined axial compression and flexure (Nosho 1996; Saadatmanesh et al. 1996; Chaallal and Shahawy 2000; Sheikh and Yau 2002; Iacobucci et al. 2003; Bousias et al. 2004; Elnabelsy and Saatcioglu 2004; Harajli and Rteil 2004; Sause et al. 2004; Memon and Sheikh 2005).

For the purpose of predicting the effect of FRP confinement on strength enhancement, Eq. (12-1) is applicable when the eccentricity present in the member is less than or equal to $0.1h$. When the eccentricity is larger than $0.1h$, the methodology and equations presented in Section 12.1 can be used to determine the concrete material properties of the member cross section under compressive stress. Based on that, the P-M diagram for the FRP-confined member can be constructed using well-established procedures (Bank 2006).

The following limitations apply for members subjected to combined axial compression and bending:

- The effective strain in the FRP jacket should be limited to the value given in Eq. (12-12) to ensure the shear integrity of the confined concrete

$$\varepsilon_{fe} = 0.004 \le \kappa_\varepsilon \varepsilon_{fu} \tag{12-12}$$

- The strength enhancement can only be considered when the applied ultimate axial force and bending moment, P_u and M_u, fall above the line connecting the origin and the balanced point in the P-M diagram for
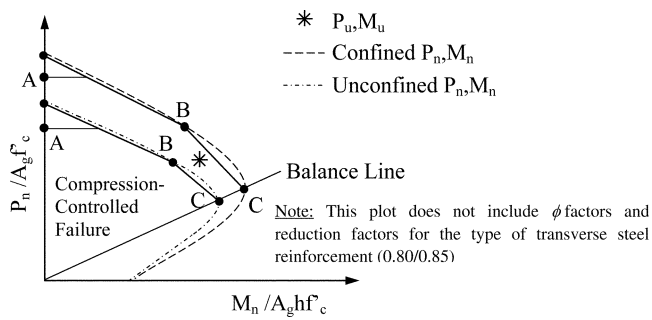
Fig. 12.4—Representative interaction diagram.

the unconfined member (Fig. 12.4). This limitation stems from the fact that strength enhancement is only of significance for members in which compression failure is the controlling mode (Bank 2006).

P-M diagrams may be developed by satisfying strain compatibility and force equilibrium using the model for the stress-strain behavior for FRP-confined concrete presented in Eq. (12-2). For simplicity, the portion of the unconfined and confined P-M diagrams corresponding to compression-controlled failure can be reduced to two bilinear curves passing through three points (Fig 12.4). For values of eccentricity greater than $0.1h$ and up to the point corresponding to the balanced condition, the methodology provided in Appendix A may be used for the computation of a simplified interaction diagram. The values of the ϕ factors as established in ACI 318-05 for both circular and noncircular cross sections apply.

12.3—Ductility enhancement

Increased ductility of a section results from the ability to develop greater compressive strains in the concrete before compressive failure (Seible et al. 1997). The FRP jacket can also serve to delay buckling of longitudinal steel reinforcement in compression and to clamp lap splices of longitudinal steel reinforcement.

For seismic applications, FRP jackets should be designed to provide a confining stress sufficient to develop concrete compression strains associated with the displacement demands. The maximum compressive strain in concrete for an FRP-confined member can be found by use of Eq. (12-6). Shear forces should also be evaluated in accordance with Chapter 11 to prevent brittle shear failure in accordance with ACI 318-05.

12.3.1 *Circular cross sections*—The maximum compressive strain for an FRP-confined members with circular cross sections can be found from Eq. (12-6) with f'_{cc} from Eq. (12-3) and using $\kappa_b = 1.0$.

12.3.2 *Noncircular cross sections*—The maximum compressive strain for FRP-confined members with square or rectangular sections can be found from Eq. (12-6), with f'_{cc} from Eq. (12-3), and using κ_b as given in Eq. (12-10). The confining effect of FRP jackets should be assumed to be negligible for rectangular sections with aspect ratio h/b exceeding 2.0, or face dimensions b or h exceeding 36 in. (900 mm), unless testing demonstrates their effectiveness.

12.4—Pure axial tension

FRP systems can be used to provide additional tensile strength to a concrete member. Due to the linear-elastic nature of FRP materials, the tensile contribution of the FRP system is directly related to its strain level and is calculated using Hooke's Law.

The level of tension provided by the FRP is limited by the design tensile strength of the FRP and the ability to transfer stresses into the substrate through bond (Nanni et al. 1997). The effective strain in the FRP can be determined based on the criteria given for shear strengthening in Eq. (11-6) through (11-9). The value of k_1 in Eq. (11-7) can be taken as 1.0. A minimum bond length of $2L_e$ (where L_e is the active bond length defined previously in Eq. (11-8)) should be provided to develop this level of strain.

CHAPTER 13—FRP REINFORCEMENT DETAILS

This chapter offers guidance for detailing externally bonded FRP reinforcement. Detailing will typically depend on the geometry of the structure, the soundness and quality of the substrate, and the levels of load that are to be sustained by the FRP sheets or laminates. Many bond-related failures can be avoided by following these general guidelines for detailing FRP sheets or laminates:

* Do not turn inside corners such as at the intersection of beams and joists with the underside of slabs;
* Provide a minimum 1/2 in. (13 mm) radius when the sheet is wrapped around outside corners;
* Provide adequate development length; and
* Provide sufficient overlap when splicing FRP plies.

13.1—Bond and delamination

The actual distribution of bond stress in an FRP laminate is complicated by cracking of the substrate concrete. The general elastic distribution of interfacial shear stress and normal stress along an FRP laminate bonded to uncracked concrete is shown in Fig. 13.1.

For an FRP system installed according to Part 3 of this guide, the weak link in the concrete/FRP interface is the concrete. The soundness and tensile strength of the concrete substrate will limit the overall effectiveness of the bonded FRP system. Design requirements to mitigate FRP debonding failure modes are discussed in Section 10.1.1.

13.1.1 *FRP debonding*—In reinforced concrete members having relatively long shear spans or where the end peeling (refer to Section 13.1.2) has been effectively mitigated, debonding may initiate at flexural cracks, flexural/shear cracks, or both, near the region of maximum moment. For point-loading condition, the shear span is the distance from a point load to the nearest support. Under loading, these cracks open and induce high interfacial shear stress that causes FRP debonding that propagates across the shear span in the direction of decreasing moment. Typically, this failure does not engage the aggregate in the concrete, progressing through the thin mortar-rich layer comprising the surface of the concrete beam. This failure mode is exacerbated in regions having a high shear-moment ratio.
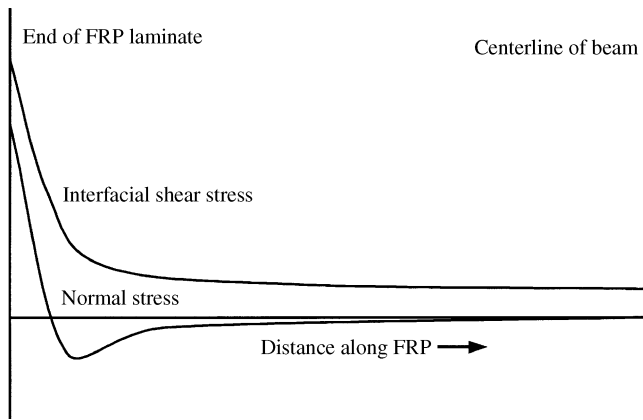
Fig. 13.1—Conceptual interfacial shear and normal stress distributions along the length of a bonded FRP laminate (Roberts and Haji-Kazemi 1989; Malek et al. 1998).
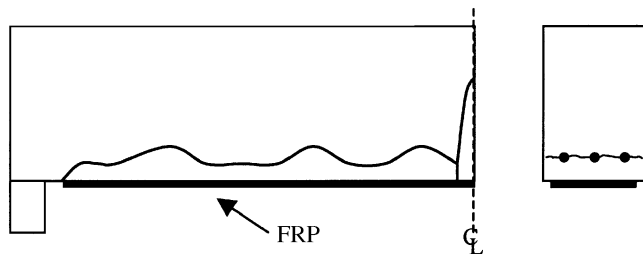

Fig. 13.2—Delamination caused by tension failure of the concrete cover.

Mechanical anchorages can be effective in increasing stress transfer (Khalifa et al. 1999), although their efficacy is believed to result from their ability to resist the tensile normal stresses rather than in enhancing the interfacial shear capacity (Quattlebaum et al. 2005). Limited data suggest a modest increase in FRP strain at debonding can be achieved with the provision of transverse anchoring FRP wraps (Reed et al. 2005). The performance of any anchorage system should be substantiated through testing.

13.1.2 *FRP end peeling*—FRP end peeling (also referred to as concrete cover delamination) can also result from the normal stresses developed at the ends of externally bonded FRP reinforcement. With this type of delamination, the existing internal reinforcing steel essentially acts as a bond breaker in a horizontal plane, and the concrete cover pulls away from the rest of the beam (this may be exacerbated if epoxy-coated steel reinforcement was used in the existing member), as shown in Fig. 13.2.

The tensile concrete cover splitting failure mode is controlled, in part, by the level of stress at the termination point of the FRP. In general, the FRP end peeling failure mode can be mitigated by using anchorage (transverse FRP stirrups), by minimizing the stress at the FRP curtailment by locating the curtailment as close to the region of zero moment as possible, or by both. When the factored shear force at the termination point is greater than 2/3 the concrete shear strength ($V_u > 0.67V_c$), the FRP laminates should be anchored with transverse reinforcement to prevent the concrete cover layer from splitting. The area of the transverse clamping FRP U-wrap reinforcement $A_{f,anchor}$ can be determined in accordance with Eq. (13-1) (Reed et al. 2005)

$$A_{fanchor} = \frac{(A_f f_{fu})_{longitudinal}}{(E_f \kappa_v \varepsilon_{fu})_{anchor}} \qquad (13\text{-}1)$$

In which κ_v is calculated using Eq. (11-7). Instead of detailed analysis, the following general guidelines for the location of cutoff points for the FRP laminate can be used to avoid end peeling failure mode:

- For simply supported beams, a single-ply FRP laminate should be terminated at least a distance equal to l_{df} past the point along the span corresponding to the cracking moment M_{cr}. For multiple-ply laminates, the termination points of the plies should be tapered. The outermost ply should be terminated not less than l_{df} past the point along the span corresponding to the cracking moment. Each successive ply should be terminated not less than an additional 6 in. (150 mm) beyond the previous ply (Fig. 13.3); and

- For continuous beams, a single-ply FRP laminate should be terminated $d/2$ or 6 in. (150 mm) minimum beyond the inflection point (point of zero moment resulting from factored loads). For multiple-ply laminates, the termination points of the plies should be tapered. The outermost ply should be terminated no less than 6 in. (150 mm) beyond the inflection point. Each successive ply should be terminated no less than an additional 6 in. (150 mm) beyond the previous ply. For example, if a three-ply laminate is required, the ply directly in contact with the concrete substrate should be terminated at least 18 in. (450 mm) past the inflection point (Fig. 13.3). These guidelines apply for positive and negative moment regions.

13.1.3 *Development length*—The bond capacity of FRP is developed over a critical length l_{df}. To develop the effective FRP stress at a section, the available anchorage length of FRP should exceed the value given by Eq. (13-2) (Teng et al. 2001).

$$l_{df} = 0.057\sqrt{\frac{nE_f t_f}{\sqrt{f_c'}}} \quad \text{in in.-lb units}$$

$$l_{df} = \sqrt{\frac{nE_f t_f}{\sqrt{f_c'}}} \quad \text{in SI units} \qquad (13\text{-}2)$$

13.2—Detailing of laps and splices

Splices of FRP laminates should be provided only as permitted on drawings, specifications, or as authorized by the licensed design professional as recommended by the system manufacturer.

The fibers of FRP systems should be continuous and oriented in the direction of the largest tensile forces. Fiber continuity can be maintained with a lap splice. For FRP systems, a lap splice should be made by overlapping the fibers along their length. The required overlap, or lap-splice

(a) Simply supported beam   *(b) Continuous beam*
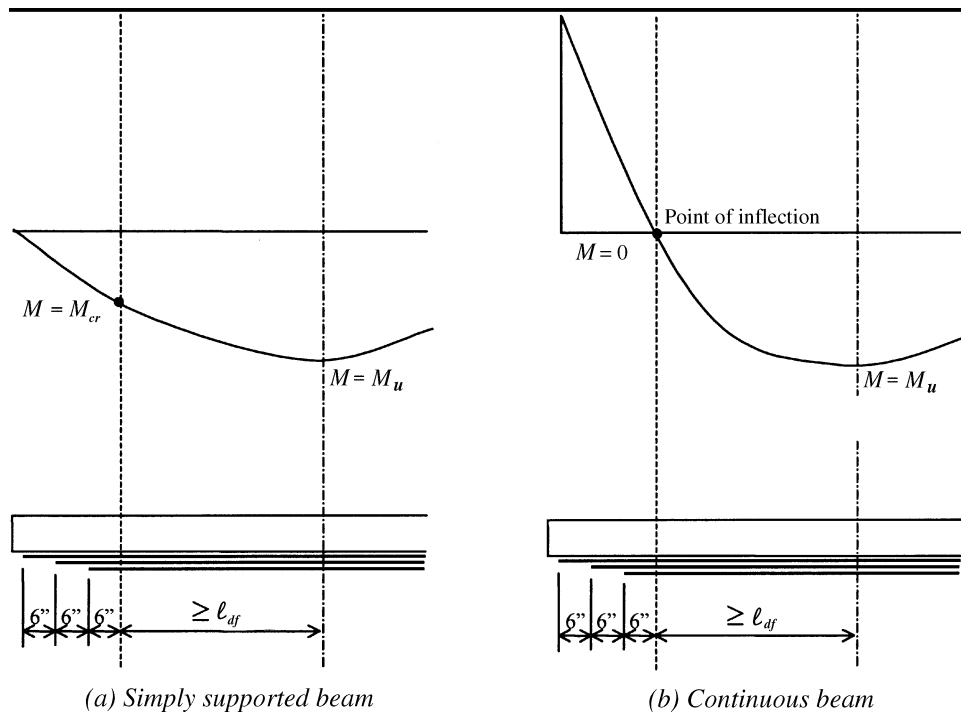
Fig. 13.3—Graphical representation of the guidelines for allowable termination points of a three-ply FRP laminate.

length, depends on the tensile strength and thickness of the FRP material system and on the bond strength between adjacent layers of FRP laminates. Sufficient overlap should be provided to promote the failure of the FRP laminate before debonding of the overlapped FRP laminates. The required overlap for an FRP system should be provided by the material manufacturer and substantiated through testing that is independent of the manufacturer.

Jacket-type FRP systems used for column members should provide appropriate development area at splices, joints, and termination points to ensure failure through the FRP jacket thickness rather than failure of the spliced sections.

For unidirectional FRP laminates, lap splices are required only in the direction of the fibers. Lap splices are not required in the direction transverse to the fibers. FRP laminates consisting of multiple unidirectional sheets oriented in more than one direction or multidirectional fabrics require lap splices in more than one direction to maintain the continuity of the fibers and the overall strength of the FRP laminates.

13.3—Bond of near-surface-mounted systems

For NSM systems, the minimum dimension of the grooves should be taken at least 1.5 times the diameter of the FRP bar (De Lorenzis and Nanni 2001b; Hassan and Rizkalla 2003). When a rectangular bar with large aspect ratio is used, however, the limit may lose significance due to constructibility. In such a case, a minimum groove size of $3.0a_b \times 1.5b_b$, as depicted in Fig. 13.4, is suggested, where a_b is the smallest bar dimension. The minimum clear groove spacing for NSM FRP bars should be greater than twice the depth of the NSM groove to avoid overlapping of the tensile stresses around the NSM bars. Furthermore, a clear edge distance of
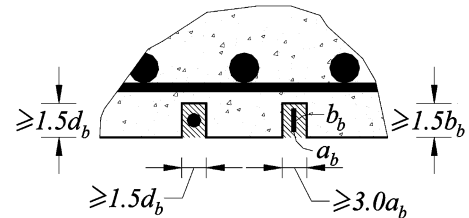
Fig. 13.4—Minimum dimensions of grooves.

four times the depth of the NSM groove should be provided to minimize the edge effects that could accelerate debonding failure (Hassan and Rizkalla 2003).

Bond properties of the NSM FRP bars depend on many factors such as cross-sectional shape and dimensions and surface properties of the FRP bar (Hassan and Rizkalla 2003; De Lorenzis et al. 2004). Figure 13.5 shows the equilibrium condition of an FRP bar with an embedded length equal to its development length l_{db} having a bond strength of τ_{max}. Using a triangular stress distribution, the average bond strength can be expressed as $\tau_b = 0.5\tau_{max}$. Average bond strength τ_b for NSM FRP bars in the range of 500 to 3000 psi (3.5 to 20.7 MPa) has been reported (Hassan and Rizkalla 2003; De Lorenzis et al. 2004); therefore, $\tau_b = 1000$ psi (6.9 MPa) is recommended for calculating the bar development length. Via force equilibrium, the following equations for development length can be derived

$$l_{db} = \frac{d_b}{4(\tau_b)}f_{fd} \quad \text{for circular bars} \qquad (13-3)$$
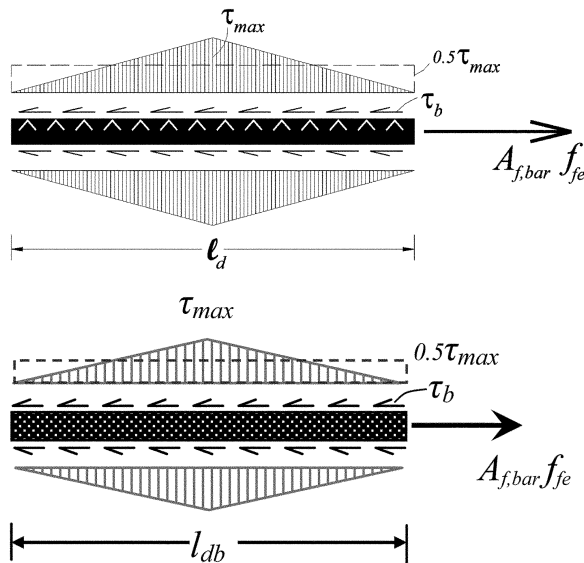
Fig. 13.5—Transfer of force in NSM FRP bars.

$$l_{db} = \frac{a_b b_b}{2(a_b + b_b)(\tau_b)} f_{fd} \text{ for rectangular bars} \quad (13\text{-}4)$$

CHAPTER 14—DRAWINGS, SPECIFICATIONS, AND SUBMITTALS

14.1—Engineering requirements

Although federal, state, and local codes for the design of externally bonded FRP systems do not exist, other applicable code requirements may influence the selection, design, and installation of the FRP system. For example, code requirements related to fire or potable water may influence the selection of the coatings used with the FRP system. All design work should be performed under the guidance of a licensed design professional familiar with the properties and applications of FRP strengthening systems.

14.2—Drawings and specifications

The licensed design professional should document calculations summarizing the assumptions and parameters used to design the FRP strengthening system and should prepare design drawings and project specifications. The drawings and specifications should show, at a minimum, the following information specific to externally applied FRP systems:
- FRP system to be used;
- Location of the FRP system relative to the existing structure;
- Dimensions and orientation of each ply, laminate, or NSM bar;
- Number of plies and bars and the sequence of installation;
- Location of splices and lap length;
- General notes listing design loads and allowable strains in the FRP laminates;
- Material properties of the FRP laminates and concrete substrate;
- Concrete surface preparation requirements, including corner preparation, groove dimensions for NSM bars, and maximum irregularity limitations;

- Installation procedures, including surface temperature and moisture limitations, and application time limits between successive plies;
- Curing procedures for FRP systems;
- Protective coatings and sealants, if required;
- Shipping, storage, handling, and shelf-life guidelines;
- Quality control and inspection procedures, including acceptance criteria; and
- In-place load testing of installed FRP system, if necessary.

14.3—Submittals

Specifications should require the FRP system manufacturer, installation contractor, inspection agency (if required), and all those involved with the project to submit product information and evidence of their qualifications and experience to the licensed design professional for review.

14.3.1 *FRP system manufacturer*—Submittals required of the FRP system manufacturer should include:
- Product data sheets indicating the physical, mechanical, and chemical characteristics of the FRP system and all its constituent materials;
- Tensile properties of the FRP system, including the method of reporting properties (net fiber or gross laminate), test methods used, and the statistical basis used for determining the properties (Section 4.3);
- Installation instructions, maintenance instructions, and general recommendations regarding each material to be used. Installation procedures should include surface preparation requirements;
- Manufacturer's MSDS for all materials to be used;
- QC procedure for tracking FRP materials and material certifications;
- Durability test data for the FRP system in the types of environments expected;
- Structural test reports pertinent to the proposed application; and
- Reference projects.

14.3.2 *FRP system installation contractor*—Submittals required of the FRP system installation contractor should include:
- Documentation from the FRP system manufacturer of having been trained to install the proposed FRP system;
- Project references, including installations similar to the proposed installation. For example, for an overhead application, the contractor should submit a list of previous installations involving the installation of the proposed FRP system in an overhead application;
- Evidence of competency in surface preparation techniques;
- QC testing procedures including voids and delaminations, FRP bond to concrete, and FRP tensile properties; and
- Daily log or inspection forms used by the contractor.

14.3.3 *FRP system inspection agency*—If an independent inspection agency is used, submittals required of that agency should include:
- A list of inspectors to be used on the project and their qualifications;
- Sample inspection forms; and
- A list of previous projects inspected by the inspector.

PART 5—DESIGN EXAMPLES
CHAPTER 15—DESIGN EXAMPLES
15.1—Calculation of FRP system tensile properties

This example illustrates the derivation of material properties based on net-fiber area versus the properties based on gross-laminate area. As described in Section 4.3.1, both methods of determining material properties are valid. It is important, however, that any design calculations consistently use material properties based on only one of the two methods (for example, if the gross-laminate thickness is used in any calculation, the strength based on gross-laminate area should be used in the calculations as well). Reported design properties should be based on a population of 20 or more coupons tested in accordance with ASTM D3039. Reported properties should be statistically adjusted by subtracting three standard deviations from the mean tensile stress and strain, as discussed in Section 4.3.1.

A test panel is fabricated from two plies of a carbon fiber/resin unidirectional FRP system using the wet layup technique. Based on the known fiber content of this FRP system, the net-fiber area is 0.0065 in.^{2}/in. (0.165 mm^2/mm) width per ply. After the system has cured, five 2 in. (50.8 mm) wide test coupons are cut from the panel. The test coupons are tested in tension to failure in accordance with ASTM D3039. Tabulated in Table 15.1 are the results of the tension tests.

Table 15.1—FRP system tension test results

	Specimen width		Measured coupon thickness		Measured rupture load	
Coupon ID	in.	mm	in.	mm	kips	kN
T-1	2	50.8	0.055	1.40	17.8	79.2
T-2	2	50.8	0.062	1.58	16.4	72.9
T-3	2	50.8	0.069	1.75	16.7	74.3
T-4	2	50.8	0.053	1.35	16.7	74.3
T-5	2	50.8	0.061	1.55	17.4	77.4
Average	2	50.8	0.060	1.52	17.0	75.6

Net-fiber area property calculations		Gross-laminate area property calculations	
Calculate A_f using the known, net-fiber area ply thickness: $A_f = nt_f w_f$	$A_f = (2)(0.0065 \text{ in.}^2/\text{in.})(2 \text{ in.}) = 0.026 \text{ in.}^2$ $A_f = (2)(0.165 \text{ mm}^2/\text{mm})(50.8 \text{ mm}) = 16.8 \text{ mm}^2$	Calculate A_f using the average, measured laminate thickness: $A_f = t_f w_f$	$A_f = (0.060 \text{ in.})(2 \text{ in.}) = 0.120 \text{ in.}^2$ $A_f = (1.52 \text{ mm})(50.8 \text{ mm}) = 77.4 \text{ mm}^2$
Calculate the average FRP system tensile strength based on net-fiber area: $\overline{f_{fu}} = \dfrac{\text{Average rupture load}}{A_f}$	$\overline{f_{fu}} = \dfrac{17 \text{ kips}}{0.026 \text{ in.}^2} = 650 \text{ ksi}$ $\overline{f_{fu}} = \dfrac{75.62 \text{ kN}}{16.8 \text{ mm}^2} = 4.5 \text{ kN/mm}^2$	Calculate the average FRP system tensile strength based on gross-laminate area: $\overline{f_{fu}} = \dfrac{\text{Average rupture load}}{A_f}$	$\overline{f_{fu}} = \dfrac{17 \text{ kips}}{0.120 \text{ in.}^2} = 140 \text{ ksi}$ $\overline{f_{fu}} = \dfrac{75.62 \text{ kN}}{77.4 \text{ mm}^2} = 0.997 \text{ kN/mm}^2$
Calculate the average FRP system tensile strength per unit width based on net-fiber area: $\overline{p_{fu}} = \dfrac{\overline{f_{fu}} A_f}{w_f}$	$\overline{p_{fu}} = \dfrac{(650 \text{ ksi})(0.026 \text{ in.}^2)}{2 \text{ in.}} = 8.4 \text{ kips/in.}$ $\overline{p_{fu}} = \dfrac{(4.5 \text{ kN/mm}^2)(16.8 \text{ mm}^2)}{50.8 \text{ mm}} = 1.49 \text{ kN/mm}$	Calculate the average FRP system tensile strength per unit width based on laminate area: $\overline{p_{fu}} = \dfrac{\overline{f_{fu}} A_f}{w_f}$	$\overline{p_{fu}} = \dfrac{(140 \text{ ksi})(0.120 \text{ in.}^2)}{2 \text{ in.}} = 8.4 \text{ kips/in.}$ $\overline{p_{fu}} = \dfrac{(0.98 \text{ kN/mm}^2)(77.4 \text{ mm}^2)}{50.8 \text{ mm}} = 1.49 \text{ kN/mm}$

15.2—Comparison of FRP systems' tensile properties

Two FRP systems are being considered for strengthening concrete members. The mechanical properties of two FRP systems are available from respective manufacturers. System A consists of dry, carbon-fiber unidirectional sheets and is installed with an adhesive resin using the wet layup technique. System B consists of precured carbon fiber/resin laminates that are bonded to the concrete surface with an adhesive resin. Excerpts from the data sheets provided by the FRP system manufacturers are given in Table 15.2. After reviewing the material data sheets sent by the FRP system manufacturers, the licensed design professional compares the tensile strengths of the two systems.

Table 15.2—Material properties and description of two types of FRP systems

System A (excerpts from data sheet)	System B (excerpts from data sheet)
System type: dry, unidirectional sheet	System type: precured, unidirectional laminate
Fiber type: high-strength carbon Polymer resin: epoxy	Fiber type: high-strength carbon Polymer resin: epoxy
System A is installed using a wet layup procedure where the dry carbon-fiber sheets are impregnated and adhered with an epoxy resin on-site.	*System B's precured laminates are bonded to the concrete substrate using System B's epoxy paste adhesive.*
Mechanical properties[*†‡]	Mechanical properties[*†]
t_f = 0.013 in. (0.33 mm)	t_f = 0.050 in. (1.27 mm)
f_{fu}^* = 550 ksi (3792 N/mm^2)	f_{fu}^* = 380 ksi (2620 N/mm^2)
ε_{fu}^* = 1.6%	ε_{fu}^* = 1.5%
E_f = 33,000 ksi (227,527 N/mm^2)	E_f = 22,000 ksi (151,724 N/mm^2)
Notes on System A: [*]Reported properties are based on a population of 20 or more coupons tested in accordance with ASTM D3039. [†]Reported properties have been statistically adjusted by subtracting three standard deviations from the mean tensile stress and strain. [‡]Thickness is based on the net-fiber area for one ply of the FRP system. Resin is excluded. Actual installed thickness of cured FRP is 0.04 to 0.07 in. (1.0 to 1.8 mm) per ply.	Notes on System B: [*]Reported properties are based on a population of 20 or more coupons tested in accordance with ASTM D3039. [†]Reported properties have been statistically adjusted by subtracting three standard deviations from the mean tensile stress and strain.

Because the data sheets for both systems are reporting statistically based properties, it is possible to directly compare the tensile strength and modulus of both systems.

Procedure	Calculation in inch-pound units	Calculation in SI units
Step 1A—Calculate the tensile strength per unit width of System A $p_{fu}^* = f_{fu}^* \, t_f$	p_{fu}^* = (550 ksi)(0.013 in.) = 7.15 kips/in.	p_{fu}^* = (3.79 kN/mm^2)(0.33 mm) = 1.25 kN/mm
Step 1B—Calculate the tensile strength per unit width of System B $p_{fu}^* = f_{fu}^* \, t_f$	p_{fu}^* = (380 ksi)(0.050 in.) = 19 kips/in.	p_{fu}^* = (2.62 kN/mm^2)(1.27 mm) = 3.33 kN/mm
Step 2A—Calculate the tensile modulus per unit width of System A $k_f = E_f t_f$	k_f = (33,000 ksi)(0.013 in.) = 429 kips/in.	k_f = (227.5 kN/mm^2)(0.33 mm) = 75.1 kN/mm
Step 2B—Calculate the tensile modulus per unit width of System B $k_f = E_f t_f$	k_f = (22,000 ksi)(0.050 in.) = 1100 kips/in.	k_f = (151.7 kN/mm^2)(1.27 mm) = 192.7 kN/mm
Step 3—Compare the two systems Compare the tensile strengths: p_{fu}^* (System A) p_{fu}^* (System B)	$\dfrac{p_{fu}^*(\text{System B})}{p_{fu}^*(\text{System A})} = \dfrac{19 \text{ kips/in.}}{7.5 \text{ kips/in.}} = 2.66$ ∴ three plies of System A are required for each ply of System B for an equivalent tensile strength	$\dfrac{p_{fu}^*(\text{System B})}{p_{fu}^*(\text{System A})} = \dfrac{3.33 \text{ kN/mm}}{75.1 \text{ kN/mm}} = 2.66$ ∴ three plies of System A are required for each ply of System B for an equivalent tensile strength
Compare the stiffnesses: k_f (System A) k_f (System B)	$\dfrac{k_f(\text{System B})}{k_f(\text{System A})} = \dfrac{1100 \text{ kips/in.}}{429 \text{ kips/in.}} = 2.56$ ∴ three plies of System A are required for each ply of System B for an equivalent stiffness	$\dfrac{k_f(\text{System A})}{k_f(\text{System B})} = \dfrac{192.7 \text{ kN/mm}}{75.1 \text{ kN/mm}} = 2.56$ ∴ three plies of System A are required for each ply of System B for an equivalent stiffness

Because all the design procedures outlined in this document limit the strain in the FRP material, the full nominal strength of the material is not used and should not be the basis of comparison between two material systems. When considering various FRP material systems for a particular application, the FRP systems should be compared based on equivalent stiffness only. In addition, each FRP system under consideration should have the ability to develop the strain level associated with the effective strain level required by the application without rupturing, $\varepsilon_{fu} > \varepsilon_{fe}$.

In many instances, it may be possible to vary the width of the FRP strip as opposed to the number of plies (use larger widths for systems with lower thicknesses and vice versa). In such instances, equivalent stiffness calculations typically will not yield equivalent contributions to the strength of a member. In general, thinner (lower nt_f) and wider (higher w_f) FRP systems will provide a higher level of strength to a member due to lower bond stresses. The exact equivalency, however, can only be found by performing complete calculations (according to procedures described in Chapters 10, 11, and 12 of this guide) for each system.

15.3—Flexural strengthening of an interior reinforced concrete beam with FRP laminates

A simply supported concrete beam reinforced with three No. 9 bars (Fig. 15.1) is located in an unoccupied warehouse and is subjected to a 50% increase in its live-load-carrying requirements. An analysis of the existing beam indicates that the beam still has sufficient shear strength to resist the new required shear strength and meets the deflection and crack-control serviceability requirements. Its flexural strength, however, is inadequate to carry the increased live load.

Length of the beam l	24 ft	7.32 m
Width of the beam w	12 in.	305 mm
d	21.5 in.	546 mm
h	24 in.	609.6 mm
f_c'	5000 psi	34.5 N/mm^2
f_y	60 ksi	414 N/mm^2
ϕM_n without FRP	266 k-ft	361 kN-m
Bars	No. 9	ϕ= 28.6 mm
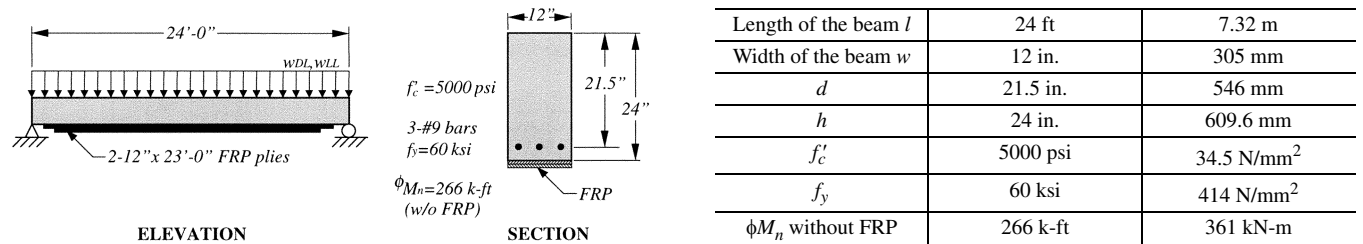
Fig. 15.1—Schematic of the idealized simply supported beam with FRP external reinforcement.

Summarized in Table 15.3 are the existing and new loadings and associated midspan moments for the beam.

Table 15.3—Loadings and corresponding moments

Loading/moment	Existing loads		Anticipated loads	
Dead loads w_{DL}	1.00 k/ft	14.6 N/mm	1.00 k/ft	14.6 N/mm
Live load w_{LL}	1.20 k/ft	17.5 N/mm	1.80 k/ft	26.3 N/mm
Unfactored loads ($w_{DL} + w_{LL}$)	2.20 k/ft	32.1 N/mm	2.80 k/ft	40.9 N/mm
Unstrengthened load limit ($1.1w_{DL} + 0.75w_{LL}$)	N/A	N/A	2.50 k/ft	35.8 N/mm
Factored loads ($1.2w_{DL} + 1.6w_{LL}$)	3.12 k/ft	45.5 N/mm	4.08 k/ft	59.6 N/mm
Dead-load moment M_{DL}	72 k-ft	98 kN-m	72 k-ft	98 kN-m
Live-load moment M_{LL}	86 k-ft	117 kN-m	130 k-ft	176 kN-m
Service-load moment M_s	158 k-ft	214 kN-m	202 k-ft	274 kN-m
Unstrengthened moment limit ($1.1M_{DL} + 0.75M_{LL}$)	N/A	N/A	177 k-ft	240 kN-m
Factored moment M_u	224 k-ft	304 kN-m	294.4 k-ft	399 kN-m

The existing reinforced concrete beam should be strengthened with the FRP system described in Table 15.4, specifically, two 12 in. (305 mm) wide x 23.0 ft (7 m) long plies bonded to the soffit of the beam using the wet layup technique.

Table 15.4—Manufacturer's reported FRP system properties

Thickness per ply t_f	0.040 in.	1.02 mm
Ultimate tensile strength f_{fu}^*	90 ksi	621 N/mm^2
Rupture strain ε_{fu}^*	0.015 in./in.	0.015 mm/mm
Modulus of elasticity of FRP laminates E_f	5360 ksi	37,000 N/mm^2

By inspection, the level of strengthening is reasonable in that it does meet the strengthening limit criteria specified in Eq. (9-1). That is, the existing moment strength without FRP, $(\phi M_n)_{w/o} = 266$ k-ft (361 kN-m), is greater than the unstrengthened moment limit, $(1.1M_{DL} + 0.75M_{LL})_{new} = 177$ k-ft (240 kN-m). The design calculations used to verify this configuration follow.

Procedure	Calculation in inch-pound units	Calculation in SI metric units
Step 1—Calculate the FRP system design material properties The beam is located in an interior space and a CFRP material will be used. Therefore, per Table 9.1, an environmental reduction factor of 0.95 is suggested. $f_{fu} = C_E f_{fu}^*$ $\varepsilon_{fu} = C_E \varepsilon_{fu}^*$	$f_{fu} = (0.95)(90 \text{ ksi}) = 85 \text{ ksi}$ $\varepsilon_{fu} = (0.95)(0.015 \text{ in./in.}) = 0.0142 \text{ in./in.}$	$f_{fu} = (0.95)(621 \text{ N/mm}^2) = 590 \text{ N/mm}^2$ $\varepsilon_{fu} = (0.95)(0.015 \text{ mm/mm}) = 0.0142 \text{ mm/mm}$
Step 2—Preliminary calculations Properties of the concrete: β_1 from ACI 318-05, Section 10.2.7.3 $E_c = 57,000\sqrt{f_c'}$ Properties of the existing reinforcing steel: Properties of the externally bonded FRP reinforcement: $A_f = n t_f w_f$	$\beta_1 = 1.05 - 0.05\dfrac{f_c'}{1000} = 0.80$ $E_c = 57,000\sqrt{5000 \text{ psi}} = 4,030,000 \text{ psi}$ $A_s = 3(1.00 \text{ in.}^2) = 3.00 \text{ in.}^2$ $A_f = (2 \text{ plies})(0.040 \text{ in./ply})(12 \text{ in.}) = 0.96 \text{ in.}^2$	$\beta_1 = 1.05 - 0.05\dfrac{f_c'}{6.9} = 0.80$ $E_c = 4700\sqrt{34.5 \text{ N/mm}^2} = 27,600 \text{ N/mm}^2$ $A_s = 3(645 \text{ mm}^2) = 1935 \text{ mm}^2$ $A_f = (2 \text{ plies})(1.02 \text{ mm/ply})(305 \text{ mm}) = 619 \text{ mm}^2$
Step 3—Determine the existing state of strain on the soffit The existing state of strain is calculated assuming the beam is cracked and the only loads acting on the beam at the time of the FRP installation are dead loads. A cracked section analysis of the existing beam gives $k = 0.334$ and $I_{cr} = 5937 \text{ in.}^4 = 2471 \times 10^6 \text{ mm}^4$ $\varepsilon_{bi} = \dfrac{M_{DL}(d_f - kd)}{I_{cr}E_c}$	$\varepsilon_{bi} = \dfrac{(864 \text{ k-in.})[24 \text{ in.} - (0.334)(21.5 \text{ in.})]}{(5937 \text{ in.}^4)(4030 \text{ ksi})}$ $\varepsilon_{bi} = 0.00061$	$\varepsilon_{bi} = \dfrac{(97.6 \text{ kN-mm})[609.6 \text{ mm} - (0.334)(546.1 \text{ mm})]}{(2471 \times 10^6 \text{ mm}^4)(27.6 \text{ kN/mm}^2)}$ $\varepsilon_{bi} = 0.00061$
Step 4—Determine the design strain of the FRP system The design strain of FRP accounting for debonding failure mode ε_{fd} is calculated using Eq. (10-2) Because the design strain is smaller than the rupture strain, debonding controls the design of the FRP system.	$\varepsilon_{fd} = 0.083\sqrt{\dfrac{5000 \text{ psi}}{2(5,360,000 \text{ psi})(0.04 \text{ in.})}}$ $= 0.009 \le 0.9(0.0142) = 0.0128$	$\varepsilon_{fd} = 0.41\sqrt{\dfrac{34.5 \text{ N/mm}^2}{2(37,000 \text{ N/mm}^2)(1.02 \text{ mm})}}$ $= 0.009 \le 0.9(0.0142) = 0.0128$
Step 5—Estimate c, the depth to the neutral axis A reasonable initial estimate of c is $0.20d$. The value of the c is adjusted after checking equilibrium. $c = 0.20d$	$c = (0.20)(21.5 \text{ in.}) = 4.30 \text{ in.}$	$c = (0.20)(546.1 \text{ mm}) = 109 \text{ mm}$

Procedure	Calculation in inch-pound units	Calculation in SI metric units
Step 6—Determine the effective level of strain in the FRP reinforcement The effective strain level in the FRP may be found from Eq. (10-3). $$\varepsilon_{fe} = 0.003\left(\frac{d_f - c}{c}\right) - \varepsilon_{bi} \le \varepsilon_{fd}$$ Note that for the neutral axis depth selected, FRP debonding would be in the failure mode because the second expression in this equation controls. If the first expression governed, then concrete crushing would be in the failure mode. Because FRP controls the failure of the section, the concrete strain at failure ε_c may be less than 0.003 and can be calculated using similar triangles: $$\varepsilon_c = (\varepsilon_{fe} + \varepsilon_{bi})\left(\frac{c}{d_f - c}\right)$$	$$\varepsilon_{fe} = 0.003\left(\frac{24 \text{ in.} - 4.3 \text{ in.}}{4.3 \text{ in.}}\right) - 0.00061 \le 0.009$$ $$\varepsilon_{fe} = 0.0131 > 0.009$$ $$\varepsilon_{fe} = \varepsilon_{fd} = 0.009$$ $$\varepsilon_c = (0.009 + 0.00061)\left(\frac{4.3 \text{ in.}}{24 \text{ in.} - 4.3 \text{ in.}}\right) = 0.0021$$	$$\varepsilon_{fe} = 0.003\left(\frac{609.6 \text{ mm} - 109.2 \text{ mm}}{109.2 \text{ mm}}\right) - 0.00061 \le 0.009$$ $$\varepsilon_{fe} = 0.0131 > 0.009$$ $$\varepsilon_{fe} = \varepsilon_{fd} = 0.009$$ $$\varepsilon_c = (0.009 + 0.00061)\left(\frac{109.2 \text{ mm}}{609.6 \text{ mm} - 109.2 \text{ mm}}\right) = 0.0021$$
Step 7—Calculate the strain in the existing reinforcing steel The strain in the reinforcing steel can be calculated using similar triangles according to Eq. (10-10). $$\varepsilon_s = (\varepsilon_{fe} + \varepsilon_{bi})\left(\frac{d - c}{d_f - c}\right)$$	$$\varepsilon_s = (0.009 + 0.00061)\left(\frac{21.5 \text{ in.} - 4.3 \text{ in.}}{24 \text{ in.} - 4.3 \text{ in.}}\right) = 0.0084$$	$$\varepsilon_s = (0.009 + 0.00061)\left(\frac{546.1 \text{ mm} - 109.2 \text{ mm}}{609.6 \text{ mm} - 109.2 \text{ mm}}\right) = 0.0084$$
Step 8—Calculate the stress level in the reinforcing steel and FRP The stresses are calculated using Eq. (10-11) and (10-9). $$f_s = E_s \varepsilon_s \le f_y$$ $$f_{fe} = E_f \varepsilon_{fe}$$	$$f_s = (29,000 \text{ ksi})(0.0084) \le 60 \text{ ksi}$$ $$f_s = 244 \text{ ksi} \le 60 \text{ ksi}$$ Hence, $f_s = 60 \text{ ksi}$ $$f_{fe} = (5360 \text{ ksi})(0.009) = 48.2 \text{ ksi}$$	$$f_s = (200 \text{ kN/mm}^2)(0.0084) \le 0.414 \text{ kN/mm}^2$$ $$f_s = 1.68 \text{ kN/mm}^2 \le 0.414 \text{ kN/mm}^2$$ Hence, $f_s = 0.414 \text{ kN/mm}^2$ $$f_{fe} = (37 \text{ kN/mm}^2)(0.009) = 0.33 \text{ kN/mm}^2$$
Step 9—Calculate the internal force resultants and check equilibrium Concrete stress block factors may be calculated using ACI 318-05. Approximate stress block factors may also be calculated based on the parabolic stress-strain relationship for concrete as follows: $$\beta_1 = \frac{4\varepsilon_c' - \varepsilon_c}{6\varepsilon_c' - 2\varepsilon_c}$$ $$\alpha_1 = \frac{3\varepsilon_c'\varepsilon_c - \varepsilon_c'^2}{3\beta_1\varepsilon_c'^2}$$ where ε_c' is strain corresponding to f_c' calculated as $$\varepsilon_c' = \frac{1.7 f_c'}{E_c}$$ Force equilibrium is verified by checking the initial estimate of c with Eq. (10-12). $$c = \frac{A_s f_s + A_f f_{fe}}{\alpha_1 f_c' \beta_1 b}$$	$$\varepsilon_c' = \frac{1.7(5000)}{4030 \times 10^6} = 0.0021$$ $$\beta_1 = \frac{4(0.0021) - 0.0021}{6(0.0021) - 2(0.0021)} = 0.749$$ $$\alpha_1 = \frac{3(0.0021)(0.0021) - (0.0021)^2}{3(0.749)(0.0021)^2} = 0.886$$ $$c = \frac{(3.00 \text{ in.}^2)(60 \text{ ksi}) + (0.96 \text{ in.}^2)(48.2 \text{ ksi})}{(0.886)(5 \text{ ksi})(0.749)(12 \text{ in.})}$$ $$c = 5.68 \text{ in.} \ne 4.30 \text{ in.} \quad \text{n.g.}$$ ∴ Revise estimate of c and repeat Steps 6 through 9 until equilibrium is achieved.	$$\varepsilon_c' = \frac{1.7(34.5)}{27,600} = 0.0021$$ $$\beta_1 = \frac{4(0.0021) - 0.0021}{6(0.0021) - 2(0.0021)} = 0.749$$ $$\alpha_1 = \frac{3(0.0021)(0.0021) - (0.0021)^2}{3(0.749)(0.0021)^2} = 0.886$$ $$c =$$ $$\frac{(1935.48 \text{ mm}^2)(414 \text{ N/mm}^2) + (619 \text{ mm}^2)(330 \text{ N/mm}^2)}{(0.886)(34.5 \text{ N/mm}^2)(0.749)(304.8 \text{ mm})}$$ $$c = 149 \text{ mm} \ne 109 \text{ in.} \quad \text{n.g.}$$ ∴ Revise estimate of c and repeat Steps 6 through 9 until equilibrium is achieved.

Procedure	Calculation in inch-pound units	Calculation in SI metric units
Step 10—Adjust c until force equilibrium is satisfied Steps 6 through 9 were repeated several times with different values of c until equilibrium was achieved. The results of the final iteration are $c = 5.17$ in.; $\varepsilon_s = 0.0083$; $f_s = f_y = 60$ ksi; $\beta_1 = 0.786$; $\alpha_1 = 0.928$; and $f_{fd} = 48.2$ ksi	$c = \dfrac{(3.00 \text{ in.}^2)(60 \text{ ksi}) + (0.96 \text{ in.}^2)(48.2 \text{ ksi})}{(0.928)(5 \text{ ksi})(0.786)(12 \text{ in.})}$ $c = 5.17$ in. ✓ **OK** ∴ the value of c selected for the final iteration is correct.	$c = \dfrac{(1935.5 \text{ mm}^2)(414 \text{ N/mm}^2) + (619 \text{ mm}^2)(330 \text{ N/mm}^2)}{(0.928)(34.5 \text{ N/mm}^2)(0.786)(304.8 \text{ mm})}$ $c = 131$ mm ✓ **OK** ∴ the value of c selected for the final iteration is correct.
Step 11—Calculate flexural strength components The design flexural strength is calculated using Eq. (10-13). An additional reduction factor, $\psi_f = 0.85$, is applied to the contribution of the FRP system. Steel contribution to bending: $M_{ns} = A_s f_s \left(d - \dfrac{\beta_1 c}{2} \right)$ FRP contribution to bending: $M_{nf} = A_f f_{fe} \left(d_f - \dfrac{\beta_1 c}{2} \right)$	$M_{ns} = (3.00 \text{ in.}^2)(60 \text{ ksi})\left(21.5 \text{ in.} - \dfrac{0.786(5.17 \text{ in.})}{2}\right)$ $M_{ns} = 3504$ k-in. $= 292$ k-ft $M_{nf} = (0.96 \text{ in.}^2)(48.2 \text{ ksi})\left(24 \text{ in.} - \dfrac{0.786(5.17 \text{ in.})}{2}\right)$ $M_{nf} = 1020$ k-in. $= 85$ k-ft	$M_{ns} = (1935.5 \text{ mm}^2)(414 \text{ N/mm}^2)$ $\left(546.1 \text{ mm} - \dfrac{0.786(131 \text{ mm})}{2}\right)$ $M_{ns} = 3.963 \times 10^8$ N-mm $= 396.3$ kN-m $M_{nf} = (619 \text{ mm}^2)(330 \text{ N/mm}^2)\left(609.6 \text{ mm} - \dfrac{0.786(131 \text{ mm})}{2}\right)$ $M_{nf} = 1.140 \times 10^8$ N-mm $= 114$ kN-m
Step 12—Calculate design flexural strength of the section The design flexural strength is calculated using Eq. (10-1) and (10-13). Because $\varepsilon_s = 0.0083 > 0.005$, a strength reduction factor of $\phi = 0.90$ is appropriate per Eq. (10-5). $\phi M_n = \phi [M_{ns} + \psi_f M_{nf}]$	$\phi M_n = 0.9[292 \text{ k-ft} + 0.85(85 \text{ k-ft})]$ $\phi M_n = 327$ k-ft $\geq M_u = 294$ k-ft ∴ the strengthened section is capable of sustaining the new required moment strength.	$\phi M_n = 0.9[396.3 \text{ kN-m} + 0.85(114 \text{ kN-m})]$ $\phi M_n = 443$ kN-m $\geq M_u = 399$ kN-m ∴ the strengthened section is capable of sustaining the new required moment strength.
Step 13—Check service stresses in the reinforcing steel and the FRP Calculate the elastic depth to the cracked neutral axis. This can be simplified for a rectangular beam without compression reinforcement as follows: $k = \sqrt{\left(\rho_s \dfrac{E_s}{E_c} + \rho_f \dfrac{E_f}{E_c}\right)^2 + 2\left(\rho_s \dfrac{E_s}{E_c} + \rho_f \dfrac{E_f}{E_c}\left(\dfrac{d_f}{d}\right)\right)}$ $\qquad - \left(\rho_s \dfrac{E_s}{E_c} + \rho_f \dfrac{E_f}{E_c}\right)$ Calculate the stress level in the reinforcing steel using Eq. (10-14) and verify that it is less than the recommended limit per Eq. (10-6). $f_{s,s} = \dfrac{\left[M_s + \varepsilon_{bi} A_f E_f \left(d_f - \dfrac{kd}{3}\right)\right](d - kd)E_s}{A_s E_s \left(d - \dfrac{kd}{3}\right)(d - kd) + A_f E_f \left(d_f - \dfrac{kd}{3}\right)(d_f - kd)}$ $f_{s,s} \leq 0.80 f_y$	*See EQUATION NOTE I (U.S.) after Step 14. $k = 0.343$ $kd = (0.343)(21.5 \text{ in.}) = 7.37$ in. †See EQUATION NOTE II (U.S.) after Step 14. $f_{s,s} = 40.4$ ksi $\leq (0.80)(60 \text{ ksi}) = 48$ ksi ∴ the stress level in the reinforcing steel is within the recommended limit.	**See EQUATION NOTE I (SI) after Step 14. $k = 0.343$ $kd = (0.343)(546.1 \text{ mm}) = 187$ mm ††See EQUATION NOTE II (SI) after Step 14. $f_{s,s} = 279$ N/mm^2 $\leq (0.80)(410 \text{ N/mm}^2) = 330$ N/mm^2 ∴ the stress level in the reinforcing steel is within the recommended limit.

Procedure	Calculation in inch-pound units	Calculation in SI metric units
Step 14—Check creep rupture limit at service of the FRP Calculate the stress level in the FRP using Eq. (10-15) and verify that it is less than creep-rupture stress limit given in Table 10.1. Assume that the full service load is sustained. $$f_{f,s} = f_{s,s}\left(\frac{E_f}{E_s}\right)\left(\frac{d_f - kd}{d - kd}\right) - \varepsilon_{bi}E_f$$ For a carbon FRP system, the sustained plus cyclic stress limit is obtained from Table 10.1: Sustained plus cyclic stress limit = $0.55f_{fu}$	$f_{f,s} = 40.4 \text{ ksi}\left(\dfrac{5360 \text{ ksi}}{29,000 \text{ ksi}}\right)\left(\dfrac{24 \text{ in.} - 7.37 \text{ in.}}{21.5 \text{ in.} - 7.37 \text{ in.}}\right)$ $- (0.00061)(5360 \text{ ksi})$ $f_{f,s} = 5.60 \text{ ksi} \le (0.55)(85 \text{ ksi}) = 47 \text{ ksi}$ ∴ the stress level in the FRP is within the recommended sustained plus cyclic stress limit.	$f_{f,s} = 0.278 \text{ kN/mm}^2\left(\dfrac{37 \text{ kN/mm}^2}{200 \text{ kN/mm}^2}\right)\left(\dfrac{609.6 \text{ mm} - 187 \text{ mm}}{546 \text{ mm} - 187 \text{ mm}}\right)$ $- (0.00061)(38 \text{ N/mm}^2)$ $f_{f,s} = 38 \text{ N/mm}^2 \le (0.55)(590 \text{ N/mm}^2) = 324 \text{ N/mm}^2$ ∴ the stress level in the FRP is within the recommended sustained plus cyclic stress limit.

*EQUATION NOTE I (U.S.):

$$k = \sqrt{\left(0.0116\left(\frac{29,000}{4030}\right) + 0.00372\left(\frac{5360}{4030}\right)\right)^2 + 2\left(0.0116\left(\frac{29,000}{4030}\right) + 0.00372\left(\frac{5360}{4030}\right)\left(\frac{24 \text{ in.}}{21.5 \text{ in.}}\right)\right)} - \left(0.0116\left(\frac{29,000}{4030}\right) + 0.00372\left(\frac{5360}{4030}\right)\right)$$

**EQUATION NOTE I (SI):

$$k = \sqrt{\left(0.0116\left(\frac{200}{27.6}\right) + 0.00372\left(\frac{37}{27.6}\right)\right)^2 + 2\left(0.0116\left(\frac{200}{27.6}\right) + 0.00372\left(\frac{37}{27.6}\right)\left(\frac{609.6 \text{ mm}}{546 \text{ mm}}\right)\right)} - \left(0.0116\left(\frac{200}{27.6}\right) + 0.00372\left(\frac{37}{27.6}\right)\right)$$

†EQUATION NOTE II (U.S.):

$$f_{s,s} = \frac{\left[2424 \text{ k-in.} + (0.00061)(0.96 \text{ in.}^2)(5360 \text{ ksi})\left(24 \text{ in.} - \dfrac{7.37 \text{ in.}}{3}\right)\right](21.5 \text{ in.} - 7.37 \text{ in.})(29,000 \text{ ksi})}{(3.00 \text{ in.}^2)(29,000 \text{ ksi})\left(21.5 \text{ in.} - \dfrac{7.37 \text{ in.}}{3}\right)(21.5 \text{ in.} - 7.37 \text{ in.}) + (0.96 \text{ in.}^2)(5360 \text{ ksi})\left(24 \text{ in.} - \dfrac{7.37 \text{ in.}}{3}\right)(24 \text{ in.} - 7.37 \text{ in.})}$$

††EQUATION NOTE II (SI):

$$f_{s,s} = \frac{\left[273,912 \text{ kN-mm} + (0.00061)(619 \text{ mm}^2)(37 \text{ kN/mm}^2)\left(609.6 \text{ mm} - \dfrac{187 \text{ mm}}{3}\right)\right](546 \text{ mm} - 187 \text{ mm})(200 \text{ kN/mm}^2)}{(1935 \text{ mm}^2)(200 \text{ kN/mm}^2)\left(546 \text{ mm} - \dfrac{187 \text{ mm}}{3}\right)(546 \text{ mm} - 187 \text{ mm}) + (619 \text{ mm}^2)(37 \text{ kN/mm}^2)\left(607 \text{ mm} - \dfrac{187 \text{ mm}}{3}\right)(607 \text{ mm} - 187 \text{ mm})}$$

In detailing the FRP reinforcement, the FRP should be terminated a minimum of l_{df}, calculated per Eq. (13-2), past the point on the moment diagram that represents cracking. The factored shear force at the termination should also be checked against the shear force that causes FRP end peeling, estimated as 2/3 of the concrete shear strength. If the shear force is greater than 2/3 of the concrete shear strength, the FRP strips should be extended further toward the supports. U-wraps may also be used to reinforce against cover delamination.

15.4—Flexural strengthening of an interior reinforced concrete beam with NSM FRP bars

An existing reinforced concrete beam (Fig. 15.2) is to be strengthened using the loads given in Table 15.3 and the NSM FRP system described in Table 15.5. Specifically, three No. 3 CFRP bars are to be used at a distance 23.7 in. (602.1 mm) from the extreme top fiber of the beam.
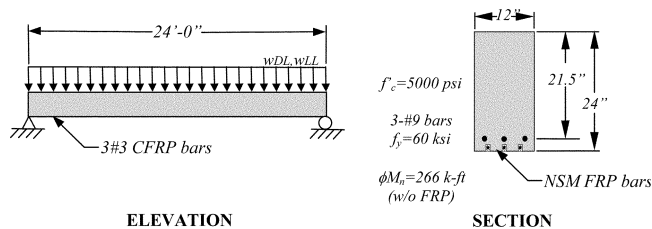
Fig. 15.2—Schematic of the idealized simply supported beam with FRP external reinforcement.

Table 15.5—Manufacturer's reported NSM FRP system properties

Area per No. 3 bar	0.10 in.^{2}	64.5 mm^2
Ultimate tensile strength f_{fu}^*	250 ksi	1725 N/mm^2
Rupture strain ε_{fu}^*	0.013 in./in.	0.013 mm/mm
Modulus of elasticity of FRP laminates E_f	19,230 ksi	132,700 N/mm^2

By inspection, the level of strengthening is reasonable in that it does meet the strengthening limit criteria put forth in Eq. (10-1). That is, the existing flexural strength without FRP, $(\phi M_n)_{w/o} = 266$ k-ft (361 kN-m), is greater than the unstrengthened moment limit, $(1.1M_{DL} + 0.75M_{LL})_{new} = 177$ k-ft (240 kN-m). The design calculations used to verify this configuration follow.

Procedure	Calculation in inch-pound units	Calculation in SI metric units
Step 1—Calculate the FRP system design material properties The beam is located in an interior space and a CFRP material will be used. Therefore, per Table 9.1, an environmental reduction factor of 0.95 is suggested. $f_{fu} = C_E f_{fu}^*$ $\varepsilon_{fu} = C_E \varepsilon_{fu}^*$	$f_{fu} = (0.95)(250 \text{ ksi}) = 237.5 \text{ ksi}$ $\varepsilon_{fu} = (0.95)(0.013 \text{ in./in.}) = 0.0123 \text{ in./in.}$	$f_{fu} = (0.95)(1725 \text{ N/mm}^2) = 1639 \text{ N/mm}^2$ $\varepsilon_{fu} = (0.95)(0.013 \text{ mm/mm}) = 0.0123 \text{ mm/mm}$
Step 2—Preliminary calculations Properties of the concrete: β_1 from ACI 318-05, Section 10.2.7.3 $E_c = 57{,}000\sqrt{f_c'}$	$\beta_1 = 1.05 - 0.05\dfrac{f_c'}{1000} = 0.85$ $E_c = 57{,}000\sqrt{5000 \text{ psi}} = 4{,}030{,}000 \text{ psi}$ $A_s = 3(1.00 \text{ in.}^2) = 3.00 \text{ in.}^2$ $A_f = (3 \text{ bars})(0.01 \text{ in.}^2/\text{bar}) = 0.3 \text{ in.}^2$	$\beta_1 = 1.05 - 0.05\dfrac{f_c'}{6.9} = 0.85$ $E_c = 4700\sqrt{34.5 \text{ N/mm}^2} = 27{,}600 \text{ N/mm}^2$ $A_s = 3(645.2 \text{ mm}^2) = 1935 \text{ mm}^2$ $A_f = (3 \text{ bars})(64.5 \text{ mm}^2/\text{bar}) = 194 \text{ mm}^2$
Step 3—Determine the existing state of strain on the soffit The existing state of strain is calculated assuming the beam is cracked and the only loads acting on the beam at the time of the FRP installation are dead loads. A cracked section analysis of the existing beam gives $k = 0.334$ and $I_{cr} = 5937 \text{ in.}^4 = 2471 \times 10^6 \text{ mm}^4$ $\varepsilon_{bi} = \dfrac{M_{DL}(d_f - kd)}{I_{cr}E_c}$	$\varepsilon_{bi} = \dfrac{(864 \text{ k-in.})[23.7 \text{ in.} - (0.334)(21.5 \text{ in.})]}{(5937 \text{ in.}^4)(4030 \text{ ksi})}$ $\varepsilon_{bi} = 0.00061$	$\varepsilon_{bi} = \dfrac{(97.6 \text{ kN-mm})[602 \text{ mm} - (0.334)(546 \text{ mm})]}{(2471 \times 10^6 \text{ mm}^4)(27.6 \text{ kN/mm}^2)}$ $\varepsilon_{bi} = 0.00061$
Step 4—Determine the bond-dependent coefficient of the FRP system Based on the manufacturer's recommendation, the dimensionless bond-dependent coefficient for flexure κ_m is 0.7.	$\kappa_m = 0.7$	$\kappa_m = 0.7$
Step 5—Estimate c, the depth to the neutral axis A reasonable initial estimate of c is $0.20d$. The value of the c is adjusted after checking equilibrium. $c = 0.20d$	$c = (0.20)(21.5 \text{ in.}) = 4.30 \text{ in.}$	$c = (0.20)(546 \text{ mm}) = 109 \text{ mm}$
Step 6—Determine the effective level of strain in the FRP reinforcement The effective strain level in the FRP may be found from Eq. (10-3). $\varepsilon_{fe} = 0.003\left(\dfrac{d_f - c}{c}\right) - \varepsilon_{bi} \le \kappa_m \varepsilon_{fd}$ Note that for the neutral axis depth selected, FRP debonding would be the failure mode because the second expression in this equation controls. If the first expression governed, then concrete crushing would be the failure mode. Because FRP controls the failure of the section, the concrete strain at failure, ε_c, may be less than 0.003 and can be calculated using similar triangles: $\varepsilon_c = (\varepsilon_{fd} + \varepsilon_{bi})\left(\dfrac{c}{d_f - c}\right)$	$\varepsilon_{fe} = 0.003\left(\dfrac{23.7 \text{ in.} - 4.3 \text{ in.}}{4.3 \text{ in.}}\right) - 0.00061 = 0.0129$ $\kappa_m \varepsilon_{fd} = 0.7(0.0123) = 0.00865$ Hence, $\varepsilon_{fe} = 0.00865$ (Mode of failure is FRP debonding) $\varepsilon_c = (0.00865 + 0.00061)\left(\dfrac{4.3}{23.7 - 4.3}\right) = 0.0020$	$\varepsilon_{fe} = 0.003\left(\dfrac{602 \text{ mm} - 109 \text{ mm}}{109 \text{ mm}}\right) - 0.00061 = 0.0129$ $\kappa_m \varepsilon_{fd} = 0.7(0.0123) = 0.00865$ Hence, $\varepsilon_{fe} = 0.00865$ (Mode of failure is FRP debonding) $\varepsilon_c = (0.00865 + 0.00061)\left(\dfrac{109}{602 - 109}\right) = 0.0020$

Procedure	Calculation in inch-pound units	Calculation in SI metric units
Step 7—Calculate the strain in the existing reinforcing steel The strain in the reinforcing steel can be calculated using similar triangles according to Eq. (10-10). $\varepsilon_s = (\varepsilon_{fe} + \varepsilon_{bi})\left(\dfrac{d-c}{d_f-c}\right)$	$\varepsilon_s = (0.00865 + 0.00061)\left(\dfrac{21.5-4.3}{23.7-4.3}\right) = 0.0082$	$\varepsilon_s = (0.00865 + 0.00061)\left(\dfrac{546-109}{602-109}\right) = 0.0082$
Step 8—Calculate the stress level in the reinforcing steel and FRP The stresses are calculated using Eq. (10-11) and (10-9). $f_s = E_s\varepsilon_s \le f_y$ $f_{fe} = E_f\varepsilon_{fe}$	$f_s = (29{,}000 \text{ ksi})(0.0082) \le 60 \text{ ksi}$ $f_s = 238 \text{ ksi} \le 60 \text{ ksi}$ Hence, $f_s = 60 \text{ ksi}$ $f_{fe} = (19{,}230 \text{ ksi})(0.00865) = 166 \text{ ksi}$	$f_s = (200 \text{ kN/mm}^2)(0.0082) \le 0.414 \text{ kN/mm}^2$ $f_s = 1.64 \text{ kN/mm}^2 \le 0.414 \text{ kN/mm}^2$ Hence, $f_s = 0.414 \text{ kN/mm}^2$ $f_{fe} = (132{,}700 \text{ N/mm}^2)(0.00865) = 1147 \text{ N/mm}^2$
Step 9—Calculate the internal force resultants and check equilibrium Concrete stress block factors may be calculated using ACI 318-05. Approximate stress block factors may also be calculated based on the parabolic stress-strain relationship for concrete as follows: $\beta_1 = \dfrac{4\varepsilon_c' - \varepsilon_c}{6\varepsilon_c' - 2\varepsilon_c}$ $\alpha_1 = \dfrac{3\varepsilon_c'\varepsilon_c - \varepsilon_c^2}{3\beta_1\varepsilon_c'^2}$ where ε_c' is strain corresponding to f_c' calculated as $\varepsilon_c' = \dfrac{1.7f_c'}{E_c}$ Force equilibrium is verified by checking the initial estimate of c with Eq. (10-12). $c = \dfrac{A_s f_s + A_f f_{fe}}{\alpha_1 f_c' \beta_1 b}$	$\varepsilon_c' = \dfrac{1.7(5000)}{4030 \times 10^6} = 0.0021$ $\beta_1 = \dfrac{4(0.0021) - 0.002}{6(0.0021) - 2(0.002)} = 0.743$ $\alpha_1 = \dfrac{3(0.0021)(0.002) - (0.002)^2}{3(0.743)(0.0021)^2} = 0.870$ $c = \dfrac{(3.00 \text{ in.}^2)(60 \text{ ksi}) + (0.3 \text{ in.}^2)(166 \text{ ksi})}{(0.87)(5 \text{ ksi})(0.743)(12 \text{ in.})}$ $c = 5.92 \text{ in.} \ne 4.30 \text{ in.}$ n.g. $\therefore$ Revise estimate of c and repeat Steps 6 through 9 until equilibrium is achieved.	$\varepsilon_c' = \dfrac{1.7(34.5)}{27{,}606} = 0.0021$ $\beta_1 = \dfrac{4(0.0021) - 0.002}{6(0.0021) - 2(0.002)} = 0.743$ $\alpha_1 = \dfrac{3(0.0021)(0.002) - (0.002)^2}{3(0.743)(0.0021)^2} = 0.870$ $c =$ $\dfrac{(1935 \text{ mm}^2)(414 \text{ N/mm}^2) + (194 \text{ mm}^2)(1147 \text{ N/mm}^2)}{(0.87)(34.5 \text{ N/mm}^2)(0.743)(305 \text{ mm})}$ $c = 150 \text{ mm} \ne 109 \text{ in.}$ n.g. $\therefore$ Revise estimate of c and repeat Steps 6 through 9 until equilibrium is achieved.
Step 10—Adjust c until force equilibrium is satisfied Steps 6 through 9 were repeated several times with different values of c until equilibrium was achieved. The results of the final iteration are $c = 5.26$ in.; $\varepsilon_s = 0.0082$; $f_s = f_y = 60$ ksi; $\varepsilon_{fe} = 0.00865$; $\varepsilon_c = 0.0027$; $\beta_1 = 0.786$; $\alpha_1 = 0.928$; and $f_{fe} = 166$ ksi	$c = \dfrac{(3.00 \text{ in.}^2)(60 \text{ ksi}) + (0.3 \text{ in.}^2)(166 \text{ ksi})}{(0.928)(5 \text{ ksi})(0.786)(12 \text{ in.})}$ $c = 5.25 \text{ in.} \approx 5.26 \text{ in.}$ ✓ **OK** $\therefore$ the value of c selected for the final iteration is correct.	$c = \dfrac{(1935 \text{ mm}^2)(414 \text{ N/mm}^2) + (193 \text{ mm}^2)(1147 \text{ N/mm}^2)}{(0.928)(34.5 \text{ N/mm}^2)(0.786)(305 \text{ mm})}$ $c = 133 \text{ mm} \approx 134 \text{ mm}$ ✓ **OK** $\therefore$ the value of c selected for the final iteration is correct.

Procedure	Calculation in inch-pound units	Calculation in SI metric units
Step 11—Calculate flexural strength components The design flexural strength is calculated using Eq. (10-13). An additional reduction factor, $\psi_f = 0.85$, is applied to the contribution of the FRP system. Steel contribution to bending: $$M_{ns} = A_s f_s\left(d - \frac{\beta_1 c}{2}\right)$$	$M_{ns} = (3.0 \text{ in.}^2)(60 \text{ ksi})\left(21.5 \text{ in.} - \frac{0.786(5.25 \text{ in.})}{2}\right)$ $M_{ns} = 3498$ k-in. $= 291$ k-ft	$M_{ns} = (1935 \text{ mm}^2)(414 \text{ N/mm}^2)\left(546 \text{ mm} - \frac{0.786(133 \text{ mm})}{2}\right)$ $M_{ns} = 394$ kN-m
FRP contribution to bending: $$M_{nf} = A_f f_{fe}\left(d_f - \frac{\beta_1 c}{2}\right)$$	$M_{nf} = (0.3 \text{ in.}^2)(166 \text{ ksi})\left(23.7 \text{ in.} - \frac{0.786(5.25 \text{ in.})}{2}\right)$ $M_{nf} = 1077$ k-in. $= 90$ k-ft	$M_{nf} = (194 \text{ mm}^2)(1147 \text{ N/mm}^2)\left(602.1 \text{ mm} - \frac{0.786(133 \text{ mm})}{2}\right)$ $M_{nf} = 122$ kN-m
Step 12—Calculate design flexural strength of the section The design flexural strength is calculated using Eq. (10-1) and (10-13). Because $\varepsilon_s = 0.0082 > 0.005$, a strength reduction factor of $\phi = 0.90$ is appropriate per Eq. (10-5). $$\phi M_n = \phi[M_{ns} + \psi_f M_{nf}]$$	$\phi M_n = 0.9[291 \text{ k-ft} + 0.85(90 \text{ k-ft})]$ $\phi M_n = 331 \text{ k-ft} \geq M_u = 294 \text{ k-ft}$ $\therefore$ the strengthened section is capable of sustaining the new required flexural strength.	$\phi M_n = 0.9[394 \text{ kN-m} + 0.85(122 \text{ kN-m})]$ $\phi M_n = 448 \text{ kN-m} \geq M_u = 398 \text{ kN-m}$ $\therefore$ the strengthened section is capable of sustaining the new required flexural strength.
Step 13—Check service stresses in the reinforcing steel and the FRP Calculate the elastic depth to the cracked neutral axis. This can be simplified for a rectangular beam without compression reinforcement as follows: $$k = \sqrt{\left(\rho_s\frac{E_s}{E_c} + \rho_f\frac{E_f}{E_c}\right)^2 + 2\left(\rho_s\frac{E_s}{E_c} + \rho_f\frac{E_f}{E_c}\left(\frac{d_f}{d}\right)\right)}$$ $$- \left(\rho_s\frac{E_s}{E_c} + \rho_f\frac{E_f}{E_c}\right)$$	*See EQUATION NOTE I (U.S.) after Step 14. $k = 0.345$ $kd = (0.345)(21.5 \text{ in.}) = 7.4 \text{ in.}$	**See EQUATION NOTE I (SI) after Step 14. $k = 0.345$ $kd = (0.345)(546 \text{ mm}) = 188 \text{ mm}$
Calculate the stress level in the reinforcing steel using Eq. (10-14) and verify that it is less than the recommended limit per Eq. (10-6). $$f_{s,s} = \frac{\left[M_s + \varepsilon_{bi}A_f E_f\left(d_f - \frac{kd}{3}\right)\right](d - kd)E_s}{A_s E_s(d - \frac{kd}{3})(d - kd) + A_f E_f(d_f - \frac{kd}{3})(d_f - kd)}$$ $$f_{s,s} \leq 0.80 f_y$$	†See EQUATION NOTE II (U.S.) after Step 14. $f_{s,s} = 40.3 \text{ ksi} \leq (0.80)(60 \text{ ksi}) = 48 \text{ ksi}$ $\therefore$ the stress level in the reinforcing steel is within the recommended limit.	††See EQUATION NOTE II (SI) after Step 14. $f_{s,s} = 278 \text{ N/mm}^2 \leq (0.80)(410 \text{ N/mm}^2) = 330 \text{ N/mm}^2$ $\therefore$ the stress level in the reinforcing steel is within the recommended limit.

Procedure	Calculation in inch-pound units	Calculation in SI metric units
Step 14—Check creep rupture limit at service of the FRP Calculate the stress level in the FRP using Eq. (10-15) and verify that it is less than creep-rupture stress limit given in Table 10.1. Assume that the full service load is sustained. $$f_{f,s} = f_{s,s}\left(\frac{E_f}{E_s}\right)\left(\frac{d_f - kd}{d - kd}\right) - \varepsilon_{bi}E_f$$ For a carbon FRP system, the sustained plus cyclic stress limit is obtained from Table 10.1: Sustained plus cyclic stress limit = $0.55 f_{fu}$	$f_{f,s} = 40.3 \text{ ksi}\left(\frac{19,230 \text{ ksi}}{29,000 \text{ ksi}}\right)\left(\frac{23.7 \text{ in.} - 7.4 \text{ in.}}{21.5 \text{ in.} - 7.4 \text{ in.}}\right)$ $- (0.00061)(19,230 \text{ ksi})$ $f_{f,s} = 19 \text{ ksi} \le (0.55)(85 \text{ ksi}) = 50 \text{ ksi}$ ∴ the stress level in the FRP is within the recommended sustained plus cyclic stress limit.	$f_{f,s} = 0.278 \text{ kN/mm}^2\left(\frac{133 \text{ kN/mm}^2}{200 \text{ kN/mm}^2}\right)\left(\frac{602 \text{ mm} - 188 \text{ mm}}{546 \text{ mm} - 188 \text{ mm}}\right)$ $- (0.00061)(133 \text{ N/mm}^2)$ $f_{f,s} = 134 \text{ N/mm}^2 \le (0.55)(590 \text{ N/mm}^2) = 324.5 \text{ N/mm}^2$ ∴ the stress level in the FRP is within the recommended sustained plus cyclic stress limit.

*EQUATION NOTE I (U.S.):

$$k = \sqrt{\left(0.0116\left(\frac{29,000}{4030}\right) + 0.0012\left(\frac{19,230}{4030}\right)\right)^2 + 2\left(0.0116\left(\frac{29,000}{4030}\right) + 0.0012\left(\frac{19,230}{4030}\right)\left(\frac{23.7 \text{ in.}}{21.5 \text{ in.}}\right)\right)} - \left(0.0116\left(\frac{29,000}{4030}\right) + 0.0012\left(\frac{19,230}{4030}\right)\right)$$

**EQUATION NOTE I (SI):

$$k = \sqrt{\left(0.0116\left(\frac{200}{27.6}\right) + 0.0012\left(\frac{133}{27.6}\right)\right)^2 + 2\left(0.0116\left(\frac{200}{27.6}\right) + 0.0012\left(\frac{133}{27.6}\right)\left(\frac{602 \text{ mm}}{546 \text{ mm}}\right)\right)} - \left(0.0116\left(\frac{200}{27.6}\right) + 0.0012\left(\frac{133}{27.6}\right)\right)$$

†EQUATION NOTE II (U.S.):

$$f_{s,s} = \frac{\left[2424 \text{ k-in.} + (0.00061)(0.3 \text{ in.}^2)(19,230 \text{ ksi})\left(23.7 \text{ in.} - \frac{7.4 \text{ in.}}{3}\right)\right](21.5 \text{ in.} - 7.4 \text{ in.})(29,000 \text{ ksi})}{(3.00 \text{ in.}^2)(29,000 \text{ ksi})\left(21.5 \text{ in.} - \frac{7.4 \text{ in.}}{3}\right)(21.5 \text{ in.} - 7.4 \text{ in.}) + (0.3 \text{ in.}^2)(19,230 \text{ ksi})\left(23.7 \text{ in.} - \frac{7.4 \text{ in.}}{3}\right)(23.7 \text{ in.} - 7.4 \text{ in.})}$$

††EQUATION NOTE II (SI):

$$f_{s,s} = \frac{\left[273,912 \text{ kN-mm} + (0.00061)(194 \text{ mm}^2)(132.7 \text{ kN/mm}^2)\left(602 \text{ mm} - \frac{188 \text{ mm}}{3}\right)\right](546 \text{ mm} - 188 \text{ mm})(200 \text{ kN/mm}^2)}{(1935 \text{ mm}^2)(200 \text{ kN/mm}^2)\left(546 \text{ mm} - \frac{188 \text{ mm}}{3}\right)(546 \text{ mm} - 188 \text{ mm}) + (194 \text{ mm}^2)(132.7 \text{ kN/mm}^2)\left(602 \text{ mm} - \frac{188 \text{ mm}}{3}\right)(602 \text{ mm} - 188 \text{ mm})}$$

In detailing the FRP reinforcement, FRP bars should be terminated at a distance equal to the bar development length past the point on the moment diagram that represents cracking.

15.5—Flexural strengthening of an interior prestressed concrete beam with FRP laminates

A number of continuous prestressed concrete beams with five 1/2 in. (12.7 mm) diameter bonded strands (Fig. 15.3) are located in a parking garage that is being converted to an office space. All prestressing strands are Grade 270 ksi (1860 N/mm^2) low-relaxation seven-wire strands. The beams require an increase in their live-load-carrying capacity from 50 lb/ft^2 (244 kg/m^2) to 75 lb/ft^2 (366 kg/m^2). The beams are also required to support an additional dead load of 10 lb/ft^2. Analysis indicates that each existing beam has adequate flexural capacity to carry the new loads in the negative moment region at the supports but is deficient in flexure at midspan and in shear at the supports. The beam meets the deflection and crack control serviceability requirements. The cast-in-place beams support a 4 in. (100 mm) slab. For bending at midspan, beams should be treated as T-sections. Summarized in Table 15.6 are the existing and new loads and associated midspan moments for the beam. FRP system properties are shown in Table 15.4, shown again on this page for convenience.
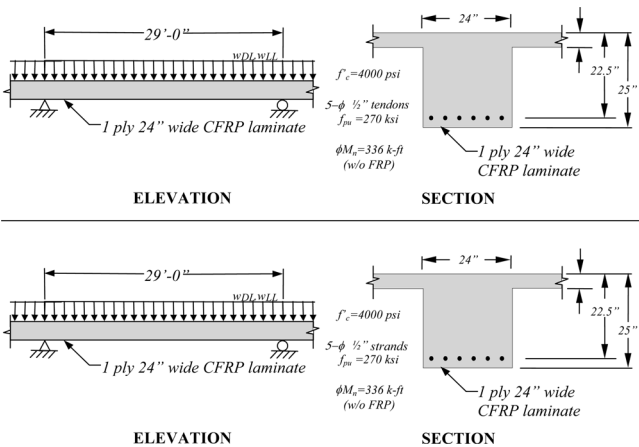

Fig. 15.3—Schematic of the idealized continuous prestressed beam with FRP external reinforcement.

Length of the beam l	29 ft	8.84 m
Bay width l_2	30 ft	9.14 m
Width of beam w	24 in.	610 mm
d_p	22.5 in.	571 mm
h	25 in.	635 mm
Effective flange width b_f	87 in.	2210 mm
Flange thickness h_f	4 in.	102 mm
f_c'	4000 psi	27.6 N/mm^2
Strands diameter	1/2 in.	12.7 mm
f_{pe}	165 ksi	1138 N/mm^2
f_{py}	230 ksi	1586 N/mm^2
f_{pu}	270 ksi	1860 N/mm^2
E_p	28,500 ksi	1.96×10^5 N/mm^2
ϕM_n without FRP	336 k-ft	455 kN-m

Table 15.6—Loadings and corresponding moments

Loading/moment	Existing loads		Anticipated loads	
Dead loads w_{DL}	2.77 k/ft	40.4 N/mm	3.09 k/ft	45.1 N/mm
Live load w_{LL}	1.60 k/ft	23.3 N/mm	2.4 k/ft	35 N/mm
Unfactored loads ($w_{DL} + w_{LL}$)	4.37 k/ft	63.8 N/mm	5.49 k/ft	80.2 N/mm
Unstrengthened load limit ($1.1w_{DL} + 0.75w_{LL}$)	N/A	N/A	5.2 k/ft	75.9 N/mm
Factored loads ($1.2w_{DL} + 1.6w_{LL}$)	5.88 k/ft	85.9 N/mm	7.55 k/ft	110.2 N/mm
Dead-load moment M_{DL}	147 k-ft	199 kN-m	162 k-ft	220.2 kN-m
Live-load moment M_{LL}	85 k-ft	115 kN-m	126 k-ft	171.1 kN-m
Service-load moment M_s	232 k-ft	314 kN-m	288 k-ft	391.3 kN-m
Unstrengthened moment limit ($1.1M_{DL} + 0.75M_{LL})_{new}$	N/A	N/A	273 k-ft	371 kN-m
Factored moment M_u	312 k-ft	423 kN-m	397 k-ft	538 kN-m

By inspection, the level of strengthening is reasonable in that it does meet the strengthening limit criteria put forth in Eq. (10-1). That is, the existing flexural strength without FRP, $(\phi M_n)_{w/o} = 336$ k-ft (455 kN-m), is greater than the unstrengthened moment limit, $(1.1M_{DL} + 0.75M_{LL})_{new} = 273$ k-ft (370 kN-m). The design calculations used to verify this configuration follow. The beam is to be strengthened using the FRP system described in Table 15.4. A one-ply, 24 in. (610 mm) wide strip of FRP is considered for this evaluation.

Table 15.4—Manufacturer's reported FRP system properties

Thickness per ply t_f	0.040 in.	1.02 mm
Ultimate tensile strength f_{fu}^*	90 ksi	621 N/mm^2
Rupture strain ε_{fu}^*	0.015 in./in.	0.015 mm/mm
Modulus of elasticity of FRP laminates E_f	5360 ksi	37,000 N/mm^2

Procedure	Calculation in inch-pound units	Calculation in SI metric units
Step 1—Calculate the FRP-system design material properties The beam is located in an interior space and a CFRP material will be used. Therefore, per Table 9.1, an environmental reduction factor of 0.95 is suggested. $f_{fu} = C_E f_{fu}^*$ $\varepsilon_{fu} = C_E \varepsilon_{fu}^*$	$f_{fu} = (0.95)(90 \text{ ksi}) = 85 \text{ ksi}$ $\varepsilon_{fu} = (0.95)(0.015 \text{ in./in.}) = 0.0142 \text{ in./in.}$	$f_{fu} = (0.95)(621 \text{ N/mm}^2) = 590 \text{ N/mm}^2$ $\varepsilon_{fu} = (0.95)(0.015 \text{ mm/mm}) = 0.0142 \text{ mm/mm}$
Step 2—Preliminary calculations Properties of the concrete: β_1 from ACI 318-05, Section 10.2.7.3 $E_c = 57{,}000\sqrt{f_c'}$ Properties of the existing prestressing steel: Area of FRP reinforcement: $A_f = n t_f w_f$ Cross-sectional area: $A_{cg} = b_e h_f + b_w(h - h_f)$ Distance from the top fiber to the section centroid: $y_t = \dfrac{b_f \dfrac{h_f^2}{2} + b_w(h-h_f)\left(h_f + \dfrac{(h-h_f)}{2}\right)}{A_{cg}}$ Gross moment of inertia: $I_g = \dfrac{b_f h_f^3}{12} + b_f h_f\left(y_t - \dfrac{h_f}{2}\right)^2$ $+ \dfrac{b_w(h-h_f)^3}{12} + b_w(h-h_f)\left(y_t - \dfrac{h-h_f}{2}\right)^2$ Radius of gyration: $r = \sqrt{\dfrac{I_g}{A_{cg}}}$ Effective prestressing strain: $\varepsilon_{pe} = \dfrac{f_{pe}}{E_p}$ Effective prestressing force: $P_e = A_{ps} f_{pe}$ Eccentricity of prestressing force: $e = d_p - y_t$	$\beta_1 = 1.05 - 0.05\dfrac{f_c'}{1000} = 0.85$ $E_c = 57{,}000\sqrt{4000 \text{ psi}} = 3{,}605{,}000 \text{ psi}$ $A_{ps} = 5(0.153 \text{ in.}^2) = 0.765 \text{ in.}^2$ $A_f = (1 \text{ ply})(0.040 \text{ in./ply})(24 \text{ in.}) = 0.96 \text{ in.}^2$ $A_{cg} = (87 \text{ in.})(4 \text{ in.}) + (24 \text{ in.})(25 \text{ in.} - 4 \text{ in.}) = 852 \text{ in.}^2$ $y_t = \dfrac{87 \text{ in.} \times \dfrac{4 \text{ in.}^2}{2} + 24 \text{ in.} \times 21 \times 14.5}{852} = 9.39 \text{ in.}$ $I_g = \dfrac{87 \text{ in.} \times 4 \text{ in.}^3}{12} + 87 \text{ in.} \times 4 \text{ in.}(9.39 \text{ in.} - 2)^2$ $+ \dfrac{24 \text{ in.} \times 21^3}{12} + 24 \text{ in.} \times 21(9.39 - 14.5)^2 = 51{,}150 \text{ in.}^4$ $r = \sqrt{\dfrac{51{,}150}{852}} = 7.75 \text{ in.}$ $\varepsilon_{pe} = \dfrac{265}{28{,}500} = 0.00589$ $P_e = 0.765 \times 165 = 126.2 \text{ kips}$ $e = 22.5 - 9.39 = 13.1 \text{ in.}$	$\beta_1 = 1.05 - 0.05\dfrac{f_c'}{6.9} = 0.85$ $E_c = 4700\sqrt{27.6 \text{ N/mm}^2} = 24{,}700 \text{ N/mm}^2$ $A_{ps} = 5(99 \text{ mm}^2) = 495 \text{ mm}^2$ $A_f = (1 \text{ ply})(1.0 \text{ mm/ply})(610 \text{ mm}) = 610 \text{ mm}^2$ $A_{cg} = (2210 \text{ mm})(102 \text{ mm})$ $+ (610 \text{ mm})(612 \text{ mm} - 102 \text{ mm}) = 5.5 \times 10^5 \text{ mm}^2$ $y_t = \dfrac{2210 \text{ mm} \times \dfrac{102 \text{ mm}^2}{2} + 610 \text{ mm} \times 533 \times 368}{5.5 \times 10^5}$ $= 238 \text{ mm}$ $I_g = \dfrac{2210 \text{ mm} \times 102 \text{ mm}^3}{12} + 2210 \text{ mm} \times 102 \text{ mm}(238 - 51)^2$ $+ \dfrac{610 \text{ mm} \times 533^3}{12} + 610 \text{ mm} \times 533(238 - 368)^2 = 2.13 \times 10^{10} \text{ mm}$ $r = \sqrt{\dfrac{2.13 \times 10^{10}}{5.5 \times 10^5}} = 197 \text{ mm}$ $\varepsilon_{pe} = \dfrac{1138}{1.96 \times 10^5} = 0.00589$ $P_e = 495 \times 1138 = 563{,}310 \text{ N}$ $e = 571 - 238 = 333 \text{ mm}$
Step 3—Determine the existing state of strain on the soffit The existing state of strain is calculated assuming the beam is uncracked and the only loads acting on the beam at the time of the FRP installation are dead loads. Distance from extreme bottom fiber to the section centroid: $y_b = h - y_t$ Initial strain in the beam soffit: $\varepsilon_{bi} = \dfrac{-P_e}{E_c A_{cg}}\left(1 + \dfrac{e y_b}{r^2}\right) + \dfrac{M_{DL} y_b}{E_c I_g}$	 $y_b = 25 - 9.39 = 15.61 \text{ in.}$ $\varepsilon_{bi} = \dfrac{-126.2}{3605 \times 852}\left(1 + \dfrac{13.1 \times 15.6}{7.75^2}\right) + \dfrac{147 \times 12 \times 15.6}{3605 \times 51{,}150}$ $\varepsilon_{bi} = -3 \times 10^{-5}$	 $y_b = 635 - 238 = 397 \text{ mm}$ $\varepsilon_{bi} = \dfrac{-563{,}310}{24{,}700 \times 5.5 \times 10^5}\left(1 + \dfrac{333 \times 397}{197^2}\right) + \dfrac{199 \times 10^6 \times 397}{24{,}700 \times 2.13 \times 10^{10}}$ $\varepsilon_{bi} = -3 \times 10^{-5}$

Procedure	Calculation in inch-pound units	Calculation in SI metric units
Step 4—Determine the design strain of the FRP system The design strain of FRP accounting for debonding failure mode ε_{fd} is calculated using Eq. (10-2) Because the design strain is smaller than the rupture strain, debonding controls the design of the FRP system.	$\varepsilon_{fd} = 0.083 \sqrt{\dfrac{4000 \text{ psi}}{1\,(5{,}360{,}000 \text{ psi})(0.04 \text{ in.})}}$ $= 0.0113 \le 0.9(0.0142) = 0.0128$	$\varepsilon_{fd} = 0.042 \sqrt{\dfrac{27.6 \text{ N/mm}^2}{1\,(37{,}000 \text{ N/mm}^2)(1.016 \text{ mm})}}$ $= 0.0113 \le 0.9(0.0142) = 0.0128$
Step 5—Estimate c, the depth to the neutral axis A reasonable initial estimate of c is $0.1h$. The value of the c is adjusted after checking equilibrium. $c = 0.1h$	$c = (0.1)(25 \text{ in.}) = 2.50 \text{ in.}$	$c = (0.1)(635 \text{ mm}) = 63.5 \text{ mm}$
Step 6—Determine the effective level of strain in the FRP reinforcement The effective strain level in the FRP may be found from Eq. (10-3). $\varepsilon_{fe} = 0.003\left(\dfrac{d_f - c}{c}\right) - \varepsilon_{bi} \le \varepsilon_{fd}$ Note that for the neutral axis depth selected, FRP debonding would be the failure mode because the second expression in this equation controls. If the first (limiting) expression governed, then FRP rupture would be the failure mode.	$\varepsilon_{fe} = 0.003\left(\dfrac{25 - 2.5}{2.5}\right) - 0.00003 = 0.027$ $> \varepsilon_{fd} = 0.0113$ Failure is governed by FRP debonding $\varepsilon_{fe} = \varepsilon_{fd} = 0.0113$	$\varepsilon_{fe} = 0.003\left(\dfrac{635 - 63.5}{63.5}\right) - 0.00003 = 0.027$ $\varepsilon_{fd} = 0.0113$ Failure is governed by FRP debonding $\varepsilon_{fe} = \varepsilon_{fd} = 0.0113$
Step 7—Calculate the strain in the existing prestressing steel The strain in the prestressing steel can be calculated using Eq. (10-23b) and (10-22). $\varepsilon_{pnet} = (\varepsilon_{fe} + \varepsilon_{bi})\left(\dfrac{d_p - c}{d_f - c}\right)$ $\varepsilon_{ps} = \varepsilon_{pe} + \dfrac{P_e}{A_c E_c}\left(1 + \dfrac{e^2}{r^2}\right) + \varepsilon_{pnet} \le 0.035$	$\varepsilon_{pnet} = (0.0113 + 0.00003)\left(\dfrac{22.5 - 2.5}{25 - 2.5}\right)$ $\varepsilon_{pnet} = 0.01$ $\varepsilon_{ps} = 0.00589 + \dfrac{126.2}{852 \times 3605}\left(1 + \dfrac{13.1^2}{7.75^2}\right) + 0.01$ $\varepsilon_{ps} = 0.016 \le 0.035$	$\varepsilon_{pnet} = (0.0113 + 0.00003)\left(\dfrac{571 - 63.5}{635 - 63.5}\right)$ $\varepsilon_{pnet} = 0.01$ $\varepsilon_{ps} = 0.00589 + \dfrac{563{,}310}{5.5 \times 10^5 \times 24{,}700}\left(1 + \dfrac{333^2}{197^2}\right) + 0.01$ $\varepsilon_{ps} = 0.016 \le 0.035$
Step 8—Calculate the stress level in the prestressing steel and FRP The stresses are calculated using Eq. (10-24b) and (10-21). $f_{ps} = \begin{cases} 28{,}500\varepsilon_{ps} & \text{for } \varepsilon_{ps} \le 0.0086 \\ 270 - \dfrac{0.04}{\varepsilon_{ps} - 0.007} & \text{for } \varepsilon_{ps} > 0.0086 \end{cases}$ $f_{fe} = E_f \varepsilon_{fe}$	$f_{ps} = 270 - \dfrac{0.04}{0.016 - 0.007} = 265.6 \text{ ksi}$ $f_{fe} = (5360 \text{ ksi})(0.0113) = 60.6 \text{ ksi}$	$f_{ps} = 1860 - \dfrac{0.276}{0.016 - 0.007} = 1831 \text{ N/mm}^2$ $f_{fe} = (37{,}000 \text{ N/mm}^2)(0.0113) = 418 \text{ N/mm}^2$

Procedure	Calculation in inch-pound units	Calculation in SI metric units
Step 9—Calculate the equivalent concrete compressive stress block parameters α_1 and β_1 The strain in concrete at failure can be calculated from strain compatibility as follows: $$\varepsilon_c = (\varepsilon_{fe} + \varepsilon_{bi})\left(\frac{c}{d_f - c}\right)$$ The strain ε_c' corresponding to f_c' is calculated as $$\varepsilon_c' = \frac{1.7 f_c'}{E_c}$$ Concrete stress block factors can be estimated using ACI 318-05. Approximate stress block factors may be calculated from the parabolic stress-strain relationship for concrete and is expressed as follows: $$\beta_1 = \frac{4\varepsilon_c' - \varepsilon_c}{6\varepsilon_c' - 2\varepsilon_c}$$ $$\alpha_1 = \frac{3\varepsilon_c'\,\varepsilon_c - \varepsilon_c^2}{3\beta_1\varepsilon_c'^2}$$	$$\varepsilon_c = (0.0113 + 0.00003)\left(\frac{2.5}{25 - 2.5}\right) = 0.0013$$ $$\varepsilon_c' = \frac{1.7(4000)}{3605 \times 10^6} = 0.0019$$ $$\beta_1 = \frac{4(0.0019) - 0.0013}{6(0.0019) - 2(0.0013)} = 0.716$$ $$\alpha_1 = \frac{3(0.0019)(0.0013) - (0.0013)^2}{3(0.716)(0.0019)^2} = 0.738$$	$$\varepsilon_c = (0.0113 + 0.00003)\left(\frac{63.5}{635 - 63.5}\right) = 0.0013$$ $$\varepsilon_c' = \frac{1.7(27.6)}{24{,}700} = 0.0019$$ $$\beta_1 = \frac{4(0.0019) - 0.0013}{6(0.0019) - 2(0.0013)} = 0.716$$ $$\alpha_1 = \frac{3(0.0019)(0.0013) - (0.0013)^2}{3(0.716)(0.0019)^2} = 0.738$$
Step 10—Calculate the internal force resultants and check equilibrium Force equilibrium is verified by checking the initial estimate of c with Eq. (10-25). $$c = \frac{A_p f_{ps} + A_f f_{fe}}{\alpha_1 f_c' \beta_1 b}$$	$$c = \frac{(0.765 \text{ in.}^2)(265.6 \text{ ksi}) + (0.96 \text{ in.}^2)(60.6 \text{ ksi})}{(0.738)(4 \text{ ksi})(0.716)(87 \text{ in.})}$$ $c = 1.42$ in. $\neq 2.50$ in. n.g. ∴ Revise estimate of c and repeat Steps 6 through 10 until equilibrium is achieved.	$$c =$$ $$\frac{(495 \text{ mm}^2)(1831 \text{ N/mm}^2) + (620 \text{ mm}^2)(418 \text{ N/mm}^2)}{(0.738)(27.6 \text{ N/mm}^2)(0.716)(2210 \text{ mm})}$$ $c = 36$ mm $\neq 63.5$ in. n.g. ∴ Revise estimate of c and repeat Steps 6 through 10 until equilibrium is achieved.
Step 11—Adjust c until force equilibrium is satisfied Steps 6 through 10 were repeated several times with different values of c until equilibrium was achieved. The results of the final iteration are $c = 1.86$ in.; $\varepsilon_{ps} = 0.016$; $f_{ps} = f_y = 265.6$ ksi; $\varepsilon_{fe} = 0.0113$; $f_{fe} = 60.6$ ksi; $\varepsilon_c = 0.00091$; $\alpha_1 = 0.577$; and $\beta_1 = 0.698$.	$$c = \frac{(0.765 \text{ in.}^2)(265.6 \text{ ksi}) + (0.96 \text{ in.}^2)(60.6 \text{ ksi})}{(0.577)(4 \text{ ksi})(0.698)(87 \text{ in.})}$$ $c = 1.86$ in. $= 1.86$ in. ✓ **OK** ∴ the value of c selected for the final iteration is correct.	$$c = \frac{(495 \text{ mm}^2)(1831 \text{ N/mm}^2) + (620 \text{ mm}^2)(418 \text{ N/mm}^2)}{(0.577)(27.6 \text{ N/mm}^2)(0.698)(2210 \text{ mm})}$$ $c = 47$ mm $= 47$ mm ✓ **OK** ∴ the value of c selected for the final iteration is correct.
Step 12—Calculate flexural strength components The design flexural strength is calculated using Eq. (10-26). An additional reduction factor, $\psi_f = 0.85$, is applied to the contribution of the FRP system. Prestressing steel contribution to bending: $$M_{np} = A_p f_{ps}\left(d_p - \frac{\beta_1 c}{2}\right)$$ FRP contribution to bending: $$M_{nf} = A_s f_{fe}\left(d_f - \frac{\beta_1 c}{2}\right)$$	$$M_{np} = (0.765 \text{ in.}^2)(265.6 \text{ ksi})\left(22.5 \text{ in.} - \frac{0.70(1.86 \text{ in.})}{2}\right)$$ $M_{np} = 4440$ k-in. $= 370$ k-ft $$M_{nf} = (0.96 \text{ in.}^2)(60.6 \text{ ksi})\left(25 \text{ in.} - \frac{0.70(1.86 \text{ in.})}{2}\right)$$ $M_{nf} = 1417$ k-in. $= 118$ k-ft	$$M_{np} = (495 \text{ mm}^2)(1830 \text{ N/mm}^2)\left(571.5 \text{ mm} - \frac{0.70(47 \text{ mm})}{2}\right)$$ $M_{np} = 501.6 \times 10^6$ N-mm $= 501.6$ kN-m $$M_{nf} = (620 \text{ mm}^2)(418 \text{ N/mm}^2)\left(635 \text{ mm} - \frac{0.70(47 \text{ mm})}{2}\right)$$ $M_{nf} = 160.1 \times 10^6$ N-mm $= 160.1$ kN-m

Procedure	Calculation in inch-pound units	Calculation in SI metric units
Step 13—Calculate design flexural strength of the section The design flexural strength is calculated using Eq. (10-1) and (10-26). Because $\varepsilon_{ps} = 0.016 > 0.015$, a strength reduction factor of $\phi = 0.90$ should be used per Eq. (10-5). An additional reduction factor $\psi_f = 0.85$ is used to calculate the FRP contribution to nominal capacity. $$\phi M_n = \phi[M_{np} + \psi_f M_{nf}]$$	$\phi M_n = 0.9[370 \text{ k-ft} + 0.85(118 \text{ k-ft})]$ $\phi M_n = 423 \text{ k-ft} \geq M_u = 397 \text{ k-ft}$ ∴ the strengthened section is capable of sustaining the new required flexural strength.	$\phi M_n = 0.9[506.1 \text{ kN-m} + 0.85(160.1 \text{ kN-m})]$ $\phi M_n = 573 \text{ kN-m} \geq M_u = 538 \text{ kN-m}$ ∴ the strengthened section is capable of sustaining the new required flexural strength.
Step 14—Check service condition of the section Calculate the cracking moment and compare the service moment: $$f_r = 7.5\sqrt{f_c'}$$ $$M_{cr} = \frac{f_r I_g}{y_b} + P_e\left(e + \frac{r^2}{y_b}\right)$$	$f_r = 7.5\sqrt{4000} = 474 \text{ psi} = 0.474 \text{ ksi}$ $M_{cr} = \frac{0.474 \times 51{,}150}{15.61} + 126.2\left(13.1 + \frac{7.75^2}{15.61}\right)$ $M_{cr} = 3695 \text{ k-in.} = 308 \text{ k-ft}$ $> M_s = 288 \text{ k-ft}$ ∴ the strengthened section is uncracked at service.	$f_r = 7.5\sqrt{27.6} = 3.67 \text{ N/mm}^2$ $M_{cr} = \frac{3.67 \times 2.13 \times 10^{10}}{397} + 563{,}310\left(333 + \frac{197^2}{397}\right)$ $M_{cr} = 439{,}950{,}000 \text{ N-mm} = 440 \text{ kN-mm}$ $> M_s = 391.3 \text{ kN-m}$ ∴ the strengthened section is uncracked at service.
Step 15—Check stress in prestressing steel at service condition Calculate the cracking moment and compare to service moment: $$\varepsilon_{ps,s} = \varepsilon_{pe} + \frac{P_e}{A_c E_c}\left(1 + \frac{e^2}{r^2}\right) + \frac{M_s e}{E_c I_g}$$ Calculate the steel stress using Eq. (10-24a): $$f_{ps,s} = \begin{cases} 28{,}500\varepsilon_{ps,s} & \text{for } \varepsilon_{ps,s} \leq 0.0086 \\ 270 - \dfrac{0.04}{\varepsilon_{ps,s} - 0.07} & \text{for } \varepsilon_{ps,s} > 0.0086 \end{cases}$$ Check the service stress limits of Eq. (10-20): $$f_{ps,s} \leq 0.82 f_{py}$$ $$f_{ps,s} \leq 0.74 f_{pu}$$	$\varepsilon_{ps,s} = 0.00589 + \frac{126.2}{852 \times 3605}\left(1 + \frac{13.1^2}{7.75^2}\right) + \frac{289 \times 12 \times 13.1}{3605 \times 51{,}150}$ $\varepsilon_{ps,s} = 0.0063 \leq 0.0086$ $f_{ps,s} = 28{,}500(0.0063) = 180 \text{ ksi}$ $f_{ps,s} = 180 \text{ ksi} < 0.82(230) = 189 \text{ ksi}$ **OK** $f_{ps,s} = 180 \text{ ksi} < 0.74(270) = 200 \text{ ksi}$ **OK**	$\varepsilon_{ps,s} = 0.00589 + \frac{563{,}310}{5.5 \times 10^5 \times 24{,}700}\left(1 + \frac{333^2}{197^2}\right)$ $\quad + \frac{391.3 \times 10^6 \times 333}{24{,}700 \times 2.13 \times 10^{10}}$ $\varepsilon_{ps,s} = 0.0063 \leq 0.0086$ $f_{ps,s} = 1.96 \times 10^5 (0.0063) = 1238 \text{ N/mm}^2$ $f_{ps,s} = 1238 \text{ N/mm}^2 < 0.82(1586) = 1300 \text{ N/mm}^2$ **OK** $f_{ps,s} = 1238 \text{ N/mm}^2 < 0.74(1860) = 1376 \text{ N/mm}^2$ **OK**
Step 16—Check stress in concrete at service condition Calculate the cracking moment and compare to service moment: $$\varepsilon_{c,s} = \frac{-P_e}{A_c E_c}\left(1 + \frac{e^2}{r^2}\right) - \frac{M_s y_t}{E_c I_g}$$ $$f_{c,s} = E_c \varepsilon_{c,s}$$ $$f_{c,s} \leq 0.45 f_c'$$	$\varepsilon_{c,s} = \frac{-26.2}{852 \times 3605}\left(1 + \frac{13.1^2}{7.75^2}\right) - \frac{289 \times 12 \times 9.39}{3605 \times 51{,}150}$ $\varepsilon_{c,s} = 0.00016$ $f_{c,s} = 3{,}605{,}000 \text{ psi }(0.00016) = 577 \text{ psi}$ $0.45 f_c' = 0.45(4000) = 1800 \text{ psi}$ $f_{c,s} = 577 \text{ psi} < 0.45 f_c' = 1800 \text{ psi}$ **OK**	$\varepsilon_{c,s} = \frac{-563{,}310}{5.5 \times 10^5 \times 24{,}700}\left(1 + \frac{333^2}{197^2}\right) - \frac{391.3 \times 10^6 \times 238}{24{,}700 \times 2.13 \times 10^{10}}$ $\varepsilon_{c,s} = 0.00016$ $f_{c,s} = 24{,}700 \text{ N/mm}^2 (0.00016) = 3.95 \text{ N/mm}^2$ $0.45 f_c' = 0.45(27.6) = 12.42 \text{ N/mm}^2$ $f_{c,s} = 3.95 \text{ N/mm}^2 < 0.45 f_c' = 12.42 \text{ N/mm}^2$ **OK**

Procedure	Calculation in inch-pound units	Calculation in SI metric units
Step 17—Check service stresses in the FRP reinforcement The stress in the FRP at service condition can be calculated using Eq. (10-29): $f_{f,s} = \left(\dfrac{E_f}{E_c}\right)\dfrac{M_s y_b}{I} - \varepsilon_{bi} E_f$ Because the section is uncracked at service, the gross moment of inertia of the section must be used. The calculated stress in FRP should be checked against the limits in Table 10.1. For carbon FRP: $f_{f,s} \le 0.55 f_{fu}$	$f_{f,s} = \left(\dfrac{5360\ \text{ksi}}{3605\ \text{ksi}}\right)\dfrac{289\ \text{k-ft} \times 12\ \text{in./ft} \times 15.61\ \text{in.}}{51{,}150\ \text{in.}^4}$ $-0.00003 \times 5360\ \text{ksi}$ $f_{f,s} = 1.41\ \text{ksi}$ $0.55 f_{fu} = 0.55(85) = 47\ \text{ksi}$ $f_{f,s} = 1.41\ \text{ksi} < 0.55 f_{fu} = 47\ \text{ksi}$ **OK**	$f_{f,s} = \left(\dfrac{37{,}700\ \text{N/mm}^2}{24{,}700\ \text{N/mm}^2}\right)\dfrac{391.3 \times 10^6\ \text{N/mm} \times 397\ \text{mm}}{2.13 \times 10^{10}\ \text{mm}^4}$ $-0.00003 \times 37{,}700\ \text{N/mm}^2$ $f_{f,s} = 9.7\ \text{N/mm}^2$ $0.55 f_{fu} = 0.55(586) = 322\ \text{N/mm}^2$ $f_{f,s} = 9.7\ \text{N/mm}^2 < 0.55 f_{fu} = 322\ \text{N/mm}^2$ **OK**

In detailing the FRP reinforcement, the FRP should be terminated a minimum of l_{df}, calculated per Eq. (13-2), past the point on the moment diagram that represents cracking. The factored shear force at the termination should also be checked against the shear force that causes FRP end peeling, estimated as 2/3 of the concrete shear strength. If the shear force is greater than 2/3 of the concrete shear strength, FRP strips should be extended further toward the supports. U-wraps may also be used to reinforce against cover delamination.

15.6—Shear strengthening of an interior T-beam

A reinforced concrete T-beam ($f_c' = 3000$ psi = 20.7 N/mm^2) located inside of an office building is subjected to an increase in its live-load-carrying requirements. An analysis of the existing beam indicates that the beam is still satisfactory for flexural strength; however, its shear strength is inadequate to carry the increased live load. Based on the analysis, the nominal shear strength provided by the concrete is $V_c = 44.2$ kips = 196.6 kN, and the nominal shear strength provided by steel shear reinforcement is $V_s = 19.6$ kips = 87.2 kN. Thus, the design shear strength of the existing beam is $\phi V_{n,existing} = 0.75(44.2$ kips $+ 19.6$ kips) = 47.85 kips = 213 kN. The factored required shear strength, including the increased live load, at a distance d away from the support is $V_u = 57$ kips = 253.5 kN. Figure 15.4 shows the shear diagram with the locations where shear strengthening is required along the length of the beam.

Supplemental FRP shear reinforcement is designed as shown in Fig. 15.5 and summarized in Table 15.7. Each FRP strip consists of one ply ($n = 1$) of a flexible carbon sheet installed by wet layup. The FRP system manufacturer's reported material properties are shown in Table 15.8.
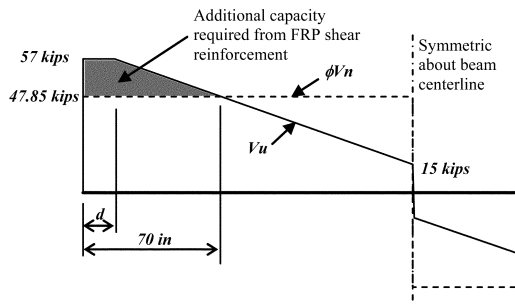

Fig. 15.4—Shear diagram showing demand versus existing strength. The FRP reinforcement should correct the deficiency shown shaded.
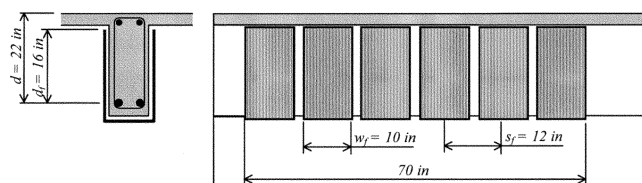

Fig. 15.5—Configuration of the supplemental FRP shear reinforcement.

Table 15.7—Configuration of the supplemental FRP shear reinforcement

d	22 in.	559 mm
d_{fv}	16 in.	406 mm
Width of each sheet w_f	10 in.	254 mm
Span between each sheet s_f	12 in.	305 mm
FRP strip length	70 in.	1778 mm

Table 15.8—Manufacturer's reported FRP system properties

Thickness per ply t_f	0.0065 in.	0.165 mm
Ultimate tensile strength f_{fu}^*	550,000 psi	3790 N/mm^2
Rupture strain ε_{fu}^*	0.017 in./in.	0.017 mm/mm
Modulus of elasticity E_f	33,000,000 psi	227,530 N/mm^2

The design calculations used to arrive at this configuration follow.

Procedure	Calculation in inch-pound units	Calculation in SI metric units
Step 1—Compute the design material properties The beam is located in an enclosed and conditioned space and a CFRP material will be used. Therefore, per Table 9.1, an environmental-reduction factor of 0.95 is suggested. $f_{fu} = C_E f_{fu}^*$ $\varepsilon_{fu} = C_E \varepsilon_{fu}^*$	 $f_{fu} = (0.95)(550 \text{ ksi}) = 522.5 \text{ ksi}$ $\varepsilon_{fu} = (0.95)(0.017) = 0.016$	 $f_{fu} = (0.95)(3.79 \text{ kN/mm}^2) = 3.60 \text{ kN/mm}^2$ $\varepsilon_{fu} = (0.95)(0.017) = 0.016$
Step 2—Calculate the effective strain level in the FRP shear reinforcement The effective strain in FRP U-wraps should be determined using the bond-reduction coefficient κ_v. This coefficient can be computed using Eq. (11-7) through (11-10). $L_e = \dfrac{2500}{(nt_f E_f)^{0.58}}$ $k_1 = \left(\dfrac{f_c'}{4000}\right)^{2/3}$ $k_2 = \left(\dfrac{d_{fv} - L_e}{d_{fv}}\right)$ $\kappa_v = \dfrac{k_1 k_2 L_e}{468 \varepsilon_{fu}} \le 0.75$ The effective strain can then be computed using Eq. (11-6b) as follows: $\varepsilon_{fe} = \kappa_v \varepsilon_{fu} \le 0.004$	 $L_e = \dfrac{2500}{[(1)(0.0065 \text{ in.})(33 \times 10^6 \text{ psi})]^{0.58}} = 2.0 \text{ in.}$ $k_1 = \left(\dfrac{3000 \text{ psi}}{4000}\right)^{2/3} = 0.825$ $k_2 = \left(\dfrac{16 \text{ in.} - 2.0 \text{ in.}}{16 \text{ in.}}\right) = 0.875$ $\kappa_v = \dfrac{(0.82)(0.875)(2 \text{ in.})}{468(0.016)} = 0.193 \le 0.75$ $\varepsilon_{fe} = 0.193(0.016) = 0.0031 \le 0.004$	 $L_e = \dfrac{416}{[(1)(0.1651 \text{ mm})(227.5 \times 10^3 \text{ kN/mm}^2)]^{0.58}} = 50.8 \text{ mm}$ $k_1 = \left(\dfrac{20.7 \text{ kN/mm}^2}{254}\right)^{2/3} = 0.825$ $k_2 = \left(\dfrac{406 \text{ mm} - 50.8 \text{ mm}}{406 \text{ mm}}\right) = 0.875$ $\kappa_v = \dfrac{(0.82)(0.875)(50.8 \text{ mm})}{11,910(0.016)} = 0.193 \le 0.75$ $\varepsilon_{fe} = 0.193(0.016) = 0.0031 \le 0.004$
Step 3—Calculate the contribution of the FRP reinforcement to the shear strength The area of FRP shear reinforcement can be computed as: $A_{fv} = 2nt_f w_f$ The effective stress in the FRP can be computed from Hooke's law. $f_{fe} = \varepsilon_{fe} E_f$ The shear contribution of the FRP can be then calculated from Eq. (11-3): $V_f = \dfrac{A_{fv} f_{fe}(\sin\alpha + \cos\alpha) d_{fv}}{s_f}$	 $A_{fv} = 2(1)(0.0065 \text{ in.})(10 \text{ in.}) = 0.13 \text{ in.}^2$ $f_{fe} = (0.0031)(33,000 \text{ ksi}) = 102 \text{ ksi}$ $V_f = \dfrac{(0.13 \text{ in.}^2)(102 \text{ ksi})(1)(16 \text{ in.})}{(12 \text{ in.})}$ $V_f = 17.7 \text{ kips}$	 $A_{fv} = 2(1)(0.1651 \text{ mm})(254 \text{ mm}) = 83.87 \text{ mm}^2$ $f_{fe} = (0.0031)(227.6 \text{ kN/mm}^2) = 0.703 \text{ kN/mm}^2$ $V_f = \dfrac{(83.87 \text{ mm}^2)(0.703 \text{ kN/mm}^2)(1)(406 \text{ mm})}{(304.8 \text{ mm})}$ $V_f = 78.5 \text{ kN}$
Step 4—Calculate the shear strength of the section The design shear strength can be computed from Eq. (11-2) with $\psi_f = 0.85$ for U-wraps. $\phi V_n = \phi(V_c + V_s + \psi_f V_f)$	 $\phi V_n = 0.75[44.2 + 19.6 + (0.85)(17.7)]$ $\phi V_n = 59 \text{ kips} > V_u = 57 \text{ kips}$ $\therefore$ the strengthened section is capable of sustaining the required shear strength.	 $\phi V_n = 0.75[196.6 + 87.2 + (0.85)(78.5)]$ $\phi V_n = 263 \text{ kN} > V_u = 253.3 \text{ kN}$ $\therefore$ the strengthened section is capable of sustaining the required shear strength.

15.7—Shear strengthening of an exterior column

A 24 x 24 in. (610 x 610 mm) square column requires an additional 60 kips of shear strength (ΔV_u = 60 kips). The column is located in an unenclosed parking garage and experiences wide variation in temperature and climate. A method of strengthening the column using FRP is sought.

An E-glass-based FRP complete wrap is selected to retrofit the column. The properties of the FRP system, as reported by the manufacturer, are shown in Table 15.9. The design calculations to arrive at the number of complete wraps required follow.

Table 15.9—Manufacturer's reported FRP system properties[*]

Thickness per ply t_f	0.051 in.	1.3 mm
Guaranteed ultimate tensile strength f_{fu}^*	80,000 psi	552 N/mm^2
Guaranteed rupture strain ε_{fu}^*	0.020 in./in.	0.020 mm/mm
Modulus of elasticity E_f	4,000,000 psi	27,600 N/mm^2

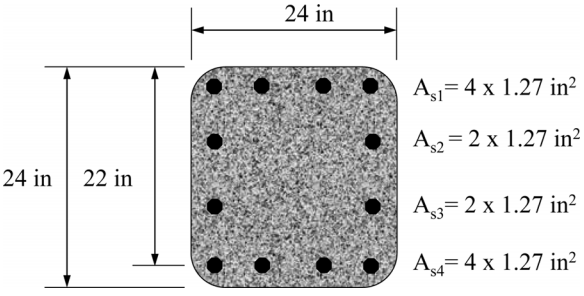[*]The reported properties are laminate properties.

Procedure	Calculation in inch-pound units	Calculation in SI metric units
Step 1—Compute the design material properties The column is located in an exterior environment and a GFRP material will be used. Therefore, per Table 9.1, an environmental reduction factor of 0.65 is suggested. $f_{fu} = C_E f_{fu}^*$ $\varepsilon_{fu} = C_E \varepsilon_{fu}^*$	$f_{fu} = (0.65)(80\ \text{ksi}) = 52\ \text{ksi}$ $\varepsilon_{fu} = (0.65)(0.020) = 0.013$	$f_{fu} = (0.65)(552\ \text{N/mm}^2) = 358.5\ \text{N/mm}^2$ $\varepsilon_{fu} = (0.65)(0.020) = 0.013$
Step 2—Calculate the effective strain level in the FRP shear reinforcement The effective strain in a complete FRP wrap can be determined from Eq. (11-6a): $\varepsilon_{fe} = 0.004 \le 0.75\varepsilon_{fu}$	$\varepsilon_{fe} = 0.004 \le 0.75(0.013) = 0.010$ $\therefore$ use an effective strain of $\varepsilon_{fe} = 0.004$.	$\varepsilon_{fe} = 0.004 \le 0.75(0.013) = 0.010$ $\therefore$ use an effective strain of $\varepsilon_{fe} = 0.004$.
Step 3—Determine the area of FRP reinforcement required The required shear contribution of the FRP reinforcement can be computed based on the increase in strength needed, the strength reduction factor for shear, and a partial-reduction factor ψ_f = 0.95 for completely wrapped sections in shear. $V_{f,\ reqd} = \dfrac{\Delta V_u}{\phi(\psi_f)}$ The required area of FRP can be determined by reorganizing Eq. (11-3). The required area is left in terms of the spacing. $A_{fv,\ reqd} = \dfrac{V_{f,\ reqd}s_f}{\varepsilon_{fe}E_f(\sin\alpha + \cos\alpha)d_f}$	$V_{f,\ reqd} = \dfrac{60\ \text{kips}}{0.85(0.95)} = 74.3\ \text{kips}$ $A_{fv,\ reqd} = \dfrac{(74.3\ \text{kips})s_f}{(0.004)(4000\ \text{ksi})(1)(24\ \text{in.})} = 0.194s_f$	$V_{f,\ reqd} = \dfrac{266.9\ \text{kN}}{0.85(0.95)} = 330.5\ \text{kN}$ $A_{fv,\ reqd} = \dfrac{(330.5\ \text{kN})s_f}{(0.004)(27.6\ \text{kN/mm}^2)(1)(610\ \text{mm})} = 4.91s_f$
Step 4—Determine the number of plies and strip width and spacing The number of plies can be determined in terms of the strip width and spacing as follows: $n = \dfrac{A_{f,\ reqd}}{2t_f w_f}$	$n = \dfrac{0.194s_f}{2(0.051\ \text{in.})w_f} = 1.90\dfrac{s_f}{w_f}$ $\therefore$ use two plies ($n = 2$) continuously along the height of the column ($s_f = w_f$).	$n = \dfrac{4.91s_f}{2(1.3\ \text{mm})w_f} = 1.90\dfrac{s_f}{w_f}$ $\therefore$ use two plies ($n = 2$) continuously along the height of the column ($s_f = w_f$).

15.8—Strengthening of a noncircular concrete column for axial load increase

A 24 x 24 in. (610 x 610 mm) square column requires an additional 20% of axial load-carrying capacity. Concrete and steel reinforcement material properties as well as details of the cross section of the column are shown in Table 15.10. The column is located in an interior environment, and a CFRP material will be used. A method of strengthening the column is sought.

Table 15.10—Column cross section details and material properties

$A_{s1} = 4 \times 1.27 \text{ in}^2$

$A_{s2} = 2 \times 1.27 \text{ in}^2$

$A_{s3} = 2 \times 1.27 \text{ in}^2$

$A_{s4} = 4 \times 1.27 \text{ in}^2$

f_c'	6.5 ksi	45 MPa
f_y	60 ksi	400 MPa
r_c	1 in.	25 mm
Bars	12 No. 10	12φ32
A_g	576 in.^{2}	3716 cm^2
A_{st}	15.24 in.^{2}	98 cm^2
ρ_g, %	2.65	2.65
ϕP_n without FRP	2087 kip	9281 kN
$\phi P_{n(req)}$	2504 kip	11,138 kN

Note: The column features steel ties for transverse reinforcement.

A carbon-based FRP complete wrap is selected to retrofit the columns. The properties of the FRP system, as reported by the manufacturer, are shown in Table 15.11. The design calculations to arrive at the number of required complete wraps follow.

Table 15.11—Manufacturer's reported FRP system properties

Thickness per ply t_f	0.013 in.	0.33 mm
Ultimate tensile strength f_{fu}^*	550 ksi	3792 MPa
Rupture strain ε_{fu}^*	0.0167 in./in.	0.0167 mm/mm
Modulus of elasticity E_f	33,000 ksi	227,527 MPa

Procedure	Calculation in inch-pound units	Calculation in SI metric units
Step 1—Compute the design FRP material properties The column is located in an interior environment and a CFRP material will be used. Therefore, per Table 9.1, an environmental reduction factor of 0.95 is suggested. $f_{fu} = C_E f_{fu}^*$ $\varepsilon_{fu} = C_E \varepsilon_{fu}^*$	 $f_{fu} = (0.95)(550 \text{ ksi}) = 522.5 \text{ ksi}$ $\varepsilon_{fu} = (0.95)(0.0167) = 0.0159 \text{ in./in.}$	 $f_{fu} = (0.95)(3792 \text{ MPa}) = 3603 \text{ MPa}$ $\varepsilon_{fu} = (0.95)(0.0167) = 0.0159 \text{ mm/mm}$
Step 2—Determine the required maximum compressive strength of confined concrete f_{cc}' f_{cc}' can be obtained by reordering Eq. (12-1): $f_{cc}' = \dfrac{1}{0.85(A_g - A_{st})}\left(\dfrac{\phi P_{n,req}}{0.80\phi} - f_y A_{st}\right)$	$f_{cc}' = \dfrac{1}{0.85 \times (576 \text{ in.}^2 - 15.24 \text{ in.}^2)} \times$ $\left(\dfrac{2504 \text{ kip}}{0.80 \times 0.65} - 60 \text{ ksi} \times 15.24 \text{ in.}^2\right)$ $f_{cc}' = 8.18 \text{ ksi}$	$f_{cc}' = \dfrac{1}{0.85 \times (371,612 \text{ mm}^2 - 9832 \text{ mm}^2)} \times$ $\left(\dfrac{11,138 \text{ kN}}{0.80 \times 0.65} - 414 \text{ MPa} \times 9832 \text{ mm}^2\right)$ $f_{cc}' = 56.4 \text{ MPa}$

Procedure	Calculation in inch-pound units	Calculation in SI metric units
Step 3—Determine the maximum confining pressure due to the FRP jacket, f_l f_l can be obtained by reordering Eq. (12-3): $$f_l = \frac{f'_{cc} - f'_c}{3.3\kappa_a}$$ where $$\kappa_a = \frac{A_e}{A_c}\left(\frac{b}{h}\right)^2$$ $$\frac{A_e}{A_c} = \frac{1 - \frac{\left[\left(\frac{b}{h}\right)(h - 2r_c)^2 + \left(\frac{h}{b}\right)(b - 2r_c)^2\right]}{3A_g} - \rho_g}{1 - \rho_g}$$	$$f_l = \frac{8.18 \text{ ksi} - 6.5 \text{ ksi}}{3.3 \times 0.425} = 1.2 \text{ ksi}$$ $$\kappa_a = 0.425(1)^2 = 0.425$$ $$\frac{A_e}{A_c} = \frac{1 - \frac{[2 \times (1)(24 \text{ in.} - 2 \times 1 \text{ in.})^2]}{3 \times 576 \text{ in.}^2} - 0.0265}{1 - 0.0265}$$ $$\frac{A_e}{A_c} = 0.425$$	$$f_l = \frac{56.4 \text{ MPa} - 44.8 \text{ MPa}}{3.3 \times 0.425} = 8.3 \text{ MPa}$$ $$\kappa_a = 0.425(1)^2 = 0.425$$ $$\frac{A_e}{A_c} = \frac{1 - \frac{[2 \times (1)(610 \text{ mm} - 2 \times 25 \text{ mm})^2]}{3 \times 371,612 \text{ mm}^2} - 0.0265}{1 - 0.0265}$$ $$\frac{A_e}{A_c} = 0.425$$
Step 4—Determine the number of plies n n can be obtained by reordering Eq. (12-4): $$n = \frac{f_l\sqrt{b^2 + h^2}}{\psi_f 2E_f t_f \varepsilon_{fe}}$$ $$\varepsilon_{fe} = \kappa_\varepsilon \varepsilon_{fu}$$ Checking the minimum confinement ratio: $$\frac{f_l}{f'_c} \geq 0.08$$	$$n = \frac{1.2 \text{ ksi}\sqrt{(24 \text{ in.})^2 + (24 \text{ in.})^2}}{0.95 \times 2 \times 33,000 \text{ ksi} \times 0.013 \text{ in.} \times (8.8 \times 10^{-3} \text{ in./in.})}$$ $$n = 5.7 \approx 6 \text{ plies}$$ $$\varepsilon_{fe} = 0.55 \times 0.0159 \text{ in./in.} = 8.8 \times 10^{-3} \text{ in./in.}$$ $$\frac{f_l}{f'_c} = \frac{1.2 \text{ ksi}}{6.5 \text{ ksi}} = 0.18 > 0.08 \quad \textbf{OK}$$	$$n = \frac{8.3 \text{ MPa}\sqrt{(610 \text{ mm})^2 + (610 \text{ mm})^2}}{0.95 \times 2 \times 227,527 \text{ MPa} \times 0.33 \text{ mm} \times (8.8 \times 10^{-3} \text{ mm/mm})}$$ $$n = 5.7 \approx 6 \text{ plies}$$ $$\varepsilon_{fe} = 0.55 \times 0.0159 \text{ mm/mm} = 8.8 \times 10^{-3} \text{ mm/mm}$$ $$\frac{f_l}{f'_c} = \frac{8.3 \text{ MPa}}{44.8 \text{ MPa}} = 0.18 > 0.08 \quad \textbf{OK}$$
Step 5—Verify that the ultimate axial strain of the confined concrete $\varepsilon_{ccu} \leq 0.01$ ε_{ccu} can be obtained using Eq. (12-6): $$\varepsilon_{ccu} = \varepsilon'_c\left(1.5 + 12\kappa_b\frac{f_l}{f'_c}\left(\frac{\varepsilon_{fe}}{\varepsilon'_c}\right)^{0.45}\right)$$ where $$\kappa_b = \frac{A_e}{A_c}\left(\frac{h}{b}\right)^{0.5}$$ If the case that ε_{ccu} was to be greater than 0.01, then f'_{cc} should be recalculated from the stress-strain model using Eq. (12-2).	$$\varepsilon_{cc} = (0.002 \text{ in./in.})\left(1.5 + 12 \times 0.425 \times\right.$$ $$\left.\frac{1.2 \text{ ksi}}{6.5 \text{ ksi}}\left(\frac{8.8 \times 10^{-3} \text{ in./in.}}{0.002 \text{ in./in.}}\right)^{0.45}\right)$$ $$\varepsilon_{cc} = 0.0067 \text{ in./in.} < 0.01 \quad \textbf{OK}$$ $$\kappa_b = 0.425(1)^{0.5} = 0.425$$	$$\varepsilon_{cc} = (0.002 \text{ mm/mm})\left(1.5 + 12 \times 0.425 \times\right.$$ $$\left.\frac{8.3 \text{ MPa}}{44.8 \text{ MPa}}\left(\frac{8.8 \times 10^{-3} \text{ mm/mm}}{0.002 \text{ mm/mm}}\right)^{0.45}\right)$$ $$\varepsilon_{cc} = 0.0067 \text{ mm/mm} < 0.01 \quad \textbf{OK}$$ $$\kappa_b = 0.425(1)^{0.5} = 0.425$$

15.9—Strengthening of a noncircular concrete column for increase in axial and bending forces

The column in Example 15.6 is subjected to an ultimate axial compressive load P_u = 1900 kip (8451 kN) and an ultimate bending moment M_u = 380 kip-ft (515 kN-m) (e = 0.1h). It is sought to increase load demands by 30% at constant eccentricity (P_u = 2470 kip, M_u = 494 kip-ft). Note: 1 kN/mm^2 = 1000 MPa or 1 MPa = 10^{-3} kN/mm^2.

Procedure	Calculation in inch-pound units	Calculation in SI metric units
Step 1—Determine the simplified curve for the unstrengthened column (n = 0 plies) Points A, B, and C can be obtained by well-known procedures, and also by using Eq. (D-1) to (D-5) considering ψ_f = 1; f'_{cc} = f'_c; E_2 = 0; and ε_{ccu} = ε_{cu} = 0.003.	$\phi P_{n(A)}$ = 2087 kip; $\phi M_{n(A)}$ = 0 kip-ft $\phi P_{n(B)}$ = 1858 kip; $\phi M_{n(B)}$ = 644 kip-ft $\phi P_{n(C)}$ = 928 kip; $\phi M_{n(C)}$ = 884 kip-ft	$\phi P_{n(A)}$ = 9283 kN; $\phi M_{n(A)}$ = 0 kN-m $\phi P_{n(B)}$ = 8265 kN; $\phi M_{n(B)}$ = 873 kN-m $\phi P_{n(C)}$ = 4128 kN; $\phi M_{n(C)}$ = 1199 kN-m
Step 2—Determine the simplified curve for a strengthened column A wrapping system composed of six plies will be the starting point to construct the bilinear Curve A-B-C and then be compared with the position of the required P_u and M_u. Points A, B, and C of the curve can be computed using Eq. (12-1), (D-1), and (D-2): $\phi P_{n(A)} = \phi 0.8(0.85 f'_{cc}\,(A_g - A_{st}) + f_y A_{st})$ $\phi P_{n(B,C)} = \phi(A(y_t)^3 + B(y_t)^2 + C(y_t) + D) + \Sigma A_{si}f_{si}]$ $\phi M_{n(B,C)} = \phi(E(y_t)^4 + F(y_t)^3 + G(y_t)^2 + H(y_t) + I) + \Sigma A_{si}f_{si}d_i$ The coefficients A, B, C, D, E, F, G, H, and I of the previous expressions are given by Eq. (D-3): $A = \dfrac{-b(E_c - E_2)^2}{12 f'_c}\left(\dfrac{\varepsilon_{ccu}}{c}\right)^2$ $B = \dfrac{b(E_c - E_2)}{2}\left(\dfrac{\varepsilon_{ccu}}{c}\right)$ $C = b f'_c$ $D = b f'_c + \dfrac{bcE_2}{2}(\varepsilon_{ccu})$ $E = \dfrac{-b(E_c - E_2)^2}{16 f'_c}\left(\dfrac{\varepsilon_{ccu}}{c}\right)^2$ $F = b\left(c - \dfrac{h}{2}\right)\dfrac{(E_c - E_2)^2}{12 f'_c}\left(\dfrac{\varepsilon_{ccu}}{c}\right)^2 + \dfrac{b(E_c - E_2)}{3}\left(\dfrac{\varepsilon_{ccu}}{c}\right)$ $G = -\left(\dfrac{b}{2}f'_c + b\left(c - \dfrac{h}{2}\right)\dfrac{(E_c - E_2)}{2}\left(\dfrac{\varepsilon_{ccu}}{c}\right)\right)$ $H = b f'_c\left(c - \dfrac{h}{2}\right)$ $I = \dfrac{bc^2}{2}f'_c - bc f'_c\left(c - \dfrac{h}{2}\right) + \dfrac{bc^2 E_2}{3}(\varepsilon_{ccu})$ $-\dfrac{bcE_2}{2}\left(c - \dfrac{h}{2}\right)(\varepsilon_{ccu})$	**Point A:** Nominal axial capacity: $\phi P_{n(A)}$ = 0.65 × 0.8(0.85 × 8.26 ksi × (576 in.^{2} – 15.24 in.^{2}) + 60 ksi + 15.24 in.^{2} $\phi P_{n(A)}$ = 2523 kip where f'_{cc} = 6.5 ksi + 3.3(0.425)(1.26 ksi) f'_{cc} = 8.26 ksi $f_l = \dfrac{0.95 \times 2 \times 33{,}000\ \text{ksi} \times 6 \times 0.013\ \text{in.} \times \left(0.55 \times 0.0159\frac{\text{in.}}{\text{in.}}\right)}{\sqrt{(24\ \text{in.})^2 + (24\ \text{in.})^2}}$ f_l = 1.26 ksi **Point B:** Nominal axial capacity: $\phi P_{n(B)}$ = 0.65[–0.22 kip/in.^{3}(15.33 in.)^3 + 10.17 ksi (15.33 in.)^2 – 56 kip/in.(15.33 in.) + 3645.2 kips] + 5.08 in.^{2} (60 ksi) + 2.54 in.^{2}(60 ksi) + 2.54 in.^{2} (37.21 ksi)] $\phi P_{n(B)}$ = 2210 kip where $A = \dfrac{-24\ \text{in.}(4595\ \text{ksi} - 190.7\ \text{ksi})^2}{12 \times 6.5\ \text{ksi}}\left(\dfrac{0.0042\ \text{in./in.}}{22\ \text{in.}}\right)^2$ = –0.22 kip/in.^{3} $B = \dfrac{24\ \text{in.}(4595\ \text{ksi} - 190.7\ \text{ksi})}{2}\left(\dfrac{0.0042\ \text{in./in.}}{22\ \text{in.}}\right)$ = 10.17 ksi C = –24 in. × 6.5 ksi = –156 kip/in. D = 24 in. × 22 in. × 6.5 ksi + $\dfrac{24\ \text{in.} \times 22\ \text{in.} \times 190.7\ \text{ksi}}{2}$ (0.0042 in./in.) D = 3645.2 kip	**Point A:** Nominal axial capacity: $\phi P_{n(A)}$ = 0.65 × 0.8(0.85 × 56.96 MPa × (371,612 mm^2 – 9832 mm^2) + 414 MPa + 9232 mm^2 $\phi P_{n(A)}$ = 11,223 kN where f'_{cc} = 44.8 MPa + 3.3(0.425)(8.7 MPa) f'_{cc} = 56.96 MPa $f_l = \dfrac{0.95 \times 2 \times 227{,}500\ \text{MPa} \times 6 \times 0.33\ \text{mm} \times \left(0.55 \times 0.0159\frac{\text{mm}}{\text{mm}}\right)}{\sqrt{(610\ \text{mm})^2 + (610\ \text{mm})^2}}$ f_l = 8.67 MPa **Point B:** Nominal axial capacity: $\phi P_{n(B)}$ = 0.65[–6.003 × 10^{-5} kN/mm^3(389 mm)^3 + 70.14 × 10^{-3} kN/mm^2(389 mm)^2 – 27.32 kN/mm(389 mm) + 16,215 kN] + 3277 mm^2(414 MPa) + 1639 mm^2(414 MPa) + 1639 mm^2(257 ksi) $\phi P_{n(B)}$ = 9892 kN where $A = \dfrac{-610\ \text{mm}\,(31{,}685\ \text{MPa} - 1315\ \text{MPa})^2}{12 \times 44.8\ \text{MPa}}\left(\dfrac{0.0042\ \text{mm/mm}}{559\ \text{mm}}\right)^2$ = –6.003 × 10^{-5} kN/mm^3 $B = \dfrac{600\ \text{mm}(31{,}685\ \text{MPa} - 1315\ \text{MPa})}{2}\left(\dfrac{0.0042\ \text{mm/mm}}{559\ \text{mm}}\right)$ = 70.14 × 10^{-3} kN/mm^2 C = –610 mm × 44.84 MPa = –27.32 kN/mm D = 610 mm × 559 mm × 44.8 MPa + $\dfrac{610\ \text{mm} \times 559\ \text{mm} \times 1315\ \text{MPa}}{2}$ (0.0042 mm/mm) D = 16,215 kN

Procedure	Calculation in inch-pound units	Calculation in SI metric units
Step 2—(cont.) Key parameters of the stress-strain model:	For the calculation of the coefficients, it is necessary to compute key parameters from the stress-strain model:	For the calculation of the coefficients, it is necessary to compute key parameters from the stress-strain model:
$y_t = c\dfrac{\varepsilon_t'}{\varepsilon_{ccu}}$	$y_t = 22\text{ in.} \times \dfrac{0.003\text{ in./in.}}{0.0042\text{ in./in.}} = 15.33\text{ in.}$	$y_t = 559\text{ mm} \times \dfrac{0.003\text{ mm/mm}}{0.0042\text{ mm/mm}} = 389\text{ mm}$
$c = \begin{cases} d & \text{for Point B} \\ d\dfrac{\varepsilon_{ccu}}{\varepsilon_{sy}+\varepsilon_{ccu}} & \text{for Point C} \end{cases}$	$c = 22\text{ in.}$	$c = 559\text{ mm}$
$\varepsilon_t' = \dfrac{2f_c'}{E_c - E_2}$	$\varepsilon_t' = \dfrac{2\times 6.5\text{ ksi}}{4595\text{ ksi} - 190.7\text{ ksi}} = 0.003\text{ in./in.}$	$\varepsilon_t' = \dfrac{2\times 44.8\text{ MPa}}{31{,}685\text{ MPa} - 1315\text{ MPa}} = 0.003\text{ mm/mm}$
$E_2 = \dfrac{f_{cc}' - f_c'}{\varepsilon_{ccu}}$	$E_2 = \dfrac{7.31\text{ ksi} - 6.5\text{ ksi}}{0.0042\text{ in./in.}} = 190.7\text{ ksi}$	$E_2 = \dfrac{50.4\text{ MPa} - 44.8\text{ MPa}}{0.0042\text{ mm/mm}} = 1315\text{ MPa}$
$f_{cc}' = f_c' + 3.3\kappa_a f_l$	$f_{cc}' = 6.5\text{ ksi} + 3.3(0.425)(0.58\text{ ksi}) = 7.31\text{ ksi}$	$f_{cc}' = 44.8\text{ MPa} + 3.3(0.425)(3.97\text{ MPa}) = 50.4\text{ MPa}$
$\varepsilon_{ccu} = \varepsilon_c'\left(1.5 + 12\kappa_b\dfrac{f_l}{f_c'}\left(\dfrac{\varepsilon_{fe}}{\varepsilon_c'}\right)^{0.45}\right)$	$\varepsilon_{ccu}=0.002\text{ in./in.}\left(1.5 + 12\times 0.425\left(\dfrac{0.58\text{ ksi}}{6.5\text{ ksi}}\right)\left(\dfrac{0.004\text{ in./in.}}{0.002\text{ in./in.}}\right)^{0.45}\right)$ $\varepsilon_{ccu} = 0.0042\text{ in./in.}$	$\varepsilon_{ccu}=0.002\text{ mm/mm}\left(1.5 + 12\times 0.425\left(\dfrac{3.97\text{ MPa}}{44.8\text{ MPa}}\right)\left(\dfrac{0.004\text{ mm/mm}}{0.002\text{ mm/mm}}\right)^{0.45}\right)$ $\varepsilon_{ccu} = 0.0042\text{ mm/mm}$
$\varepsilon_{fe} = \min(0.004, \kappa_\varepsilon\varepsilon_{fu})$		
$\kappa_a = \dfrac{A_e}{A_c}\left(\dfrac{b}{h}\right)^2$	$\kappa_a = \kappa_b = 0.425$	$\kappa_a = \kappa_b = 0.425$
$\kappa_b = \dfrac{A_e}{A_c}\left(\dfrac{h}{b}\right)^{0.5}$		
$f_l = \dfrac{\psi_f 2E_f n t_f \varepsilon_{fe}}{\sqrt{b^2+h^2}}$	$f_l = \dfrac{0.95\times 2\times 33{,}000\text{ ksi}\times 6\times 0.013\text{ in.}\times(0.004\text{ in./in.})}{\sqrt{(24\text{ in.})^2+(24\text{ in.})^2}}$	$f_l = \dfrac{0.95\times 2\times 227{,}527\text{ MPa}\times 6\times 0.33\text{ mm}\times(0.004\text{ mm/mm})}{\sqrt{(610\text{ mm})^2+(610\text{ mm})^2}}$
Notes: The designer should bear in mind that, for the case of pure compression, the effective strain in the FRP, ε_{fe}, is limited by $\kappa_\varepsilon\varepsilon_{fu}$ and, in the case of combined axial and bending, by $\varepsilon_{fe} = \min(0.004, \kappa_\varepsilon\varepsilon_{fu})$.	Checking the minimum confinement ratio: $f_l/f_c' = 0.58\text{ ksi}/6.5\text{ ksi} = 0.09 \ge 0.08$ **OK**	Checking the minimum confinement ratio: $f_l/f_c' = 3.97\text{ MPa}/44.8\text{ MPa} = 0.09 \ge 0.08$ **OK**
	The strains in each layer of steel are determined by similar triangles in the strain distribution. The corresponding stresses are then given by: $f_{s1} = \varepsilon_{s1}E_s = 0.0038\text{ in./in.}\times 29{,}000\text{ ksi} \rightarrow 60\text{ ksi}$ $f_{s2} = \varepsilon_{s2}E_s = 0.0026\text{ in./in.}\times 29{,}000\text{ ksi} \rightarrow 60\text{ ksi}$ $f_{s3} = \varepsilon_{s3}E_s = 0.0013\text{ in./in.}\times 29{,}000\text{ ksi} = 37.2\text{ ksi}$ $f_{s4} = \varepsilon_{s4}E_s = 0\text{ in./in.}\times 29{,}000\text{ ksi} = 0\text{ ksi}$	The strains in each layer of steel are determined by similar triangles in the strain distribution. The corresponding stresses are then given by: $f_{s1} = \varepsilon_{s1}E_s = 0.0038\text{ mm/mm}\times 200{,}000\text{ MPa} \rightarrow 414\text{ MPa}$ $f_{s2} = \varepsilon_{s2}E_s = 0.0026\text{ mm/mm}\times 200{,}000\text{ MPa} \rightarrow 414\text{ MPa}$ $f_{s3} = \varepsilon_{s3}E_s = 0.0013\text{ mm/mm}\times 200{,}000\text{ MPa} = 257\text{ MPa}$ $f_{s4} = \varepsilon_{s4}E_s = 0\text{ mm/mm}\times 200{,}000\text{ MPa} = 0\text{ MPa}$
	Nominal bending moment: $\phi M_{n(B)} = 0.65[-0.166\text{ kip/in.}^3(15.33\text{ in.})^4 + 8.99\text{ ksi}(15.33\text{ in.})^3 - 179.73\text{ kip/in.}(15.33\text{ in.})^2 + 1560\text{ kip}(15.33\text{ in.}) + 4427\text{ kip-in.}] + 5.08\text{ in.}^2(60\text{ ksi})(10\text{ in.}) + 2.54\text{ in.}^2(60\text{ ksi})(3.3\text{ in.}) - 2.54\text{ in.}^2(37.21\text{ ksi})(3.3\text{ in.})$ $\phi M_{n(B)} = 682\text{ kip-ft}$ where $E = \dfrac{-24\text{ in.}(4595\text{ ksi} - 190.7\text{ ksi})^2}{16\times 6.5\text{ ksi}}\left(\dfrac{0.0042\text{ in./in.}}{22\text{ in.}}\right)^2$ $= -0.166\text{ kip/in.}^3$ $F = 24\text{ in.}(22\text{ in.} - 12\text{ in.})\times\dfrac{(4595\text{ ksi} - 190.7\text{ ksi})^2}{12\times 6.5\text{ ksi}}$ $\left(\dfrac{0.0042\text{ in./in.}}{22\text{ in.}}\right)^2 + \dfrac{24\text{ in.}(4595\text{ ksi} - 190.7\text{ ksi})}{3}\times$ $\left(\dfrac{0.0042\text{ in./in.}}{22\text{ in.}}\right) = 8.99\text{ ksi}$	Nominal bending moment: $\phi M_{n(B)} = 0.65[-4.502\times 10^{-5}\text{ kN/mm}^3(389\text{ mm})^4 + 62.01\times 10^{-3}\text{ kN/mm}^3(389\text{ mm})^3 - 31.48\text{ kN/mm}(389\text{ mm})^2 + 6939\text{ kN}(389\text{ mm}) + 500{,}162\text{ kN-mm}] + 3277\text{ mm}^2(414\text{ MPa})(254\text{ mm}) + 1639\text{ mm}^2(414\text{ MPa})(85\text{ mm}) - 1639\text{ mm}^2(257\text{ MPa})(85\text{ mm})$ $\phi M_{n(B)} = 924\text{ kN-m}$ where $E = \dfrac{-610\text{ mm}(31{,}685\text{ MPa} - 1315\text{ MPa})^2}{16\times 44.8\text{ MPa}}\left(\dfrac{0.0042\text{ mm/mm}}{559\text{ mm}}\right)^2$ $= -0.4502\times 10^{-5}\text{ kN/mm}^3$ $F = 610\text{ mm}(559\text{ mm} - 305\text{ mm})\times\dfrac{(31{,}685\text{ MPa} - 1315\text{ MPa})^2}{12\times 44.8\text{ MPa}}$ $\left(\dfrac{0.0042\text{ mm/mm}}{559\text{ mm}}\right)^2 + \dfrac{610\text{ mm}(31{,}685\text{ MPa} - 1315\text{ MPa})}{3}\times$ $\left(\dfrac{0.0042\text{ mm/mm}}{559\text{ mm}}\right) = 62.01\times 10^{-3}\text{ kN/mm}^2$

Procedure	Calculation in inch-pound units	Calculation in SI metric units
Step 2—(cont.)	$G = 6.5$ ksi $\times$ 12 in. $+$ 24 in.$(22$ in. $- 12$ in.$)$ $\times \left(\dfrac{4595\ \text{ksi} - 190.7\ \text{ksi}}{2}\right)\left(\dfrac{0.0042\ \text{in./in.}}{22\ \text{in.}}\right)$ $G = -179.73$ kip/in. $H = 6.5$ ksi $\times$ 24 in.$(22$ in. $- 12$ in.$) = 1560$ kip $I = 6.5$ ksi $\times$ 24 in. $\times \dfrac{(22\ \text{in.})^2}{2} - 6.5$ ksi$(22$ in. $- 12$ in.$)$ $\times$ 22 in. $\times$ 24 in. $+$ 190.7 ksi $\times$ 24 in. $\times$ $\dfrac{(22\ \text{in.})^2}{3}(0.0042\ \text{in./in.}) - 190.7$ ksi $\times$ 24 in. $\times$ $\dfrac{22\ \text{in.}}{3}$ $(22$ in. $- 12$ in.$)(0.0042$ in./in. $= 4427$ kip-in. The distances from each layer of steel reinforcement to the geometric centroid of the cross section are: $d_1 = 10$ in. $d_2 = d_3 = 3.3$ in. Point C: Nominal axial capacity: $\phi P_{n(C)} = 0.65[-0.49$ kip/in.$^3(10.3$ in.$)^3 + 15.14$ ksi $(10.3$ in.$)^2 - 156$ kip-in.$(10.3$ in.$) + 2448.71$ kips$]$ $+ 5.08$ in.$^2(60$ ksi$) + 2.54$ in.$^2(50.79$ ksi$) + 2.54$ in.^{2} $(-4.61$ ksi$) + 5.08$ in.$^2(-60$ ksi$)$ $\phi P_{n(C)} = 1320$ kip where $A = \dfrac{-24\ \text{in.}(4595\ \text{ksi} - 190.7\ \text{ksi})^2}{12 \times 6.5\ \text{ksi}}\left(\dfrac{0.0042\ \text{in./in.}}{14.78\ \text{in.}}\right)^2$ $= -0.49$ kip/in.^{3} $B = \dfrac{-24\ \text{in.}(4595\ \text{ksi} - 190.7\ \text{ksi})}{2}\left(\dfrac{0.0042\ \text{in./in.}}{14.78\ \text{in.}}\right)$ $= 15.14$ ksi $C = -24$ in. $\times$ 6.5 ksi $= -156$ kip/in. $D = 24$ in. $\times$ 14.78 in. $\times$ 6.5 ksi $+\ \dfrac{24\ \text{in.} \times 14.78\ \text{in.} \times 190.7\ \text{ksi}}{2} \times (0.0042\ \text{in./in.})$ $= 2448.71$ kip For the calculation of the coefficients, it is necessary to compute key parameters from the stress-strain model: $y_t = 14.78$ in.$\dfrac{0.003\ \text{in./in.}}{0.0042\ \text{in./in.}} = 10.3$ in. $c = 22$ in.$\left(\dfrac{0.0042\ \text{in./in.}}{0.0021\ \text{in./in.} + 0.0042\ \text{in./in.}}\right) = 14.78$ in. The strains in each layer of steel are determined by similar triangles in the strain distribution. The corresponding stresses are then given by: $f_{s1} = \varepsilon_{s1}E_s = 0.0037$ in./in. $\times$ 29,000 ksi $\rightarrow$ 60 ksi $f_{s2} = \varepsilon_{s2}E_s = 0.0018$ in./in. $\times$ 29,000 ksi $= 50.78$ ksi $f_{s3} = \varepsilon_{s3}E_s = -1.59 \times 10^{-4}$ in./in. $\times$ 29,000 ksi $= -4.61$ ksi $f_{s4} = \varepsilon_{s4}E_s = -0.0021$ in./in. $\times$ 29,000 ksi $= -60$ ksi	$G = 44.8$ MPa $\times$ 305 mm $+$ 610 mm$(559$ mm $- 305$ mm$)$ $\times \left(\dfrac{31{,}685\ \text{MPa} - 1315\ \text{MPa}}{2}\right)\left(\dfrac{0.0042\ \text{mm/mm}}{559\ \text{mm}}\right)$ $G = -31.48$ kN/mm $H = 44.8$ MPa $\times$ 610 mm$(559$ mm $- 305$ mm$) = 6939$ kN $I = 44.8$ MPa $\times$ 610 mm $\times \dfrac{(559\ \text{mm})^2}{2} - 44.8$ MPa $(559$ mm $- 305$ mm$) \times (559$ mm$)(610$ mm$) + 1315$ MPa $\times$ 610 mm $\times \dfrac{(559\ \text{mm})^2}{3}(0.0042\ \text{mm/mm}) - 1315$ MPa $\times$ 610 mm $\times \dfrac{559\ \text{mm}}{2}$ $(559$ mm $- 305$ mm$)(0.0042$ mm/mm$)$ $= 500{,}162$ kN-mm The distances from each layer of steel reinforcement to the geometric centroid of the cross section are: $d_1 = 254$ mm $d_2 = d_3 = 85$ mm Point C: Nominal axial capacity: $\phi P_{n(C)} = 0.65[-1.33 \times 10^{-4}$ kN/mm$^3(262$ mm$)^3 + 104.41$ $\times 10^{-3}$ kN/mm$^2 \times (262$ mm$)^2 - 27.32$ kN/mm$(262$ mm$)$ $+ 10{,}892$ kN$] + 3277$ mm$^2(414$ MPa$) + 1315$ mm$^2(350$ MPa$) + 1315$ mm^2 $(-31.8$ MPa$) + 3277$ mm$^2(-414$ MPa$)$ $\phi P_{n(C)} = 5870$ kN where $A = \dfrac{-610\ \text{mm}(31{,}681\ \text{MPa} - 1315\ \text{MPa})^2}{12 \times 44.8\ \text{MPa}}\left(\dfrac{0.0042\ \text{mm/mm}}{375\ \text{mm}}\right)^2$ $= -1.33 \times 10^{-4}$ kN/mm^3 $B = \dfrac{-610\ \text{mm}(31{,}681\ \text{MPa} - 1315\ \text{MPa})}{2}\left(\dfrac{0.0042\ \text{mm/mm}}{375\ \text{mm}}\right)$ $= -104.41 \times 10^{-3}$ kN/mm^2 $C = -610$ mm $\times$ 44.8 MPa $= -27.32$ kN/mm $D = 610$ mm $\times$ 375 mm $\times$ 44.8 MPa $+\ \dfrac{610\ \text{mm} \times 375\ \text{mm} \times 1315\ \text{MPa}}{2} \times (0.0042\ \text{mm/mm})$ $= 10{,}892$ kN For the calculation of the coefficients, it is necessary to compute key parameters from the stress-strain model: $y_t = 375$ mm$\dfrac{0.003\ \text{mm/mm}}{0.0042\ \text{mm/mm}} = 262$ mm $c = 560$ mm$\left(\dfrac{0.0042\ \text{mm/mm}}{0.0021\ \text{mm/mm} + 0.0042\ \text{mm/mm}}\right) = 375$ mm The strains in each layer of steel are determined by similar triangles in the strain distribution. The corresponding stresses are then given by: $f_{s1} = \varepsilon_{s1}E_s = 0.0037$ mm/mm $\times$ 200,000 MPa $\rightarrow$ 414 MPa $f_{s2} = \varepsilon_{s2}E_s = 0.0018$ mm/mm $\times$ 200,000 MPa $= 350$ MPa $f_{s3} = \varepsilon_{s3}E_s = -1.59 \times 10^{-4}$ mm/mm $\times$ 200,000 MPa $= -31.8$ MPa $f_{s4} = \varepsilon_{s4}E_s = -0.0021$ mm/mm $\times$ 200,000 MPa $= -414$ MPa

Procedure	Calculation in inch-pound units	Calculation in SI metric units
Step 2—(cont.)	Nominal bending moment: $$\phi M_{n(C)} = 0.65[-0.37 \text{ kip/in.}^3(10.3 \text{ in.})^4 + 11.46 \text{ ksi}$$ $$(10.3 \text{ in.})^3 - 120.08 \text{ kip/in.}(10.3 \text{ in.})^2 + 433.5 \text{ kip}$$ $$(10.3 \text{ in.}) + 11,643 \text{ kip-in.}] + 5.08 \text{ in.}^2(60 \text{ ksi})(10 \text{ in.})$$ $$+ 2.54 \text{ in.}^2(50.79 \text{ ksi})(3.33 \text{ in.}) - 2.54 \text{ in.}^2(-4.61 \text{ ksi})$$ $$(3.33 \text{ in.}) - 5.08 \text{ in.}^2(-60 \text{ ksi})(10 \text{ in.})$$ $$\phi M_{n(C)} = 992 \text{ kip-ft}$$ where $$E = \frac{-24 \text{ in.}(4595 \text{ ksi} - 190.7 \text{ ksi})^2}{16 \times 6.5 \text{ ksi}}\left(\frac{0.0042 \text{ in./in.}}{14.78 \text{ in.}}\right)^2$$ $$= -0.37 \text{ kip/in.}^3$$ $$F = 24 \text{ in.}(14.78 \text{ in.} - 12 \text{ in.})\frac{(4595 \text{ ksi} - 190.7 \text{ ksi})^2}{12 \times 6.5 \text{ ksi}}$$ $$\left(\frac{0.0042 \text{ in./in.}}{14.78 \text{ in.}}\right)^2 + \frac{24 \text{ in.}(4595 \text{ ksi} - 190.7 \text{ ksi})}{3}$$ $$\left(\frac{0.0042 \text{ in./in.}}{14.78 \text{ in.}}\right) = 11.46 \text{ ksi}$$ $$G = -6.5 \text{ ksi} \times 12 \text{ in.} + 24 \text{ in.}(14.78 \text{ in.} - 12 \text{ in.})$$ $$\times \left(\frac{4595 \text{ ksi} - 190.7 \text{ ksi}}{2}\right)\left(\frac{0.0042 \text{ in./in.}}{14.78 \text{ in.}}\right)$$ $$G = -120.08 \text{ kip/in.}$$ $$H = 6.5 \text{ ksi} \times 24 \text{ in.}(14.78 \text{ in.} - 12 \text{ in.}) = 433.5 \text{ kip}$$ $$I = 6.5 \text{ ksi} \times 24 \text{ in.} \times \frac{(14.78 \text{ in.})^2}{2} - 6.5 \text{ ksi}(14.78 \text{ in.} -$$ $$12 \text{ in.})(14.78 \text{ in.})(24 \text{ in.}) + 190.7 \text{ ksi} \times 24 \text{ in.} \times$$ $$\frac{(14.78 \text{ in.})^2}{3}(0.0042 \text{ in./in.}) - 190.7 \text{ ksi} \times 24 \text{ in.} \times$$ $$\frac{14.78 \text{ in.}}{2}(14.78 \text{ in.} - 12 \text{ in.})(0.0042 \text{ in./in.})$$ $$= 11,643 \text{ kip-in.}$$	Nominal bending moment: $$\phi M_{n(C)} = 0.65[-9.98 \times 10^{-5} \text{ kN/mm}^3(262 \text{ mm})^4 + 79 \times$$ $$10^{-3} \text{ kN/mm}^2(262 \text{ mm})^3 - 21.03 \text{ kN/mm}(262 \text{ mm})^2 +$$ $$1928 \text{ kN}(262 \text{ mm}) + 1,315,453 \text{ kN-mm}] + 3277$$ $$\text{mm}^2(414 \text{ MPa})(254 \text{ mm}) + 1639 \text{ mm}^2(-31.8 \text{ MPa})(85$$ $$\text{mm}) - 3277 \text{ mm}^2(-414 \text{ MPa}) (254 \text{ mm})$$ $$\phi M_{n(C)} = 1345 \text{ kN-m}$$ where $$E = \frac{-610 \text{ mm}(31,681 \text{ MPa} - 1315 \text{ MPa})^2}{16 \times 44.8 \text{ MPa}}\left(\frac{0.0042 \text{ mm/mm}}{375 \text{ mm}}\right)^2$$ $$= -9.98 \times 10^{-5} \text{ kN/mm}^3$$ $$F = 610 \text{ mm}(375 \text{ mm} - 305 \text{ mm}) \times \frac{(31,681 \text{ MPa} - 1315 \text{ MPa})^2}{12 \times 44.8 \text{ MPa}}$$ $$\left(\frac{0.0042 \text{ mm/mm}}{375 \text{ mm}}\right)^2 + \frac{610 \text{ mm}(31,681 \text{ MPa} - 1315 \text{ MPa})}{3} \times$$ $$\left(\frac{0.0042 \text{ mm/mm}}{375 \text{ mm}}\right) = 79 \times 10^{-3} \text{ kN/mm}^2$$ $$G = -44.8 \text{ MPa} \times 305 \text{ mm} + 610 \text{ mm}(375 \text{ mm} - 305 \text{ mm})$$ $$\times \left(\frac{31,681 \text{ MPa} - 1315 \text{ MPa}}{2}\right)\left(\frac{0.0042 \text{ mm/mm}}{375 \text{ mm}}\right)$$ $$G = -21.03 \text{ kN/mm}$$ $$H = 44.8 \text{ MPa} \times 610 \text{ mm}(375 \text{ mm} - 305 \text{ mm}) = 1928 \text{ kN}$$ $$I = 44.8 \text{ MPa} \times 610 \text{ mm} \times \frac{(375 \text{ mm})^2}{2} - 44.8 \text{ MPa}$$ $$(375 \text{ mm} - 305 \text{ mm}) \times (375 \text{ mm})(610 \text{ mm}) + 1315 \text{ MPa}$$ $$\times 610 \text{ mm} \times \frac{(375 \text{ mm})^2}{3}(0.0042 \text{ mm/mm}) - 1315 \text{ MPa} \times$$ $$610 \text{ mm} \times \frac{375 \text{ mm}}{2}(375 \text{ mm} - 305 \text{ mm})(0.0042 \text{ mm/mm})$$ $$= 1,315,453 \text{ kN-mm}$$
Step 3—Comparison of simplified partial interaction diagram with required P_u and M_u.	The following table summarizes the axial and bending nominal capacities (unstrengthened and strengthened) for Points A, B, and C. These points are plotted in the figure below.	The following table summarizes the axial and bending nominal capacities (unstrengthened and strengthened) for Points A, B, and C. These points are plotted in the figure below.

Point	$n = 0$ plies (unstrengthened member) ϕP_n, kip	ϕM_n, kip-ft	$n = 6$ plies ϕP_n, kip	ϕM_n, kip-ft
A	2087	0	2523	0
B	1858	644	2210	682
C	928	884	1320	992

Point	$n = 0$ plies (unstrengthened member) ϕP_n, kN	ϕM_n, kN-m	$n = 6$ plies ϕP_n, kN	ϕM_n, kN-m
A	9283	0	11,223	0
B	8264	873	9829	924
C	4128	1199	5870	1345

CHAPTER 16—REFERENCES
16.1—Referenced standards and reports

The standards and reports listed below were the latest editions at the time this document was prepared. Because these documents are revised frequently, the reader is advised to contact the proper sponsoring group if it is desired to refer to the latest version.

American Concrete Institute (ACI)

216R	Guide for Determining Fire Endurance of Concrete Elements
224.1R	Causes, Evaluation, and Repair of Cracks in Concrete Structures
318	Building Code Requirements for Structural Concrete and Commentary
364.1R	Guide for Evaluation of Concrete Structures before Rehabilitation
437R	Strength Evaluation of Existing Concrete Buildings
440R	Report on Fiber-Reinforced Polymer (FRP) Reinforcement for Concrete Structures
440.3R	Test Methods for Fiber-Reinforced Polymers (FRPs) for Reinforcing or Strengthening Concrete Structures
503R	Use of Epoxy Compounds with Concrete
503.4	Standard Specification for Repairing Concrete with Epoxy Mortars
546R	Concrete Repair Guide

American National Standards Institute (ANSI)

Z-129.1	Hazardous Industrial Chemicals Precautionary Labeling

American Society of Civil Engineers (ASCE)

7-05	Minimum Design Loads for Buildings and Other Structures

ASTM International

D648	Test Method for Deflection Temperature of Plastics Under Flexural Load in the Edgewise Position
D696	Test Method for Coefficient of Linear Thermal Expansion of Plastics Between –30 °C and 30 °C with a Vitreous Silica Dilatometer
D790	Test Methods for Flexural Properties of Unreinforced and Reinforced Plastics and Electrical Insulating Materials
D2240	Test Method for Rubber Hardness—Durometer Hardness
D2344/ D2344M	Test Method for Short-Beam Strength of Polymer Matrix Composite Materials and Their Laminates
D2538	Practice for Fusion of Poly Vinyl Chloride (PVC) Compounds Using a Torque Rheometer
D2584	Test Method for Ignition Loss of Cured Reinforced Resins
D2990	Test Method for Tensile, Compressive, and Flexural Creep and Creep-Rupture of Plastics
D3039	Test Method for Tensile Properties of Polymer Matrix Composite Materials

D3165	Test Method for Strength Properties of Adhesives in Shear by Tension Loading of Single-Lap-Joint Laminated Assemblies
D3171	Test Methods for Constituent Content of Composite Materials
D3418	Test Method for Transition Temperatures and Enthalpies of Fusion and Crystallization of Polymers by Differential Scanning Calorimetry
D3479/ D3479M	Test Method for Tension-Tension Fatigue of Polymer Matrix Composite Materials
D3528	Test Method for Strength Properties of Double Lap Shear Adhesive Joints by Tension Loading
D3846	Test Method for In-Plane Shear Strength of Reinforced Plastics
D4065	Practice for Plastics: Dynamic Mechanical Properties: Determination and Report of Procedures
D4475	Test Method for Apparent Horizontal Shear Strength of Pultruded Reinforced Plastic Rods by the Short-Beam Method
D4476	Test Method for Flexural Properties of Fiber Reinforced Pultruded Plastic Rods
D4541	Test Method for Pull-Off Strength of Coatings Using Portable Adhesion Testers
D4551	Standard Specification for Poly(Vinyl Chloride) (PVC) Plastic Flexible Concealed Water-Containment Membrane
D5379/ D5379	Test Method for Shear Properties of Composite Materials by the V-Notched Beam Method
D7205	Test Method for Tensile Properties of Fiber Reinforced Polymer Matrix Composite Bars
E84	Test Method for Surface Burning Characteristics of Building Materials
E119	Test Methods for Fire Tests of Building Construction and Materials
E328	Test Methods for Stress Relaxation Tests for Materials and Structures
E831	Test Method for Linear Thermal Expansion of Solid Materials by Thermomechanical Analysis
E1356	Test Method for Assignment of the Glass Transition Temperatures by Differential Scanning Calorimetry
E1640	Test Method for Assignment of the Glass Transition Temperature by Dynamic Mechanical Analysis
E2092	Test Method for Distortion Temperature in Three-Point Bending by Thermomechanical Analysis

Canadian Standards Association (CSA)

CSA S806	Design and Construction of Building Components with Fiber-Reinforced Polymers
CAN/ CSA-S6	Canadian Highway Bridge Design Code

China Association for Engineering Construction Standardization (CECS)

CECS-146	Technical Specification for Strengthening Concrete Structures with Carbon Fiber Reinforced Polymer Laminates

Code of Federal Regulations (CFR)
CFR 16, Hazardous Substances and Articles; Administration
Part 1500 and Enforcement Regulations
CFR 49, Subchapter C Transportation

International Conference of Building Officials (ICBO)(now *International Code Council*)
AC125 Acceptance Criteria for Concrete and Reinforced and Unreinforced Masonry Strengthening Using Fiber-Reinforced Composite Systems

International Concrete Repair Institute (ICRI)
03730 Guide for Surface Preparation for the Repair of Deteriorated Concrete Resulting from Reinforcing Steel Corrosion
03732 Guideline for Selecting and Specifying Concrete Surface Preparation for Sealers, Coatings, and Polymer Overlays
03739 Guideline to Using In-Situ Tensile Pull-Off Tests to Evaluate Bond of Concrete Surface Materials

These publications may be obtained from these organizations:

American Concrete Institute (ACI)
P.O. Box 9094
Farmington Hills, MI 48333-9094
www.concrete.org

American National Standards Institute (ANSI)
11 West 42nd Street
New York, NY 10036
www.ansi.org

American Society of Civil Engineers (ASCE)
1801 Alexander Bell Drive
Reston, VA 20191-4400
www.asce.org

ASTM International
100 Barr Harbor Drive
West Conshohocken, PA 19428
www.astm.org

Canadian Standards Association (CSA)
178 Rexdale Blvd.
Toronto, ON
M9W 1R3 Canada
www.csa.ca

China Association for Engineering Construction Standardization (CECS)
No. 12 Chegongzhuang St.
Xicheng District
Beijing 100044
China

Code of Federal Regulations (CFR)
Government Printing Office
732 N. Capitol St. N.W.
Washington, DC 20402
www.gpoaccess.gov/cfr/index.html

International Code Council (ICC)
500 New Jersey Avenue N.W.
6th Floor
Washington DC, 20001
www.iccsafe.org

International Concrete Repair Institute (ICRI)
3166 S. River Road Suite 132
Des Plains, IL 60018
www.icri.org

16.2—Cited references

AASHTO, 2004, "LRFD Bridge Design Specifications," Customary U.S. Units, third edition, Publication Code LRFDUS-3, AASHTO, Washington, DC.

ACI Committee 318, 2005, "Building Code Requirements for Structural Concrete (ACI 318-05) and Commentary (318R-05)," American Concrete Institute, Farmington Hills, MI, 430 pp.

Aiello, M. A.; Galati, N.; and Tegola, L. A., 2001, "Bond Analysis of Curved Structural Concrete Elements Strengthened using FRP Materials," *Fifth International Symposium on Non-Metallic (FRP) Reinforcement for Concrete Structures (FRPRCS-5)*, Cambridge-Thomas Telford, London, pp. 680-688.

Apicella, F., and Imbrogno, M., 1999, "Fire Performance of CFRP-Composites Used for Repairing and Strengthening Concrete," *Proceedings of the 5th ASCE Materials Engineering Congress*, Cincinnati, OH, May, pp. 260-266.

Arduini, M., and Nanni, A., 1997, "Behavior of Pre-Cracked RC Beams Strengthened with Carbon FRP Sheets," *Journal of Composites in Construction*, V. 1, No. 2, pp. 63-70.

Bank, L. C., 2006, *Composites for Construction: Structural Design with FRP Materials*, John Wiley & Sons, Hoboken, NJ, 560 pp.

Benmokrane, B., and Rahman, H., eds., 1998, *Durability of Fiber Reinforced Polymer (FRP) Composites for Construction*, University of Sherbrooke, Canada.

Bisby, L. A.; Green, M. F.; and Kodur, V. K. R., 2005a, "Fire Endurance of Fiber-Reinforced Polymer-Confined Concrete Columns," *ACI Structural Journal*, V. 102, No. 6, Nov.-Dec., pp. 883-891.

Bisby, L. A.; Green, M. F.; and Kodur, V. K. R., 2005b, "Response to Fire of Concrete Structures that Incorporate FRP," *Progress in Structural Engineering and Materials*, V. 7, No. 3, pp. 136-149.

Bousias, S.; Triantafillou, T.; Fardis, M.; Spathis, L.; and O'Regan, B., 2004, "Fiber-Reinforced Polymer Retrofitting of Rectangular Reinforced Concrete Columns with or without Corrosion," *ACI Structural Journal*, V. 101, No. 4, July-Aug., pp. 512-520.

Bousselham, A., and Chaallal, O., 2006, "Behavior of Reinforced Concrete T-Beams Strengthened in Shear with Carbon Fiber-Reinforced Polymer—An Experimental Study," *ACI Structural Journal*, V. 103, No. 3, May-June, pp. 339-347.

CALTRANS Division of Structures, 1996, *Prequalification Requirements for Alternative Column Casings for Seismic Retrofit (Composites)*, Section 10.1, California Department of Transportation, Sacramento, CA.

Carey, S. A., and Harries, K. A., 2005, "Axial Behavior and Modeling of Small-, Medium-, and Large-Scale Circular Sections Confined with CFRP Jackets," *ACI Structural Journal*, V. 102, No. 4, July-Aug., pp. 596-604.

Chaallal, O., and Shahawy, M., 2000, "Performance of Fiber-Reinforced Polymer-Wrapped Reinforced Concrete Column under Combined Axial-Flexural Loading," *ACI Structural Journal*, V. 97, No. 4, July-Aug., pp. 659-668.

Chajes, M.; Januska, T.; Mertz, D.; Thomson, T.; and Finch, W., 1995, "Shear Strengthening of Reinforced Concrete Beams Using Externally Applied Composite Fabrics," *ACI Structural Journal*, V. 92, No. 3, May-June, pp. 295-303.

Christensen, J. B.; Gilstrap, J. M.; and Dolan, C. W., 1996, "Composite Materials Reinforcement of Masonry Structures," *Journal of Architectural Engineering*, V. 2, No. 12, pp. 63-70.

Concrete Society, 2004, "Design Guidance for Strengthening Concrete Structures Using Fibre Composite Materials," *Technical Report* No. 55 (TR55), second edition, Surrey, 128 pp.

De Lorenzis, L.; Lundgren, K.; and Rizzo, A., 2004, "Anchorage Length of Near-Surface-Mounted FRP Bars for Concrete Strengthening—Experimental Investigation and Numerical Modeling," *ACI Structural Journal*, V. 101, No. 2, Mar.-Apr., pp. 269-278.

De Lorenzis, L., and Nanni, A., 2001b, "Characterization of FRP Rods as Near Surface Mounted Reinforcement," *Journal of Composites for Construction*, ASCE, V. 5, No. 2, pp. 114-121.

De Lorenzis, L., and Tepfers, R., 2003, "Comparative Study of Models on Confinement of Concrete Cylinders with Fiber-Reinforced Polymer Composites," *Journal of Composites for Construction*, ASCE, V. 7, No. 3, pp. 219-237.

Demers, M., and Neale, K., 1999, "Confinement of Reinforced Concrete Columns with Fibre Reinforced Composites Sheets—An Experimental Study," *Canadian Journal of Civil Engineering*, V. 26, pp. 226-241.

Deniaud, C., and Cheng, J. J. R., 2001, "Shear Behavior of Reinforced Concrete T-Beams with Externally Bonded Fiber-Reinforced Polymer Sheets," *ACI Structural Journal*, V. 98, No. 3, May-June, pp. 386-394.

Deniaud, C., and Cheng, J. J. R., 2003, "Reinforced Concrete T-Beams Strengthened in Shear with Fiber Reinforced Polymer Sheets," *Journal of Composites in Construction*, ASCE, V. 7, No. 4, pp. 302-310.

Dolan, C. W.; Rizkalla, S. H.; and Nanni, A., eds, 1999, *Fourth International Symposium on Fiber Reinforced Polymer Reinforcement for Reinforced Concrete Structures*, SP-188, American Concrete Institute, Farmington Hills, MI.

Ehsani, M. R., 1993, "Glass-Fiber Reinforcing Bars," *Alternative Materials for the Reinforcement and Prestressing of Concrete*, J. L. Clarke, Blackie Academic & Professional, London, pp. 35-54.

Ehsani, M.; Saadatmanesh, H.; and Al-Saidy, A., 1997, "Shear Behavior of URM Retrofitted with FRP Overlays," *Journal of Composites for Construction*, ASCE, V. 1, No. 1, pp. 17-25.

El-Maaddawy, T.; Chahrour, A.; and Soudki, K. A., 2006, "Effect of FRP-Wraps on Corrosion Activity and Concrete Cracking in Chloride-Contaminated Concrete Cylinders," *Journal of Composites for Construction*, ASCE, V. 10, No. 2, pp. 139-147.

Elnabelsy, G., and Saatcioglu, M., 2004, "Seismic Retrofit of Circular and Square Bridge Columns with CFRP Jackets," *Advanced Composite Materials in Bridges and Structures*, Calgary, AB, Canada, 8 pp. (CD-ROM)

El-Tawil, S.; Ogunc, C.; Okeil, A. M.; and Shahawy, M., 2001, "Static and Fatigue Analyses of RC Beams Strengthened with CFRP Laminates," *Journal of Composites for Construction*, ASCE, V. 5, No. 4, pp. 258-267.

Eshwar, N.; Ibell, T.; and Nanni, A., 2003, "CFRP Strengthening of Concrete Bridges with Curved Soffits," *International Conference Structural Faults + Repair 2003*, M. C. Forde, ed., Commonwealth Institute, London, 10 pp. (CD-ROM)

Fardis, M. N., and Khalili, H., 1981, "Concrete Encased in Fiberglass Reinforced Plastic," ACI JOURNAL, *Proceedings* V. 78, No. 6, Nov.-Dec., pp. 440-446.

Fleming, C. J., and King, G. E. M., 1967, "The Development of Structural Adhesives for Three Original Uses in South Africa," *RILEM International Symposium, Synthetic Resins in Building Construction*, Paris, pp. 75-92.

Funakawa, I.; Shimono, K.; Watanabe, T.; Asada, S.; and Ushijima, S., 1997, "Experimental Study on Shear Strengthening with Continuous Fiber Reinforcement Sheet and Methyl Methacrylate Resion," *Third International Symposium on Non-Metallic (FRP) Reinforcement for Concrete Structures (FRPRCS-3)*, V. 1, Japan Concrete Institute, Tokyo, Japan, pp. 475-482.

GangaRao, H. V. S., and Vijay, P. V., 1998, "Bending Behavior of Concrete Beams Wrapped with Carbon Fabric," *Journal of Structural Engineering*, V. 124, No. 1, pp. 3-10.

Green, M.; Bisby, L.; Beaudoin, Y.; and Labossiere, P., 1998, "Effects of Freeze-Thaw Action on the Bond of FRP Sheets to Concrete," *Proceedings of the First International Conference on Durability of Composites for Construction*, Sherbrooke, QC, Canada, Oct., pp. 179-190.

Harajli, M., and Rteil, A., 2004, "Effect of Confinement Using Fiber-Reinforced Polymer or Fiber-Reinforced Concrete on Seismic Performance of Gravity Load-Designed Columns," *ACI Structural Journal*, V. 101, No. 1, Jan.-Feb., pp. 47-56.

Harries, K. A., and Carey, S. A., 2003, "Shape and 'Gap' Effects on the Behavior of Variably Confined Concrete," *Cement and Concrete Research*, V. 33, No. 6, pp. 881-890.

Hassan, T., and Rizkalla, S., 2002, "Flexural Strengthening of Prestressed Bridge Slabs with FRP Systems," *PCI Journal*, V. 47, No. 1, pp. 76-93.

Hassan, T., and Rizkalla, S., 2003, "Investigation of Bond in Concrete Structures Strengthened with Near Surface Mounted CFRP Strips," *Journal of Composites for Construction*, ASCE, V. 7, No. 3, pp. 248-257.

Hawkins, G. F.; Steckel, G. L.; Bauer, J. L.; and Sultan, M., 1998, "Qualification of Composites for Seismic Retrofit of Bridge Columns," *Proceedings of the First International Conference on Durability of Composites for Construction*, Sherbrooke, QC, Canada, Aug., pp. 25-36.

Hognestad, E., 1951, "A Study of Combined Bending and Axial Load in Reinforced Concrete Members," *Bulletin* 399, University of Illinois Engineering Experiment Station, Urbana, IL.

Iacobucci, R.; Sheikh, S.; and Bayrak, O., 2003, "Retrofit of Square Concrete Columns with Carbon Fiber-Reinforced Polymer for Seismic Resistance," *ACI Structural Journal*, V. 100, No. 6, Nov.-Dec., pp. 785-794.

International Federation for Structural Concrete, 2001, *FIB 2001 Externally Bonded FRP Reinforcement for RC Structures*, FIB, Lausanne, 138 pp.

Kachlakev, D., and McCurry, D., 2000, "Testing of Full-Size Reinforced Concrete Beams Strengthened with FRP Composites: Experimental Results and Design Methods Verification," *Report* No. FHWA-OR-00-19, U.S. Department of Transportation Federal Highway Administration, 109 pp.

Katsumata, H.; Kobatake, Y.; and Takeda, T., 1987, "A Study on the Strengthening with Carbon Fiber for Earth-quake-Resistant Capacity of Existing Concrete Columns," *Proceedings from the Workshop on Repair and Retrofit of Existing Structures, U.S.-Japan Panel on Wind and Seismic Effects*, U.S.-Japan Cooperative Program in Natural Resources, Tsukuba, Japan, pp. 1816-1823.

Khalifa, A.; Alkhrdaji, T.; Nanni, A.; and Lansburg, S., 1999, "Anchorage of Surface-Mounted FRP Reinforcement," *Concrete International*, V. 21, No. 10, Oct., pp. 49-54.

Khalifa, A.; Gold, W.; Nanni, A.; and Abel-Aziz, M., 1998, "Contribution of Externally Bonded FRP to the Shear Capacity of RC Flexural Members," *Journal of Composites in Construction*, ASCE, V. 2, No. 4, pp. 195-203.

Kotynia, R., 2005, "Strain Efficiency of Near-Surface Mounted CFRP-Strengthened Reinforced Concrete Beams," *International Conference on Composites in Construction*, Lyon, July 11-13.

Kumahara, S.; Masuda, Y.; and Tanano, Y., 1993, "Tensile Strength of Continuous Fiber Bar Under High Temperature," *International Symposium on Fiber-Reinforced Plastic Reinforcement for Concrete Structures*, SP-138, A. Nanni and C. W. Dolan, eds., American Concrete Institute, Farmington Hills, MI, pp. 731-742.

Lam, L., and Teng, J., 2003a, "Design-Oriented Stress-Strain Model for FRP-Confined Concrete," *Construction and Building Materials*, V. 17, pp. 471-489.

Lam, L., and Teng, J., 2003b, "Design-Oriented Stress-Strain Model for FRP-Confined Concrete in Rectangular Columns," *Journal of Reinforced Plastics and Composites*, V. 22, No. 13, pp. 1149-1186.

Luo, S., and Wong, C. P., 2002, "Thermo-Mechanical Properties of Epoxy Formulations with Low Glass Transition

Temperatures," *Proceedings of the 8th International Symposium on Advanced Packaging Materials*, pp 226-231.

Malek, A.; Saadatmanesh, H.; and Ehsani, M., 1998, "Prediction of Failure Load of R/C Beams Strengthened with FRP Plate Due to Stress Concentrations at the Plate End," *ACI Structural Journal*, V. 95, No. 1, Jan.-Feb., pp. 142-152.

Malvar, L., 1998, "Durability of Composites in Reinforced Concrete," *Proceedings of the First International Conference on Durability of Composites for Construction*, Sherbrooke, QC, Canada, Aug., pp. 361-372.

Malvar, L.; Warren, G.; and Inaba, C., 1995, "Rehabilitation of Navy Pier Beams with Composite Sheets," *Second FRP International Symposium on Non-Metallic (FRP) Reinforcement for Concrete Structures*, Ghent, Belgium, Aug., pp. 533-540.

Mandell, J. F., 1982, "Fatigue Behavior of Fibre-Resin Composites," *Developments in Reinforced Plastics*, V. 2, Applied Science Publishers, London, pp. 67-107.

Mandell, J. F., and Meier, U., 1983, "Effects of Stress Ratio Frequency and Loading Time on the Tensile Fatigue of Glass-Reinforced Epoxy," *Long Term Behavior of Composites*, ASTM STP 813, ASTM International, West Conshohocken, PA, pp. 55-77.

Marshall, O. S.; Sweeney, S. C.; and Trovillion, J. C., 1999, "Seismic Rehabilitation of Unreinforced Masonry Walls," *Fourth International Symposium on Fiber Reinforced Polymer Reinforcement for Concrete Structures*, SP-188, C. W. Dolan, S. H. Rizkalla, and A. Nanni, eds., American Concrete Institute, Farmington Hills, MI, pp. 287-295.

Masoud, S. A., and Soudki, K. A., 2006, "Evaluation of Corrosion Activity in FRP Repaired RC Beams," *Cement and Concrete Composites*, V. 28, pp. 969-977.

Matthys, S.; Toutanji, H.; Audenaert, K.; and Taerwe, L., 2005, "Axial Load Behavior of Large-Scale Columns Confined with Fiber-Reinforced Polymer Composites," *ACI Structural Journal*, V. 102, No. 2, Mar.-Apr., pp. 258-267.

Matthys, S., and Triantafillou, T., 2001, "Shear and Torsion Strengthening with Externally Bonded FRP Reinforcement," *Proceedings of the International Workshop on: Composites in Construction: A Reality*, ASCE, Reston, VA, pp. 203-212.

Meier, U., 1987, "Bridge Repair with High Performance Composite Materials," *Material und Technik*, V. 4, pp. 125-128. (in German)

Meier, U., and Kaiser, H., 1991, "Strengthening of Structures with CFRP Laminates," *Advanced Composite Materials in Civil Engineering Structures*, ASCE Specialty Conference, pp. 224-232.

Memon, M., and Sheikh, S., 2005, "Seismic Resistance of Square Concrete Columns Retrofitted with Glass Fiber-Reinforced Polymer," *ACI Structural Journal*, V. 102, No. 5, Sept.-Oct., pp. 774-783.

Mindess, S., and Young, J., 1981, *Concrete*, Prentice-Hall, Englewood Cliffs, NJ, 671 pp.

Mosallam, A.; Chakrabarti, R.; Sim, S.; and Elasnadedy, H., 2000, "Seismic Response of Reinforced Concrete Moment Connections Repaired and Upgraded with FRP Composites," *Innovative Systems for Seismic Repair and Rehabilitation of*

Structures, Proceedings, SRRS2 Conference, A. Mosallam, ed., Fullerton, CA, Mar. 20-21, pp. 59-72.

Motavalli, M.; Terrasi, G. P.; and Meier, U., 1997, "On the Behavior of Hybrid Aluminum/CFRP Box Beams at Low Temperatures," *Composites— Part A: Applied Science and Manufacturing*, V. 28, No. 2, pp. 121-129.

Mutsuyoshi, H.; Uehara, K.; and Machida, A., 1990, "Mechanical Properties and Design Method of Concrete Beams Reinforced with Carbon Fiber Reinforced Plastics," *Transaction of the Japan Concrete Institute*, V. 12, Japan Concrete Institute, Tokyo, Japan, pp. 231-238.

Nanni, A., 1995, "Concrete Repair with Externally Bonded FRP Reinforcement," *Concrete International*, V. 17, No. 6, June, pp. 22-26.

Nanni, A., 1999, "Composites: Coming on Strong," *Concrete Construction*, V. 44, p. 120.

Nanni, A.; Bakis, C. E.; Boothby, T. E.; Lee, Y. J.; and Frigo, E. L., 1997, "Tensile Reinforcement by FRP Sheets Applied to RC," *9C/1-8, ICE 97 International Composites Exposition*, Nashville, TN, Jan., pp. 9C/1 to 8.

Nanni, A., and Bradford, N., 1995, "FRP Jacketed Concrete Under Uniaxial Compression," *Construction and Building Materials*, V. 9, No. 2, pp. 115-124.

Nanni, A., and Gold, W., 1998, "Strength Assessment of External FRP Reinforcement," *Concrete International*, V. 20, No. 6, June, pp. 39-42.

National Research Council, 1991, "Life Prediction Methodologies for Composite Materials," *Committee on Life Prediction Methodologies for Composites*, *NMAB-460*, National Materials Advisory Board, Washington, DC, 75 pp.

Neale, K. W., 2000, "FRPs for Structural Rehabilitation: A Survey of Recent Progress," *Progress in Structural Engineering and Materials*, V. 2, No. 2, pp. 133-138.

Neale, K. W., and Labossière, P., 1997, "State-of-the-Art Report on Retrofitting and Strengthening by Continuous Fibre in Canada," *Non-Metallic (FRP) Reinforcement for Concrete Structures*, V. 1, Japan Concrete Institute, Tokyo, Japan, pp. 25-39.

Norris, T.; Saadatmanesh, H.; and Ehsani, M., 1997, "Shear and Flexural Strengthening of R/C Beams with Carbon Fiber Sheets," *Journal of Structural Engineering*, V. 123, No. 7, pp. 903-911.

Nosho, K. J., 1996, "Retrofit of Rectangular Reinforced Concrete Columns using Carbon Fiber," MS thesis, University of Washington, Seattle, WA, 194 pp.

Nowak, A. S., and Szerszen, M. M., 2003, "Calibration of Design Code for Buildings (ACI 318): Part 1—Statistical Models for Resistance," *ACI Structural Journal*, V. 100, No. 3, May-June, pp. 377-382.

Odagiri, T.; Matsumoto, K.; and Nakai, H., 1997, "Fatigue and Relaxation Characteristics of Continuous Aramid Fiber Reinforced Plastic Rods," *Third International Symposium on Non-Metallic (FRP) Reinforcement for Concrete Structures (FRPRCS-3)*, V. 2, Japan Concrete Institute, Tokyo, Japan, pp. 227-234.

Okeil, A. M.; Bingol, Y.; and Alkhrdaji, T., 2007, "Analyzing Model Uncertainties for Concrete Beams Flexurally Strengthened with FRP Laminates," *Proceedings of the Transportation Research Board 86th Annual Meeting*, Jan. 21-25, 2007, Washington, DC, 15 pp. (CD-ROM)

PCI, 2004, *PCI Design Handbook Precast and Prestressed Concrete*, sixth edition, Prestressed/Precast Concrete Institute, Chicago, IL, 750 pp.

Pellegrino, C., and Modena, C., 2002, "Fiber Reinforced Polymer Shear Strengthening of Reinforced Concrete Beams with Transverse Steel Reinforcement," *Journal of Composites in Construction*, ASCE, V. 6, No. 2, pp. 104-111.

Pessiki, S.; Harries, K. A.; Kestner, J.; Sause, R.; and Ricles, J. M., 2001, "The Axial Behavior of Concrete Confined with Fiber Reinforced Composite Jackets," *Journal of Composites in Construction*, ASCE, V. 5, No. 4, pp. 237-245.

Porter, M. L.; Mehus, J.; Young, K. A.; O'Neil, E. F.; and Barnes, B. A., 1997, "Aging for Fiber Reinforcement in Concrete," *Proceedings of the Third International Symposium on Non-Metallic (FRP) Reinforcement for Concrete Structures*, Japan Concrete Institute, Sapporo, Japan, Oct. 14-16.

Priestley, M.; Seible, F.; and Calvi, G., 1996, *Seismic Design and Retrofit of Bridges*, John Wiley and Sons, New York, 704 pp.

Quattlebaum, J.; Harries, K. A.; and Petrou, M. F., 2005, "Comparison of Three CFRP Flexural Retrofit Systems Under Monotonic and Fatigue Loads," *Journal of Bridge Engineering*, ASCE, V. 10, No. 6, pp. 731-740.

Reed, C. E.; Peterman, R. J.; and Rasheed, H. A., 2005, "Evaluating FRP Repair Method for Cracked Prestressed Concrete Bridge Members Subjected to Repeated Loadings (Phase 1)," *KTRAN Report* No. K-TRAN: KSU-01-2, Kansas Department of Transportation, Topeka, KS, 106 pp.

Ritchie, P.; Thomas, D.; Lu, L.; and Conneley, G., 1991, "External Reinforcement of Concrete Beams Using Fiber Reinforced Plastics," *ACI Structural Journal*, V. 88, No. 4, July-Aug., pp. 490-500.

Roberts, T. M., and Haji-Kazemi, H., 1989, "Theoretical Study of the Behavior of Reinforced Concrete Beams Strengthened by Externally Bonded Steel Plates," *Proceedings of the Institute of Civil Engineers*, Part 2, V. 87, No. 9344, pp. 39-55.

Rocca, S.; Galati, N.; and Nanni, A., 2006, "Experimental Evaluation of FRP Strengthening of Large-Size Reinforced Concrete Columns," *Report* No. UTC-142, University of Missouri-Rolla, MO.

Rocca, S.; Galati, N.; and Nanni, A., 2008, "Review of Design Guidelines for FRP Confinement of Reinforced Concrete Columns of Noncircular Cross Sections," *Journal of Composites for Construction*, ASCE, V. 12, No. 1, Jan.-Feb., pp. 80-92.

Rosenboom, O. A., and Rizkalla, S. H., 2006, "Behavior of Prestressed Concrete Strengthened with Various CFRP Systems Subjected to Fatigue Loading," *Journal of Composites for Construction*, ASCE, V. 10, No. 6, Nov.-Dec., pp. 492-502.

Rostasy, F. S., 1987, "Bonding of Steel and GFRP Plates in the Area of Coupling Joints. Talbrucke Kattenbusch," *Research Report* No. 3126/1429, Federal Institute for Materials Testing, Braunschweig, Germany. (in German)

Rostasy, F. S., 1997, "On Durability of FRP in Aggressive Environments," *Third International Symposium on Non-Metallic (FRP) Reinforcement for Concrete Structures*

(FRPRCS-3), V. 2, Japan Concrete Institute, Tokyo, Japan, pp. 107-114.

Roylance, M., and Roylance, O., 1981, "Effect of Moisture on the Fatigue Resistance of an Aramid-Epoxy Composite," *Organic Coatings and Plastics Chemistry*, V. 45, American Chemical Society, Washington, DC, pp. 784-788.

Saadatmanesh, H.; Ehsani, M. R.; and Jin, L., 1996, "Seismic Strengthening of Circular Bridge Pier Models with Fiber Composites," *ACI Structural Journal*, V. 93, No. 6, Nov.-Dec., pp. 639-647.

Saadatmanesh, H., and Ehsani, M. R., eds., 1998, *Second International Conference on Composites in Infrastructure*, ICCI, V. 1 and 2, Tucson, AZ, 1506 pp.

Sato, Y.; Ueda, T.; Kakuta, Y.; and Tanaka, T., 1996, "Shear Reinforcing Effect of Carbon Fiber Sheet Attached to Side of Reinforced Concrete Beams," *Advanced Composite Materials in Bridges and Structures*, M. M. El-Badry, ed., pp. 621-627.

Sause, R.; Harries, K. A.; Walkup, S. L.; Pessiki, S.; and Ricles, J. M., 2004, "Flexural Behavior of Concrete Columns with Carbon Fiber Composite Jackets," *ACI Structural Journal*, V. 101, No. 5, Sept.-Oct., pp. 708-716.

Seible, F.; Priestley, M. J. N.; Hegemier, G. A.; and Innamorato, D., 1997, "Seismic Retrofit of RC Columns with Continuous Carbon Fiber Jackets," *Journal of Composites for Construction*, ASCE, V. 2, No. 1, pp. 52-62.

Sharaf, M. H.; Soudki, K. A; and Van Dusen, M., 2006, "CFRP Strengthening for Punching Shear of Interior Slab-Column Connections," *Journal of Composites for Construction*, ASCE, V. 10, No. 5, pp. 410-418.

Sharif, A.; Al-Sulaimani, G.; Basunbul, I.; Baluch, M.; and Ghaleb, B., 1994, "Strengthening of Initially Loaded Reinforced Concrete Beams Using FRP Plates," *ACI Structural Journal*, V. 91, No. 2, Mar.-Apr., pp. 160-168.

Sheheta, E.; Morphy, R.; and Rizkalla, S., 1999, *Fourth International Symposium on Fiber Reinforced Polymer Reinforcement for Concrete Structures*, SP-188, C. W. Dolan, S. H. Rizkalla, and A. Nanni, eds., American Concrete Institute, Farmington Hills, MI, pp. 157-167.

Sheikh, S., and Yau, G., 2002, "Seismic Behavior of Concrete Columns Confined with Steel and Fiber-Reinforced Polymers," *ACI Structural Journal*, V. 99, No. 1, Jan.-Feb., pp. 72-80.

Shield, C. K.; Busel, J. P.; Walkup S. L.; and Gremel, D. D., 2005, *Proceedings of the Seventh International Symposium on Fiber Reinforced Polymer for Reinforced Concrete Structures (FRPRCS-7)*, SP-230, American Concrete Institute, Farmington Hills, MI, 1708 pp.

Soudki, K. A., and Green, M. F., 1997, "Freeze-Thaw Response of CFRP Wrapped Concrete," *Concrete International*, V. 19, No. 8, Aug., pp. 64-67.

Spoelstra, M. R., and Monti, G., 1999, "FRP-Confined Concrete Model," *Journal of Composites for Construction*, ASCE, V. 3, No. 3, pp. 143-150.

Steckel, G.; Hawkins, G.; and Bauer, J., 1999, "Durability Issues for Composites in Infrastructure," *44th International SAMPE Symposium*, Long Beach, CA, May, pp. 2194-2208.

Szerszen, M. M., and Nowak, A. S., 2003, "Calibration of Design Code for Buildings (ACI 318): Part 2—Reliability Analysis and Resistance Factors," *ACI Structural Journal*, V. 100, No. 3, May-June, pp. 383-391.

Teng, J. G.; Chen, J. F.; Smith, S. T.; and Lam, L., 2002, *FRP Strengthened RC Structures*, John Wiley & Sons, West Sussex, UK, 266 pp.

Teng, J. G.; Lu, X. Z.; Ye, L. P.; and Jiang, J. J., 2004, "Recent Research on Intermediate Crack Induced Debonding in FRP Strengthened Beams," *Proceedings of the 4th International Conference on Advanced Composite Materials for Bridges and Structures*, Calgary, AB, Canada.

Teng, J. G.; Smith, S. T.; Yao, J.; and Chen, J. F., 2001, "Intermediate Crack Induced Debonding in RC Beams and Slabs," *Construction and Building Materials*, V. 17, No. 6-7, pp. 447-462.

Toutanji, H., 1999, "Stress-Strain Characteristics of Concrete Columns Externally Confined with Advanced Fiber Composite Sheets," *ACI Materials Journal*, V. 96, No. 3, May-June, pp. 397-404.

Triantafillou, T. C., 1998a, "Shear Strengthening of Reinforced Concrete Beams Using Epoxy-Bonded FRP Composites," *ACI Structural Journal*, V. 95, No. 2, Mar.-Apr., pp. 107-115.

Triantafillou, T. C., 1998b, "Strengthening of Masonry Structures Using Epoxy-Bonded FRP Laminates," *Journal of Composites for Construction*, ASCE, V. 3, No. 2, pp. 96-104.

Wang, N., and Evans, J. T., 1995, "Collapse of Continuous Fiber Composite Beam at Elevated Temperatures," *Composites*, V. 26, No. 1, pp. 56-61.

Wang, Y. C., and Restrepo, J. I., 2001, "Investigation of Concentrically Loaded Reinforced Concrete Columns Confined with Glass Fiber-Reinforced Polymer Jackets," *ACI Structural Journal*, V. 98, No. 3, May-June, pp. 377-385.

Williams, B. K.; Bisby, L. A.; Kodur, V. K. R.; Green, M. F.; and Chowdhury, E., 2006, "Fire Insulation Schemes for FRP-Strengthened Concrete Slabs," *Composites*, Part A, No. 37, pp. 1151-1160.

Wolf, R., and Miessler, H. J., 1989, "HLV-Spannglieder in der Praxis," *Erfahrungen Mit Glasfaserverbundstaben*, Beton, 2, pp. 47-51.

Wu, W., 1990, "Thermomechanical Properties of Fiber Reinforced Plastics (FRP) Bars," PhD dissertation, West Virginia University, Morgantown, WV, 292 pp.

Xian, G., and Karbhari, V. M., 2007, "Segmental Relaxation of Water-Aged Ambient Cured Epoxy," *Journal of Polymer Degradation and Stability*, V. 92, No. 9, pp. 1650-1659.

Yamaguchi, T.; Kato, Y.; Nishimura, T.; and Uomoto, T., 1997, "Creep Rupture of FRP Rods Made of Aramid, Carbon and Glass Fibers," *Third International Symposium on Non-Metallic (FRP) Reinforcement for Concrete Structures* (FRPRCS-3), V. 2, Japan Concrete Institute, Tokyo, Japan, pp. 179-186.

Youssef, M. N., 2003, "Stress Strain Model for Concrete Confined by FRP Composites," PhD dissertation, University of California-Irvine, Irvine, CA, 310 pp.

APPENDIX A—MATERIAL PROPERTIES OF CARBON, GLASS, AND ARAMID FIBERS

Table A1.1 presents ranges of values for the tensile properties of carbon, glass, and aramid fibers. The tabulated values are based on the testing of impregnated fiber yarns or strands in accordance with Suppliers of Advanced Composite Materials Association Test Method 16-90. The strands or fiber yarns are impregnated with resin, cured, and then tested in tension. The tabulated properties are calculated using the area of the fibers; the resin area is ignored. Hence, the properties listed in Table A1.1 are representative of unidirectional FRP systems whose properties are reported using net-fiber area (Section 4.3.1).

Table A1.2 presents ranges of tensile properties for CFRP, GFRP, and AFRP bars with fiber volumes of approximately 50 to 70%. Properties are based on gross-laminate area (Section 4.3.1).

Table A1.3 presents ranges of tensile properties for CFRP, GFRP, and AFRP laminates with fiber volumes of approximately 40 to 60%. Properties are based on gross-laminate area (Section 4.3.1). The properties are shown for unidirectional, bidirectional, and +45/–45-degree fabrics. Table A1.3 also shows the effect of varying the fiber orientation on the 0-degree strength of the laminate.

Table A1.4 gives the tensile strengths of some commercially available FRP systems. The strength of unidirectional laminates is dependent on fiber type and dry fabric weight.

These tables are not intended to provide ultimate strength values for design purposes.

Table A1.1—Typical tensile properties of fibers used in FRP systems

Fiber type	Elastic modulus		Ultimate strength		Rupture strain, minimum, %
	10^3 ksi	GPa	ksi	MPa	
Carbon					
General purpose	32 to 34	220 to 240	300 to 550	2050 to 3790	1.2
High-strength	32 to 34	220 to 240	550 to 700	3790 to 4820	1.4
Ultra-high-strength	32 to 34	220 to 240	700 to 900	4820 to 6200	1.5
High-modulus	50 to 75	340 to 520	250 to 450	1720 to 3100	0.5
Ultra-high-modulus	75 to 100	520 to 690	200 to 350	1380 to 2400	0.2
Glass					
E-glass	10 to 10.5	69 to 72	270 to 390	1860 to 2680	4.5
S-glass	12.5 to 13	86 to 90	500 to 700	3440 to 4140	5.4
Aramid					
General purpose	10 to 12	69 to 83	500 to 600	3440 to 4140	2.5
High-performance	16 to 18	110 to 124	500 to 600	3440 to 4140	1.6

Table A1.2—Tensile properties of FRP bars with fiber volumes of 50 to 70%

FRP system description	Young's modulus, 10^3 ksi (GPa)	Ultimate tensile strength, ksi (MPa)	Rupture strain, %
High-strength carbon/epoxy	17 to 24 (115 to 165)	180 to 400 (1240 to 2760)	1.2 to 1.8
E-glass/epoxy	4 to 7 (27 to 48)	70 to 230 (480 to 1580)	1.6 to 3.0
High-performance aramid	8 to 11 (55 to 76)	130 to 280 (900 to 11,930)	2.0 to 3.0

Table A1.3—Tensile properties of FRP laminates with fiber volumes of 40 to 60%

FRP system description (fiber orientation)	Young's modulus		Ultimate tensile strength		Rupture strain at 0 degrees, %
	Property at 0 degrees 10^3 ksi (GPa)	Property at 90 degrees 10^3 ksi (GPa)	Property at 0 degrees ksi (MPa)	Property at 90 degrees ksi (MPa)	
High-strength carbon/epoxy, degrees					
0	15 to 21 (100 to 140)	0.3 to 1 (2 to 7)	150 to 350 (1020 to 2080)	5 to 10 (35 to 70)	1.0 to 1.5
0/90	8 to 11 (55 to 76)	8 to 11 (55 to 75)	100 to 150 (700 to 1020)	100 to 150 (700 to 1020)	1.0 to 1.5
+45/–45	2 to 4 (14 to 28)	2 to 4 (14 to 28)	25 to 40 (180 to 280)	25 to 40 (180 to 280)	1.5 to 2.5
E-glass/epoxy, degrees					
0	3 to 6 (20 to 40)	0.3 to 1 (2 to 7)	75 to 200 (520 to 1400)	5 to 10 (35 to 70)	1.5 to 3.0
0/90	2 to 5 (14 to 34)	2 to 5 (14 to 35)	75 to 150 (520 to 1020)	75 to 150 (520 to 1020)	2.0 to 3.0
+45/–45	2 to 3 (14 to 21)	2 to 3 (14 to 20)	25 to 40 (180 to 280)	25 to 40 (180 to 280)	2.5 to 3.5
High-performance aramid/epoxy, degrees					
0	7 to 10 (48 to 68)	0.3 to 1 (2 to 7)	100 to 250 (700 to 1720)	5 to 10 (35 to 70)	2.0 to 3.0
0/90	4 to 5 (28 to 34)	4 to 5 (28 to 35)	40 to 80 (280 to 550)	40 to 80 (280 to 550)	2.0 to 3.0
+45/–45	1 to 2 (7 to 14)	1 to 2 (7 to 14)	20 to 30 (140 to 210)	20 to 30 (140 to 210)	2.0 to 3.0

Notes:
FRP composite properties are based on FRP systems having an approximate fiber volume of 50% and a composite thickness of 0.1 in. (2.5 mm). In general, FRP bars have fiber volumes of 50 to 70%, precured systems have fiber volumes of 40 to 60%, and wet layup systems have fiber volumes of 25 to 40%. Because the fiber volume influences the gross-laminate properties, precured laminates usually have higher mechanical properties than laminates created using the wet layup technique.

Zero degrees represents unidirectional fiber orientation.

Zero/90 degrees (or +45/–45 degrees) represents fiber balanced in two orthogonal directions, where 0 degrees is the direction of loading, and 90 degrees is normal to the direction of loading.

Tension is applied to 0-degree direction. All FRP bar properties are in the 0-degree direction.

Table A1.4—Ultimate tensile strength* of some commercially available FRP systems

FRP system description (fiber type/saturating resin/fabric type)	Fabric weight		Ultimate strength[†]	
	oz/yd^3	g/m^3	lb/in.	kN/mm
General purpose carbon/resin unidirectional sheet	6	200	2600	500
	12	400	3550	620
High-strength carbon/resin unidirectional sheet	7	230	1800	320
	9	300	4000	700
	18	620	5500	960
High-modulus carbon/resin unidirectional sheet	9	300	3400	600
General-purpose carbon/resin balanced sheet	9	300	1000	180
E-glass/resin unidirectional sheet	27	900	4100	720
	10	350	1300	230
E-glass/balanced fabric	9	300	680	120
Aramid/resin unidirectional sheet	12	420	4000	700
High-strength carbon/resin precured, unidirectional laminate	70[‡]	2380[‡]	19,000	3300
E-glass/vinyl ester precured, unidirectional shell	50[‡]	1700[‡]	9000	1580

[*]Values shown should not be used for design.
[†]Ultimate tensile strength per unit width of sheet or fabric.
[‡]Precured laminate weight.

APPENDIX B—SUMMARY OF STANDARD TEST METHODS

ACI 440.3R provides test methods for the short-term and long-term mechanical and durability testing of FRP rods and sheets. The recommended test methods are based on the knowledge gained from research results and literature worldwide. It is anticipated that these test methods may be considered, modified, and adopted, either in whole or in part, by a U.S. national standards-writing agency such as ASTM or AASHTO. The publication of these test methods by ACI Committee 440 is an effort to aid in this adoption.

ASTM test methods that quantify the structural behavior of FRP systems bonded to concrete are in preparation. Certain existing ASTM test methods are applicable to the FRP material. FRP materials can be tested in accordance with the methods listed in Table B1.1 as long as all exceptions to the method are listed in the test report. Durability-related tests use the same test methods but require application-specific preconditioning of specimens. Acceptance of the data generated by the listed test methods can be the basis for FRP material system qualification and acceptance.

Table B1.1—Test methods for FRP material systems

Property	ASTM test method(s)	ACI 440.3R test method	Summary of differences
Test methods for sheets, prepreg, and laminates			
Surface hardness	D2538	—	No ACI methods developed.
	D2240		
	D3418		
Coefficient of thermal expansion	D696	—	No ACI methods developed.
Glass-transition temperature	D4065	—	No ACI methods developed.
Volume fraction	D3171	—	No ACI methods developed.
	D2584		
Sheet to concrete adhesion (direct tension pull-off)	D4551	L.1	ACI method provides specific requirements for specimen preparation not found in the ASTM method
Tensile strength and modulus	D3039	L.2	ACI method provides methods for calculating tensile strength and modulus on gross cross-sectional and effective fiber area basis. Section 3.3.1 of ACI 440.2R is used to calculate design values.
Lap shear strength	D3165	L.3	ACI method provides specific requirements for specimen preparation.
	D3528		
Test methods for FRP bars			
Cross-sectional area	D7205	B.1	Two options for bar area are provided in D7205 (nominal and actual) whereas only nominal area is used in 440.3R method B.1
Longitudinal tensile strength and modulus	D7205	B.2	Strain limits for calculation of modulus are different in the two methods.
Shear strength	D5379/D5379M	B.4	The ACI method focuses on dowel action of bars and does not overlap with existing ASTM methods that focus mainly on beam shearing failure modes. Bar shear strength is of specific concern for applications where FRP rods are used to cross construction joints in concrete pavements.
	D3846		
	D2344/D2344M		
	D4475		
Durability properties	—	B.6	No existing ASTM test methods available.
Fatigue properties	D3479/D3479M	B.7	ACI methods provide specific information on anchoring bars in the test fixtures and on attaching elongation measuring devices to the bar. The ACI methods also require specific calculations that are not provided in the ASTM methods.
Creep properties	D2990	B.8	
Relaxation properties	D2990	B.9	
	E328		
Flexural tensile properties	—	B.11	No existing ASTM test methods available.
Flexural properties	D790	—	No ACI methods developed.
	D4476	—	
Coefficient of thermal expansion	E831	—	No ACI methods developed.
	D696	—	
Glass-transition temperature	E1356	—	No ACI methods developed.
	E1640		
	D648		
	E2092		
Volume fraction	D3171	—	No ACI methods developed.

APPENDIX C—AREAS OF FUTURE RESEARCH

As mentioned in the body of the document, future research is needed to provide information in areas that are still unclear or are in need of additional evidence to validate performance. The list of topics presented in this appendix provides a summary.

Materials
- Confirmation of normal (Gaussian) distribution representing the tensile strength of a population of FRP strengthening systems;
- Methods of fireproofing FRP strengthening systems;
- Behavior of FRP-strengthened members under elevated temperatures;
- Behavior of FRP-strengthened members under cold temperatures;
- Fire rating of concrete members strengthened with FRP bars;
- Effect of different coefficients of thermal expansion between FRP systems and member substrates;
- Creep-rupture behavior and endurance times of FRP systems; and
- Strength and stiffness degradation of FRP systems in harsh environments.

Flexure/axial force
- Compression behavior of noncircular members wrapped with FRP systems;
- Behavior of members strengthened with FRP systems oriented in the direction of the applied axial load;
- Effects of high concrete strength on behavior of FRP-strengthened members;
- Effects of lightweight concrete on behavior of FRP-strengthened members;

- Maximum crack width and deflection prediction and control of concrete reinforced with FRP systems; and
- Long-term deflection behavior of concrete flexural members strengthened with FRP systems.

Shear
- Effective strain of FRP systems that do not completely wrap around the section; and
- Use of FRP systems for punching shear reinforcement in two-way systems.

Detailing
- Anchoring of FRP systems.

The design guide specifically indicated that test methods are needed to determine the following properties of FRP:
- Bond characteristics and related bond-dependent coefficients;
- Creep-rupture and endurance times;
- Fatigue characteristics;
- Coefficient of thermal expansion;
- Shear strength; and
- Compressive strength.

(a) Point B

(b) Point C

Fig. D.1—Strain distributions for Points B and C for simplified interaction diagram.

APPENDIX D—METHODOLOGY FOR COMPUTATION OF SIMPLIFIED P-M INTERACTION DIAGRAM FOR NONCIRCULAR COLUMNS

P-M diagrams may be developed by satisfying strain compatibility and force equilibrium using the model for the stress strain behavior for FRP-confined concrete presented in Eq. (12-2). For simplicity, the portion of the unconfined and confined P-M diagrams corresponding to compression-controlled failure can be reduced to two bilinear curves passing through the following three points (Fig D.1). (The following only makes reference to the confined case because the unconfined one is analogous):

- Point A (pure compression) at a uniform axial compressive strain of confined concrete ε_{ccu};
- Point B with a strain distribution corresponding to zero strain at the layer of longitudinal steel reinforcement nearest to the tensile face, and a compressive strain ε_{ccu} on the compression face; and
- Point C with a strain distribution corresponding to balanced failure with a maximum compressive strain ε_{ccu} and a yielding tensile strain ε_{sy} at the layer of longitudinal steel reinforcement nearest to the tensile face.
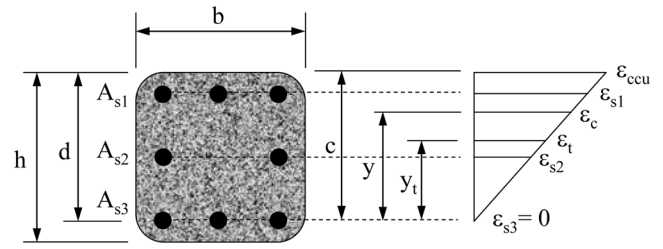
For confined concrete, the value of ϕP_n corresponding to Point A (ϕM_n equals zero) is given in Eq. (12-1), while the coordinates of Points B and C can be computed as:

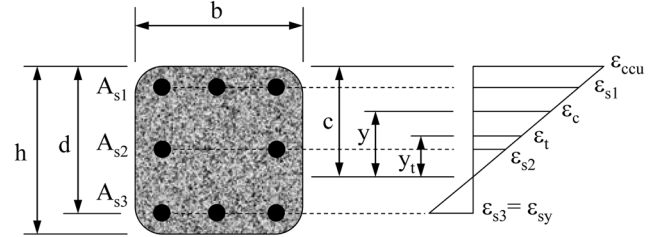$$\phi P_{n(B,C)} = \phi[(A(y_t)^3 + B(y_t)^2 + C(y_t) + D) + \sum A_{si} f_{si}] \quad \text{(D-1)}$$

$$\phi M_{n(B,C)} = \phi[(E(y_t)^4 + F(y_t)^3 + G(y_t)^2 + H(y_t) + I) + \sum A_{si} f_{si} d_i] \quad \text{(D-2)}$$

where

$$A = \frac{-b(E_c - E_2)^2}{12f_c'}\left(\frac{\varepsilon_{ccu}}{c}\right)^2 \quad \text{(D-3a)}$$

$$B = \frac{b(E_c - E_2)}{2}\left(\frac{\varepsilon_{ccu}}{c}\right) \quad \text{(D-3b)}$$

$$C = -bf_c' \quad \text{(D-3c)}$$

$$D = bcf_c' + \frac{bcE_2}{2}(\varepsilon_{ccu}) \quad \text{(D-3d)}$$

$$E = \frac{-b(E_c - E_2)^2}{16f_c'}\left(\frac{\varepsilon_{ccu}}{c}\right)^2 \quad \text{(D-3e)}$$

$$F = b\left(c - \frac{h}{2}\right)\frac{(E_c - E_2)^2}{12f_c'}\left(\frac{\varepsilon_{ccu}}{c}\right)^2 + \frac{b(E_c - E_2)}{3}\left(\frac{\varepsilon_{ccu}}{c}\right) \quad \text{(D-3f)}$$

$$G = \left(\frac{b}{2}f_c' + b\left(c - \frac{h}{2}\right)\frac{(E_c - E_2)}{2}\left(\frac{\varepsilon_{ccu}}{c}\right)\right) \quad \text{(D-3g)}$$

$$H = bf_c'\left(c - \frac{h}{2}\right) \quad \text{(D-3h)}$$

$$I = \frac{bc^2}{h}f_c' - bcf_c'\left(c - \frac{h}{2}\right) + \frac{bc^2 E_2}{3}(\varepsilon_{ccu}) - \frac{bcE_2}{2}\left(c - \frac{h}{2}\right)(\varepsilon_{ccu}) \quad \text{(D-3i)}$$

In Eq. (D-3), c is the distance from the extreme compression fiber to the neutral axis (Fig D.1) and it is given by Eq. (D-4). The parameter y_t represents the vertical coordinate within the compression region measured from the neutral axis position
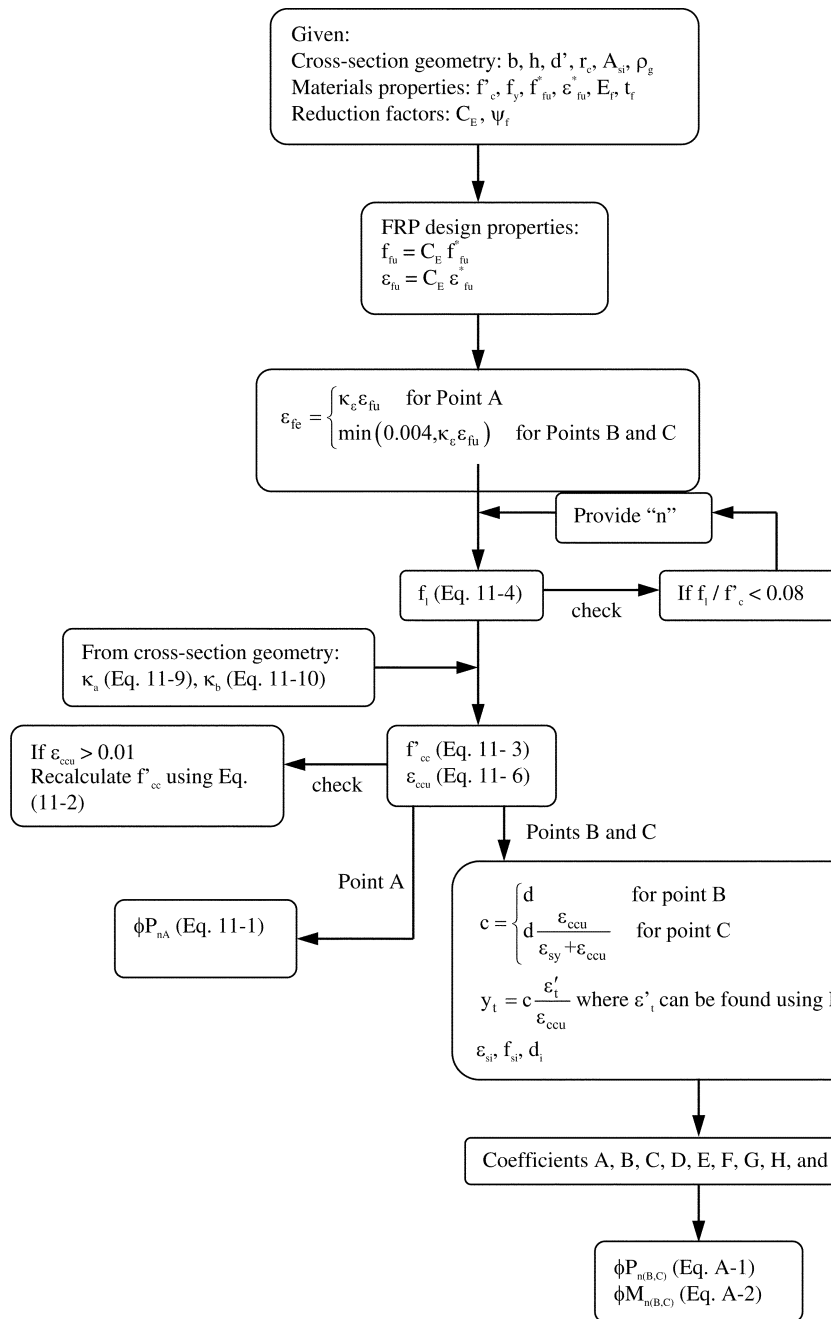
Fig. D.2—Flowchart for application of methodology.

(Fig. D.1) and corresponds to the transition strain ε_t' (Eq. (D-5) [see Fig. D.1]).

$$c = \begin{cases} d & \text{for Point B} \\ d\dfrac{\varepsilon_{ccu}}{\varepsilon_{sy} + \varepsilon_{ccu}} & \text{for Point C} \end{cases} \qquad \text{(D-4)}$$

$$y_t = c\frac{\varepsilon_t'}{\varepsilon_{ccu}} \qquad \text{(D-5)}$$

in which f_{si} is the stress in the i-th layer of longitudinal steel reinforcement. The values are calculated by similar triangles from the strain distribution corresponding to Points B and C. Depending on the neutral axis position c, the sign of f_{si} will be positive for compression and negative for tension. A flowchart illustrating the application of the proposed methodology is shown in Fig. D.2.

American Concrete Institute®

Advancing concrete knowledge

As ACI begins its second century of advancing concrete knowledge, its original chartered purpose remains "to provide a comradeship in finding the best ways to do concrete work of all kinds and in spreading knowledge." In keeping with this purpose, ACI supports the following activities:

· Technical committees that produce consensus reports, guides, specifications, and codes.

· Spring and fall conventions to facilitate the work of its committees.

· Educational seminars that disseminate reliable information on concrete.

· Certification programs for personnel employed within the concrete industry.

· Student programs such as scholarships, internships, and competitions.

· Sponsoring and co-sponsoring international conferences and symposia.

· Formal coordination with several international concrete related societies.

· Periodicals: the *ACI Structural Journal* and the *ACI Materials Journal*, and *Concrete International*.

Benefits of membership include a subscription to *Concrete International* and to an ACI Journal. ACI members receive discounts of up to 40% on all ACI products and services, including documents, seminars and convention registration fees.

As a member of ACI, you join thousands of practitioners and professionals worldwide who share a commitment to maintain the highest industry standards for concrete technology, construction, and practices. In addition, ACI chapters provide opportunities for interaction of professionals and practitioners at a local level.

American Concrete Institute
38800 Country Club Drive
Farmington Hills, MI 48331
U.S.A.
Phone: 248-848-3700
Fax: 248-848-3701

www.concrete.org

Guide for the Design and Construction of Externally Bonded FRP Systems for Strengthening Concrete Structures

The AMERICAN CONCRETE INSTITUTE

was founded in 1904 as a nonprofit membership organization dedicated to public service and representing the user interest in the field of concrete. ACI gathers and distributes information on the improvement of design, construction and maintenance of concrete products and structures. The work of ACI is conducted by individual ACI members and through volunteer committees composed of both members and non-members.

The committees, as well as ACI as a whole, operate under a consensus format, which assures all participants the right to have their views considered. Committee activities include the development of building codes and specifications; analysis of research and development results; presentation of construction and repair techniques; and education.

Individuals interested in the activities of ACI are encouraged to become a member. There are no educational or employment requirements. ACI's membership is composed of engineers, architects, scientists, contractors, educators, and representatives from a variety of companies and organizations.

Members are encouraged to participate in committee activities that relate to their specific areas of interest. For more information, contact ACI.

www.concrete.org

American Concrete Institute®
Advancing concrete knowledge